Supporting information for

$NaBH_4$-mediated syntheses of colloidal gold nanocatalysts in water: are additives really needed?

Hilary Kouawa Fokam,[a] Aleksandra Smolska,[a] Jonathan Quinson[b,a,*]

a) Biological and Chemical Engineering Department, Aarhus University, 8200 Aarhus, Denmark
b) CICA-Centro Interdisciplinar de Química e Bioloxía, Facultade de Ciencias, Universidade da Coruña, Campus de Elviña, 15008 A Coruña, Spain

* corresponding author: j.quinson@udc.es

Table of Contents

1. Literature

A large body of literature covers the use of $NaBH_4$ as reducing agent for Au NP synthesis.[1-3] The synthesis is typically performed in presence of additives as detailed in the main text. Only few examples of a surfactant-free version have been reported and are summarized in **Table S1**.

Table S1. Comparison with the literature for surfactant-free $NaBH_4$-mediated syntheses of Au NPs. RT stands for room temperature. Results from our own work are in grey cells.

Ref.	$HAuCl_4$ mM	$NaBH_4$/Au molar ratio	N_2	Volume mL	Containers	λ_{spr} nm	Diameter nm	Stability	Applications
4 *	0.13	2	YES	33	Not specified (likely glass)	515	5.5 ± 2	days	4-NP
		10	YES/NO			514	2.8 ± 1	1 month*	
		50	YES			-	-	60 min	
		100	YES			-	-	10 min	
5 **	0.17	2 10 20 50	NO	15	glass	513	5.6	1 month at RT	4-NP
6 ***	0.25	11-46	NO	N/S	N/S	520 To 537	11.4 to 22.2	N/A	Size
7 ****	0.25	2 5 10	NO	20	polypropylene centrifuge tubes	510 to 525	- 7.7 ± 3.2 -	1 month at RT	4-NP
8 *****	0.25	10	NO	10	glass scintillation vial	500 to 510	3.1 ± 0.9 7.4 ± 2.5	N/A	-
Our previous work 9	0.5	1 - 30	NO	2	PS cuvettes	508 - 545	5 - 20	months at RT	Size control
Our previous work 10	0.5	5.0 8.5 11.0	NO	2	PS cuvettes	500 - 525	5 - 15	months at RT	4-NP
Our previous work 11	0.5	5.0 8.5 11.0	NO	2 100	PS cuvettes Pyrex®	508 - 529	4.3 - 20	At least 1 month in a fridge	4-NP **EOR**
This work	**0.10** **0.20** **0.25** **0.50**	5 8 10	NO	2 **1000**	PS cuvettes Pyrex®	510 - 520	**4** **-** **10**	At least 1 month at RT	4-NP **EOR**

* Storage conditions not specified

** The surfactant-free $NaBH_4$-mediated Au NPs are used as benchmark for the 4-NP (obtained with a $NaBH_4$/Au molar ratio of 4) to assess the effect of using homemade stabilizers.

*** The exact volume was not constant but likely above 100 mL, different for all experiments. The $NaBH_4$ was added drop by drop from a 100 mM stock solution. The focus was less on obtaining NP with controlled sizes than comparing the size evaluation with different methods for NP that happen to have different sizes.

**** Note that the focus of [7] is on Au_xAg_{1-x} NPs and not Au NPs (x=1) as such.

***** Note that the focus on [8] is on the use of D_2O or mQ for Au NPs prepared at a fixed $NaBH_4$/Au molar ratio of 10.

[9] Focuses, among other experimental conditions, on the effects of using different reducing agents: $LiBH_4$, $NaBH_4$, KBH_4 for the colloidal syntheses.

[10] Focuses on the effect of using $HAuCl_4$ or $HAuBr_4$ as precursor.

[11] Focuses on the effect of the water purity and conductivity. Includes our first attempts to use Au NPs prepared by a surfactant-free $NaBH_4$-mediated synthesis for an alternative reaction to the 4-NP, i.e. for electrocatalysis with the EOR.

Our previous work focuses on surfactant-free approaches. This works focuses on the benefits or not to use additives for $NaBH_4$-mediated syntheses of Au NPs in water at RT and benchmark their activity.

2. Materials and methods

2.1. Chemicals

All chemicals were used as received: $HAuCl_4 \cdot 3H_2O$ (≥99.9%, Sigma-Aldrich); $NaBH_4$ (ReagentPlus®, 99%, Sigma-Aldrich); ultrapure water (mQ, Milli-Q, Millipore, resistivity of >18.2 MΩ•cm); trisodium citrate·$2H_2O$ (NaCt, Sigma Aldrich, BioUltra); polyvinylpyrrolidone (PVP, Sigma Aldrich, average molecular weight 10,000, a molar mass of 111.14 corresponding to the vinylpyrrolidone unit was considered for the concentrations); sodium dodecyl sulfate (SDS, Sigma Aldrich, ReagentPlus, ≥98.5%); HCl (puriss. ACS reagent, reag. ISO, Reag. Ph. Eur. fuming, ≥ 37%, Sigma Aldrich); HNO_3 (puriss ≥ 65%, Sigma Aldrich); 4-nitrophenol (4-NP, ReagentPlus®, ≥99%, Sigma-Aldrich); ethanol ($E_{99.8\%}$, Ethanol absolute, ≥99.8%, AnalaR NORMAPUR® ACS, Reag. Ph. Eur. analyse reagens, VWR); H_2SO_4 (99.999%, Sigma-Aldrich, 339741-500ML); KOH (Reag. Ph. Eur., VWR).

Extra caution was taken so that none of the chemicals was in contact with metal (e.g. metallic spatulas were not used and plastic spatulas were preferred). **Dispose of chemicals following local rules**. **Pay attention to HCl, HNO_3 and 4-NP based wastes**.

2.2. $NaBH_4$-mediated synthesis of Au NPs

General recipe

The general synthesis follows the method proposed by Astruc and co-workers,[4] with adaptations. To a solution of $HAuCl_4$ in water, $NaBH_4$ is added under vigorous stirring (here, 1500 rpm). In the present study, the synthesis was directly performed in UV-vis cuvettes made of polystyrene with a 1 cm square based and a rectangular shape, de-dusted with a gentle flow of compressed air before being used. The magnets used for stirring are PTFE cylindrical stirrer bar (8 x 3 mm), cleaned with *aqua regia* (4:1, v:v, HCl:HNO_3; ***to be handled and disposed of with care following the related safety procedures in place in the laboratory***), washed with copious amount of water, and de-dusted prior to use.[2] The chemicals were added in the order water, additives, $HAuCl_4$ and finally $NaBH_4$, unless otherwise specified. This approach is described as the *direct* method (as opposed to the *inverse* or *reverse* method where the $HAuCl_4$ would be added last, detailed later, by analogy to the terminology used for citrate-mediated syntheses[12]). All solutions were prepared using ultrapure (mQ) water. The stock solutions were 20 mM of $HAuCl_4$, 50 mM of NaCt, 50 mM of PVP (diluted to 10 mM for experiment 128 to 138 in **Table S3**), 50 mM of SDS, 100 mM of freshly prepared $NaBH_4$. The stock solution of $HAuCl_4$ was kept in a fridge at 5 °C, whereas the stock solutions of NaCt, PVP and SDS were kept at room temperature (ca. 22 °C). $NaBH_4$ was added under stirring, and the solutions capped after adding $NaBH_4$ and left to stir at room temperature for ca. 10 minutes (although the reaction proceeds in seconds). Afterwards the magnets were removed and the samples sealed with Parafilm®. The samples were then stored at room temperature in drawers.

The concentrations of $HAuCl_4$ of 0.1-0.5 mM are commonly reported to lead to successful syntheses of Au NPs.[2,4,12] At higher concentrations, the NPs tend to agglomerate. The $NaBH_4$/Au molar ratio in the range 5-10 were selected because it was found to be optimal to allow size control while minimizing the amount of $NaBH_4$ to use and at lower values no stable Au NPs were obtained. The chemicals used were selected for reasons detailed in the scope of this study. An additive/Au molar ratio from 5 or above is typically reported in the literature and serve here as a starting point.[12]

Scale up syntheses of Au NPs

For scale up experiment to 1 L the synthesis was performed in a Pyrex container using a larger magnet and a rotation of 800 rpm. Both the container and the magnet were cleaned with *aqua regia* prior to the synthesis.

Miscellaneous

For transparency, we stress that the reaction were performed in a photo-box (Puluz LED portable Photo Studio, PU5060EU, 60 cm x 60 cm x 60 cm, 60 W) that we use for other syntheses in our research facilities to control light environment,[13,14] although we did not observe any aninfluence of the light environment on the $NaBH_4$-mediated synthesis.

To minimize the effect of using different batches of $NaBH_4$, several experiments were prepared the same day with the same batch. In order to assess the effect of the time required to prepare all the samples, the first sample was reproduced and no significant difference was observed which suggests that the stock solution of $NaBH_4$ was used before it undergoes significant hydrolysis.

Note that In the case were high concentrations of precursors (around 3-5 mM) are added, the increasing amount of $NaBH_4$ used leads to gas evolution (likely H_2) and there is a risk of spillover of the solutions for small size reactors.

2.3. Statements on Sustainable Chemistry

As much as possible we try to develop sustainable synthetic approaches of NPs compatible with *Green Chemistry* and *Sustainable practices in academic research*.[15-18] The present synthesis proceeds at room temperature due to the redox properties of the gold precursor (relatively high redox potential). It can be performed with minimal equipment and using relatively benign chemicals at the exception of $NaBH_4$. In some reports, $NaBH_4$ is kept under cold conditions[19,20] or NaOH is added to obtain alkaline pH in order to minimize hydrolysis.[21] Those two approaches require more energy (ice) or chemicals (NaOH) and where here avoided to prefer the simple use of as-prepared $NaBH_4$ solutions at room temperature. It is common to use gases for NP synthesis, e.g. to obtain oxygen-free environment.[4,13,22] In order to develop simpler and more affordable syntheses, the use of gases was here avoided. The use of disposable UV-vis cuvettes generates plastic waste but allows performing the synthesis in small volume which minimizes waste. Furthermore, it limits the use of *aqua regia* to only cleaning the magnets.[2] It also facilitates storage. The use of 0.5 mM $HAuCl_4$ is on the high end of concentrations for Au NPs synthesis[2] but is relevant to explore to minimize the volume of chemicals used upon scale up. The colloidal dispersions, and most stock solutions (see experimental sections) were stored at room temperature to save energy (that the use of

fridges would consume). The recycling of the Au atoms is a natural further step,[23] but beyond the scope of this study.

It is anticipated that the achievements reported here and the overall strategy to develop surfactant-free material could be transferred to the use of alternative reducing agents such as hydrazine.[24] However, due to the safety risks and health concerns related to the use of hydrazine, that is arguably a potentially more harmful chemical than $NaBH_4$, hydrazine has not been considered in the present report.

2.4. Characterization

A focus is here given to the properties retrieved from UV-vis measurements,[13] and scanning transmission electron microscopy (STEM) analysis, complemented by XRD. UV-vis spectra are informative when it comes to Au NP characteristics as detailed in **Table S1**. To develop more sustainable research,[15] it will also not be realistic to use all characterization methods reported for Au NPs.[25,26] Complementary characterization has been reported in previous work.[4,27,28]

2.4.1. UV-vis characterization

UV-vis measurements were performed using a Shimadzu UV-1800 UV/Visible scanning spectrophotometer. The solutions were measured as-prepared or diluted to an equivalent of 0.5 mM Au in the 1 cm width squared shape UV-vis cuvettes used for the synthesis. As baseline, mQ water was used since none of the chemicals considered absorb in the range of wavelengths considered.[29]

The UV-vis spectra of Au NPs is the results of an interplay between the properties of gold, nanoscale effects (e.g. size and shape) and interactions with the solvents and/or interactions between NPs and precursor.[30] Due to their plasmonic properties (surface plasmon resonance, spr), several parameters descriptive of the Au NPs can be retrieved: λ_{spr}, A_{spr}/A_{450}, A_{380}/A_{800}, A_{650}/A_{spr} and A_{400}, all defined, detailed and summarized in **Table S2**. All samples were measured the day after synthesis. For stability study, all the samples were also measured a month after synthesis while storage was simply performed at room temperature in a drawer.

2.4.2. STEM characterization

STEM micrographs were acquired using a A FEI Talos F200X operated at 200 kV STEM. The microscope is equipped with a high-angle annular dark-field (HAADF) detector and a bright field (BF) detector. The as-prepared colloidal dispersions were dropped on copper TEM grids (Sigma-Aldrich). The samples were characterized by imaging at least 3 randomly selected areas at 3 different magnifications. Typically, at least 100 NPs were used to estimate the size (diameter) of the NPs (N values reported below correspond to the number of NPs counted). The size analysis was performed using the ImageJ software. Data are provided in **Figure S8** and **Figure S9**.

2.4.3. XRD characterization

X-ray diffraction measurements were performed using a Panalytical Aeris diffractometer configured in Bragg-Brentano geometry and equipped with a PIXcel1D detector. The instrument employed Cu Kα radiation ($K\alpha_1$ = 1.54056 Å, $K\alpha_2$ = 1.54439 Å), operates at 40 kV and 15 mA. Diffraction patterns were recorded over a 2θ range of 20-90° with a total acquisition time of 600 min per sample.

For the measurement, colloidal Au NPs (0.5 mM) were drop-cast onto a silicone sample holder. Specifically, 1 mL of the colloid was applied and oven dried at 50 °C to remove solvent, followed by the addition of another 1 mL aliquot and drying under the same conditions. To eliminate possible salt or solvent residues, the dried film was rinsed by sprinkling ethanol and gently blown with compressed air several times until no visible residues remained.

Phase identification was carried out by comparing the recorded diffraction pattern with reference data for metallic gold from ICSD database, pattern no #52249.

The average crystallite size was estimated from the (111) reflection using the Scherrer equation:

$$D = \frac{K.\lambda}{\beta.\cos(\theta)}$$

Where D is the mean crystallite size (nm), K is the shape factor (0.94), λ is the X-ray wavelength (0.15418 nm), β is the full width at half maximum (FWHM) of the (111) peak (in radians), and θ is the corresponding Bragg angle. Peak position and FWHM values obtained in degrees were converted to radians prior to calculation. After this substitution,

$$D = \frac{0.94 \text{ x } 0.15418}{\left(\text{FWHM}\,\frac{\pi}{180}\right)\cos\left(\frac{\text{peak position x } \pi}{2 \text{ x } 180}\right)}$$

2.5. 4-nitrophenol reduction

The 4-NP reduction catalyzed by Au NPs and the data analysis was performed as previously reported.[31] In a nutshell, 1 mM 4-NP in mQ water, 100 mM $NaBH_4$ in mQ water (freshly prepared) and 0.5 mM as-prepared Au NPs (Au equivalent, prepared as detailed above) were used as stock solutions. All solutions were purged with nitrogen (99.9%), excluding Au NPs due to the small volume of solution used (5 µL), before the reaction to remove dissolved oxygen.[32] 2 mL with final concentrations of 0.05 mM 4-NP, 5 mM $NaBH_4$ ($NaBH_4$/4-NP molar ratio of 100) and 0.00125 mM of Au NPs (Au equivalent, Au/4-NP molar ratio of 2.5%) were used and the reaction carried at room temperature.

To comply with the principle of sustainability in the laboratory,[15] the volume of 4-NP was minimized and the kinetics studies performed in UV-vis cuvettes directly placed in a Go Direct® UV-vis spectrophotometer

with a fixed range from 220 nm to 850 nm, recorded in ca. 1-2 seconds. The background was a solution of mQ. Spectra were recorded every 40 seconds, with the first spectra 20 seconds after Au NPs were added. The reaction was magnetically stirred at 550 rpm and performed under LED light in a photo-box (Puluz LED portable Photo Studio, PU5060EU, 60 cm x 60 cm x 60 cm, 60 W). The cuvette was sealed with a cap after the addition of the reactants. The reaction was initiated by adding the Au NPs to the mixture of $NaBH_4$ and 4-NP.

The progress of the reaction was monitored following the time-related decrease of the characteristic absorption peak of the nitrophenolate anion at 400 nm.[33] A pseudo-first-order kinetics was assumed, given the large excess of $NaBH_4$, relative to 4-NP.[4] Data obtained from the UV-Vis measurements were used to fit the kinetic model and evaluate rate constants and turnover frequency.[34] It is assumed that the concentration of 4-NP in presence of $NaBH_4$ (i.e. 4-nitrophenolate) at a given time t, is given by $C_t=C_0e^{-k_{app}t}$, where C_0 is the initial concentration of 4-NP / 4-nitrophenolate at t = 0 s. Taking into account the Beer-Lambert's law, the relationship can be expressed as $A_t=A_0e^{-k_{app}t}$, where A_t is the absorbance at 400 nm at a given time and A_0 the absorbance at t = 0 s. Thus, $-\ln(A_t/A_0)=k_{app}.t$ should be a linear function of time.[34] The turnover frequency was estimated as:

$$\text{TOF} = \frac{\mathrm{n_0}\ (mol)}{\mathrm{n_{Au}}\ (mol)}\ \frac{\text{Conversion}\ (\%)/100}{\mathrm{t}\ (h)}$$

where n_0 is the initial amount of 4-NP in moles, where n_{Au} is the nominal amount of Au in moles, t is the time required to reach a given conversion estimated from UV-vis. For the interest of the reader, the TOF were also normalized to the absorbance at 400 nm (A_{400}) retrieved from UV-vis measurements of the Au colloidal dispersion given that the A_{400} value is proportional to the amount of Au^0 in the dispersion.[35]

2.6. Ethanol oxidation reaction (EOR)

The EOR is a reaction relevant for energy conversion in alcohol fuel cells.[36,37] The general procedure previously reported was followed.[38] In a nutshell, a three-electrode set up composed of a glassy carbon (GC) working electrode (WE) with a diameter of 5 mm (0.2 cm^2), a graphite rod (Thermo Scientific Chemicals, 6.15 mm x 152 mm, 15403735) counter electrode (CE), and a saturated calomel electrode (SCE, SI Analytics™ ScienceLine Glass Single Reference Electrode, Fisher Scientitic, 10542113) or a Hg/HgO (Origalys, OGR001), electrode as reference electrode (RE), as indicated, immerged in ca. 20 mL of electrolyte in a Pyrex container. The WE was prepared by dropping and letting dry overnight at room temperature 20 µL of the as-prepared dispersions of Au NPs (0.5 mM Au) on the GC surface (polished to mirror finish using aluminum polishing slurry, 0.30 and 0.05 µm alumina, eDAQ), making a 'tip' with 1.97 μg_{Au}, 9.85 $\mu g_{Au} cm^{-2}$. All the electrochemical experiments were conducted using a computer-controlled potentiostat (Eci-100, NordicElectrochemistry) at room temperature (ca. 22 °C). We previously observed that the reaction is not mass transport limited and therefore no rotation was used.[38,39] The electrolytes were not purged with N_2 or any other gases.[38,39] The voltage expressed versus the SCE (V_{SCE}) was converted to voltage versus the relative hydrogen electrode (V_{RHE}) using the relationship: $V_{RHE} = V_{SCE} + 0.26$ (in V) in

0.5 M H_2SO_4. The voltage expressed versus the Hg/HgO ($V_{Hg/HgO}$) electrode was converted to V_{RHE} by the relationship: $V_{RHE} = V_{Hg/HgO} + 0.87$ (in V) in 1 M KOH.

There are no commonly agreed on procedures to tests catalysts for the EOR and different scan rates, electrolytes, electrolyte concentrations, amounts of catalyst, upper and lower potentials are reported cross the literature,[38,39] see also **Table S4**, not to mention the different normalizations reported. Here, each sample was tested following the same protocol for at least three different tips of the same Au NPs obtained from the same synthesis conditions. The electrochemically active surface area (ECSA), the mass activity (MA) and the specific activity (SA, activity per active surface area) were evaluated. ECSA and MA were evaluated for cyclic voltamograms and the SA was evaluated as SA = MA/ECSA. In the case of samples prepared following Protocol A where no ECSA measurement was performed, the SA was evaluated using the average ECSA retrieved from protocol B.

Note that given that the same mass of gold and same geometrical surface of electrode was used for every experiment, the reported MAs are easily converted to geometric current density by multiplying the MA in A g_{Au}^{-1} or mA mg_{Au}^{-1} by 9.85×10^{-3} to obtain the geometric current density in mA cm^{-2}.

Protocol A – EOR without ECSA evaluation

- Step 1/1:

10 scans at 50 mV s^{-1} in 1 M KOH and 1 M ethanol between -0.50 and 0.70 $V_{Hg/HgO}$ (0.37–1.57 V_{RHE})

The related mass activity (evaluated at the maximum current recorded in the forward scan of the 10th scan) and specific acidity are abbreviated MA and SA.

Protocol B – EOR with ECSA evaluation

- Step 1/2:

3 scans at 50 mV s^{-1} in 0.5 M H_2SO_4 between 0.00 and 1.50 V_{SCE} (0.26–1.76 V_{RHE})

- Step 2/2:

10 scans at 50 mV s^{-1} in 1 M KOH and 1 M ethanol between -0.50 and 0.70 $V_{Hg/HgO}$ (0.37–1.57 V_{RHE})

Step (1) was performed to evaluate the electrochemically active surface area (ECSA) via the reduction of gold oxide, illustrated in **Figure S1**,[38] evaluated by the charge passed under the reduction peak of gold in H_2SO_4 around 1.17 V_{RHE} for the 3rd scan converted to an ECSA using the conversion factor of 386 µC cm^{-2}.[40] Step (2) is to evaluate the mass activity (MA), evaluated at the maximum current recorded in the forward scan of the 10th scan. To mark the difference between results obtained following protocol A or B, the mass activity and specific activity retrieved following protocol B are referred to as MA_{acid} and SA_{acid}.

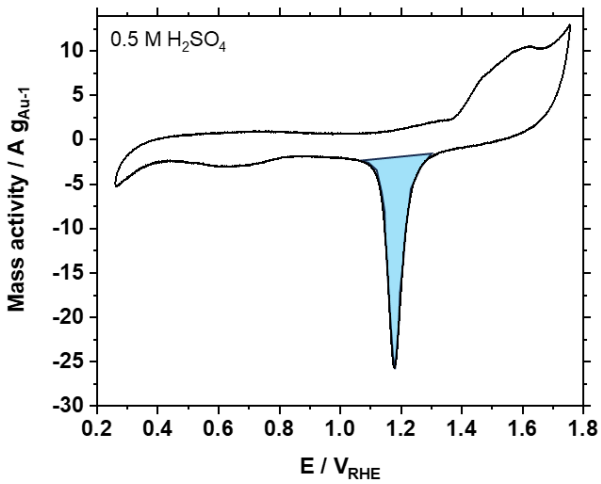

Figure S1. Illustrative CV of Au NPs in 0.5 M H_2SO_4 used to evaluate the ECSA, as detailed in Panagopoulos et al. *Materials Today Nano* 2025, 100600.[38] The charge passed on the reduction peak highlighted in blue was used.

Normalizations

Here, the conversion of Au^{III} to Au^0 is first assumed to be 100% for the synthesis and the MA and ECSA are first estimated using the nominal loading (*synthesis-to-catalysis*). To propose a relatively more accurate picture, the absorbance at 400 nm retrieved from UV–vis spectroscopy was also used to normalize the MA (MA_{A400}) and ECSA ($ECSA_{A400}$) in our previous work,[38] as A_{400} gives a relative indication of the conversion of Au^{III} to Au^0.[35] In the present study, the A_{400} values were close to each other and this normalization was not performed. Moreover, for the samples obtained using PVP, the validity of the A_{400} values relating to Au^0 can be questioned given that the samples do not show the typical plasmatic properties of larger Au NPs. to As detailed elsewhere,[38] the preference for a comparison based on the nominal amount of Au has multiple reasons. (i) To take into account the overall amount of Au used in the synthesis (cost-weighted activity, assuming the cost here will come from the amount of $HAuCl_4$ used, regardless of the overall yield). (ii) To minimize steps between Au NP synthesis and catalytic screening, no isolation / washing / processing of the NPs, or no supporting on conductive materials such as high surface area carbon, for a direct use of the as-produced colloids, alleviating here from possible support effects.

3. XRD characterization

Figure S2 shows XRD patterns for synthesized Au NPs in comparison to the reference data for metallic gold from ICSD database, pattern no #52249.

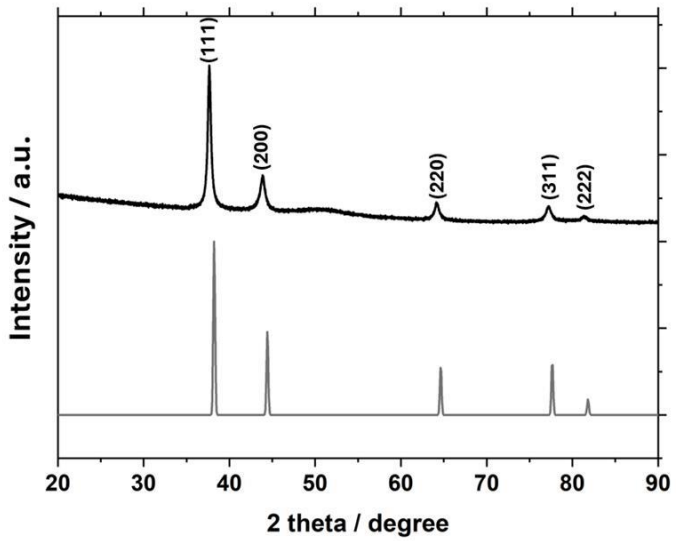

Figure S2. XRD pattern of Au NPs (black) in comparison to reference data for metallic gold from ICSD database, pattern no #52249 (grey). In this case, for Au NPs obtained using 0.5 mM $HAuCl_4$, a $NaBH_4$/Au molar ratio of 5 and 1 L of solution.

The average crystallite size was estimated from the (111) reflection and is 20.9 nm. This value is larger than the particle size measured by TEM (ADD SIZE), which is a common observation for very small nanoparticles. The discrepancy is caused because the Scherrer equation measures the size of coherently diffracting domains, which can be affected by multiple parameters, such as particle aggregation, strain and peak-fitting limitations, while TEM provides direct physical particle diameters. As seen in the XRD pattern, the (111) peak is only moderately broader than the bulk reference, indicating that Au NPs retain crystalline order. The observed diffraction peaks of Au NPs are slightly shifted to lower angles in comparison to reference pattern. This shift may be attributed to several factors, including slight instrumental misalignment of the diffractometer and possible strain within the drop-cast nanoparticle film induced during solvent evaporation.

4. UV-vis metrics

Table S2. Parameters retrieved from UV-vis spectroscopy. The relationships summarized typically assume spherical NPs within a given size range and are general (not absolute) trends. Keep in mind that the UV-vis spectra of Au NPs show features that depends on size, shapes but also the solvent / surrounding media.

Parameter	Definition	Interpretation in first approximation	Ref.
λ_{spr} nm	position of the localised surface plasmon resonance (spr)	λ_{spr} ↗ with NP sizes ↗	41
A_{spr}/A_{450} -	ratio of absorbances at λ_{spr} and 450 nm	A_{spr}/A_{450} ↗ with NP sizes ↗	41
A_{400} a.u.	absorbance at 400 nm (typically normalised)	A_{400} ↗ with relative yield ↗	35
A_{380}/A_{800} -	ratio of absorbances at 380 nm and 800 nm	A_{380}/A_{800} ↗ indicates higher stability	42
A_{650}/A_{spr} -	ratio of absorbances at 650 nm and λ_{spr}	A_{650}/A_{spr} ↗ indicates higher aggregation	43,44

a)

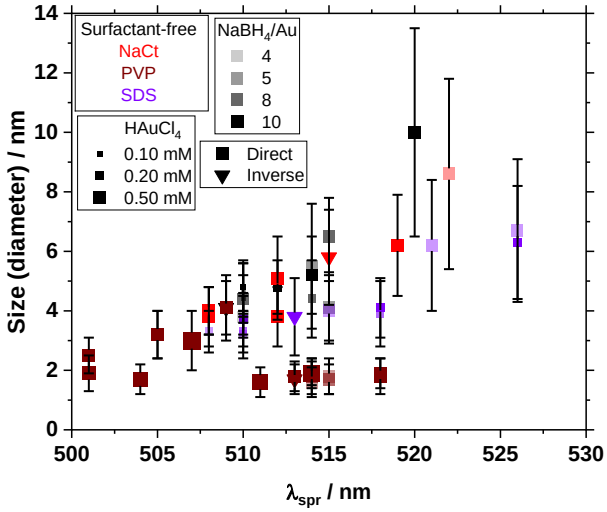

b)

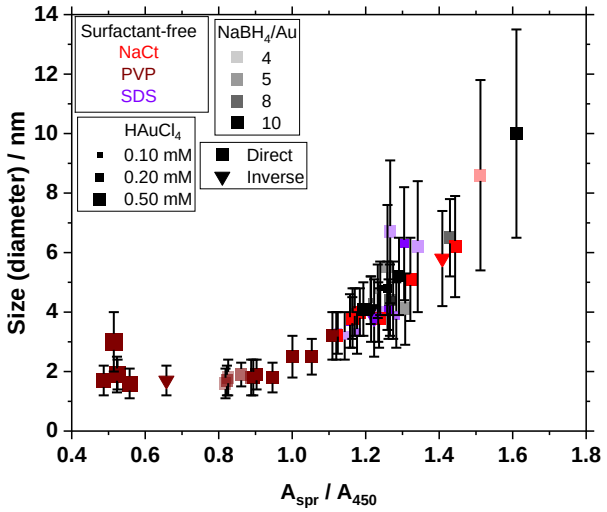

Figure S3. Relationship between Au NP size and (a) λ_{spr} and (b) A_{spr}/A_{450} values for $NaBH_4$-mediated NP synthesis using different additives (color coded, as indicated), different concentrations of $HAuCl_4$ (where the size of the data point increases with the concentration of $HAuCl_4$, for simplicity the single point data point obtained using 1, 2, 3, 4, 5 mM and PVP are not represented in the caption), different $NaBH_4$/Au molar ratios (where the transparence of the data point decreases as the $NaBH_4$/Au molar ratio increases, as indicated) and whether the direct or inverse method was used (where the (■) data point correspond to the direct method and the (▼) correspond to the inverse method, as indicated). For simplicity the Additive/Au molar ratio is not encoded here in the graphical representation but largely discussed in the manuscript and other Figures.

The results in **Figure S3** illustrate the expected correlated that the NP size (diameter for spherical NPs) increases as the λ_{spr} values increases or the A_{spr}/A_{450} value increases, in agreement with previous literature. Note that for the NPs prepared using PVP, it is harder to identify the spr due to the very small of the NPs (< 3 nm).

5. Overview of samples for parametric study

Table S3. Overview of the samples considered and related UV-vis metrics. The stock solutions of $HAuCl_4$ was 20 mM, NaCt was 50 mM, PVP was 50 mM, SDS was 50 mM, all prepared in mQ water. The colored cells indicate cell where the same overall concentration of $NaBH_4$ was used (0.5, 1.0. 2.0. 2.5 mM) for different $HAuCl_4$ concentrations when the same color is used. The experiment number in parenthesis correspond to experiments with the same chemicals and chemical concentrations.

#	$HAuCl_4$ mM	$NaBH_4$/Au	NaCt/Au	PVP/Au	SDS/Au	Last	Batch $NaBH_4$	λ_{spr} nm	A_{450}/A_{spr} -	A_{400}	A_{380}/A_{800} -	A_{650}/A_{spr} -	d nm	σ nm	N
1 (96)	0.1	5	-	-	-	$NaBH_4$	1	510	1.23	0.24	23.16	0.12	4.7	0.9	157
2	0.1	5	5	-	-	$NaBH_4$	1	518	1.28	0.24	19.15	0.12	-	-	-
3	0.1	5	10	-	-	$NaBH_4$	1	515	1.19	0.24	22.21	0.14	-	-	-
4	0.1	5	15	-	-	$NaBH_4$	1	518	1.27	0.24	19.01	0.13	-	-	-
5	0.1	5	-	5	-	$NaBH_4$	1	512	0.90	0.30	16.95	0.24	-	-	-
6	0.1	5	-	10	-	$NaBH_4$	1	512	0.93	0.29	17.99	0.22	-	-	-
7	0.1	5	-	15	-	$NaBH_4$	1	512	0.91	0.29	17.71	0.23	-	-	-
8	0.1	5	-	-	5	$NaBH_4$	1	510	1.15	0.24	27.99	0.13	-	-	-
9	0.1	5	-	-	10	$NaBH_4$	1	510	1.15	0.25	21.69	0.14	-	-	-
10	0.1	5	-	-	15	$NaBH_4$	1	515	1.24	0.25	29.55	0.12	-	-	-
11	0.1	8	-	-	-	$NaBH_4$	1	510	1.21	0.24	14.58	0.14	4.4	0.8	173
12	0.1	8	5	-	-	$NaBH_4$	1	510	1.19	0.23	25.16	0.12	-	-	-
13	0.1	8	10	-	-	$NaBH_4$	1	514	1.19	0.24	21.69	0.14	-	-	-
14	0.1	8	15	-	-	$NaBH_4$	1	518	1.22	0.24	26.86	0.13	-	-	-
15	0.1	8	-	5	-	$NaBH_4$	1	500	0.89	0.30	18.66	0.23	-	-	-
16	0.1	8	-	10	-	$NaBH_4$	1	504	0.86	0.30	17.14	0.25	-	-	-
17	0.1	8	-	15	-	$NaBH_4$	1	503	0.85	0.30	17.09	0.25	-	-	-
18	0.1	8	-	-	5	$NaBH_4$	1	508	1.15	0.24	20.85	0.14	-	-	-
19	0.1	8	-	-	10	$NaBH_4$	1	507	1.13	0.24	18.66	0.16	-	-	-
20	0.1	8	-	-	15	$NaBH_4$	1	510	1.13	0.25	14.10	0.18	-	-	-
21	0.1	10	-	-	-	$NaBH_4$	1	510	1.24	0.23	19.18	0.12	4.8	0.9	154
22	0.1	10	5	-	-	$NaBH_4$	1	510	1.17	0.24	25.72	0.13	-	-	-
23	0.1	10	10	-	-	$NaBH_4$	1	509	1.17	0.24	22.27	0.14	-	-	-
24	0.1	10	15	-	-	$NaBH_4$	1	514	1.20	0.23	22.07	0.13	-	-	-
25	0.1	10	-	5	-	$NaBH_4$	1	504	0.85	0.30	19.69	0.24	-	-	-
26	0.1	10	-	10	-	$NaBH_4$	1	504	0.86	0.30	17.16	0.25	-	-	-
27	0.1	10	-	15	-	$NaBH_4$	1	504	0.87	0.30	17.84	0.24	-	-	-
28	0.1	10	-	-	5	$NaBH_4$	1	509	1.16	0.24	20.55	0.14	-	-	-
29	0.1	10	-	-	10	$NaBH_4$	1	505	1.13	0.24	22.69	0.15	-	-	-
30	0.1	10	-	-	15	$NaBH_4$	1	518	1.22	0.25	17.16	0.16	-	-	-

31	0.2	5	-	-	-	$NaBH_4$	1	508	1.17	0.45	22.94	0.13	4.0	0.8	158
32	0.2	5	5	-	-	$NaBH_4$	1	510	1.18	0.46	27.07	0.13	-	-	-
33	0.2	5	10	-	-	$NaBH_4$	1	514	1.24	0.47	23.18	0.12	-	-	-
34	0.2	5	15	-	-	$NaBH_4$	1	514	1.31	0.46	35.64	0.10	-	-	-
35	0.2	5	-	5	-	$NaBH_4$	1	501	0.87	0.56	16.65	0.26	-	-	-
36	0.2	5	-	10	-	$NaBH_4$	1	511	0.86	0.57	16.36	0.26	-	-	-
37	0.2	5	-	15	-	$NaBH_4$	1	511	0.85	0.56	17.63	0.26	-	-	-
38	0.2	5	-	-	5	$NaBH_4$	1	507	1.13	0.47	24.93	0.14	-	-	-
39	0.2	5	-	-	10	$NaBH_4$	1	508	1.12	0.47	23.90	0.15	3.3	0.7	160
40	0.2	5	-	-	15	$NaBH_4$	1	510	1.14	0.49	18.20	0.17	3.2	0.8	170
41	0.2	8	-	-	-	$NaBH_4$	1	514	1.27	0.45	19.53	0.12	4.4	1.3	172
42	0.2	8	5	-	-	$NaBH_4$	1	514	1.23	0.47	28.81	0.12	-	-	-
43	0.2	8	10	-	-	$NaBH_4$	1	514	1.29	0.46	29.35	0.11	-	-	-
44	0.2	8	15	-	-	$NaBH_4$	1	520	1.43	0.46	23.85	0.12	-	-	-
45	0.2	8	-	5	-	$NaBH_4$	1	501	0.86	0.57	17.76	0.25	-	-	-
46	0.2	8	-	10	-	$NaBH_4$	1	501	0.82	0.58	17.65	0.26	-	-	-
47	0.2	8	-	15	-	$NaBH_4$	1	501	0.83	0.57	17.69	0.26	-	-	-
48	0.2	8	-	-	5	$NaBH_4$	1	508	1.14	0.47	26.03	0.14	-	-	-
49	0.2	8	-	-	10	$NaBH_4$	1	510	1.18	0.48	24.72	0.15	3.3	0.7	156
50	0.2	8	-	-	15	$NaBH_4$	1	518	1.28	0.50	18.13	0.18	3.9	1.1	164
51	0.2	10	-	-	-	$NaBH_4$	1	512	1.26	0.46	25.91	0.12	4.8	0.9	158
52	0.2	10	5	-	-	$NaBH_4$	1	518	1.31	0.46	26.02	0.11	-	-	-
53	0.2	10	10	-	-	$NaBH_4$	1	518	1.43	0.46	21.63	0.12	-	-	-
54	0.2	10	15	-	-	$NaBH_4$	1	522	1.33	0.46	2.18	0.52	-	-	-
55	0.2	10	-	5	-	$NaBH_4$	1	501	0.85	0.58	17.60	0.25	-	-	-
56	0.2	10	-	10	-	$NaBH_4$	1	501	0.83	0.58	17.25	0.26	-	-	-
57	0.2	10	-	15	-	$NaBH_4$	1	501	0.84	0.58	17.98	0.26	-	-	-
58	0.2	10	-	-	5	$NaBH_4$	1	510	1.16	0.47	23.49	0.14	3.7	0.9	175
59	0.2	10	-	-	10	$NaBH_4$	1	518	1.26	0.48	23.60	0.14	4.1	1	157
60	0.2	10	-	-	15		1	526	1.30	0.50	5.57	0.35	6.3	1.9	198
61 (97)	0.50	5	-	-	-	$NaBH_4$	1	515	1.31	1.09	17.83	0.13	4.1	1.2	155
62	0.50	5	5	-	-	$NaBH_4$	1	522	1.51	1.12	10.84	0.17	8.6	3.2	161
63	0.50	5	10	-	-	$NaBH_4$	1	775	1.29	0.14	0.90	0.89	-	-	-
64	0.50	5	15	-	-	$NaBH_4$	1	795	1.52	0.01	0.96	0.69	-	-	-
65	0.50	5	-	5	-	$NaBH_4$	1	515	0.83	1.38	17.02	0.27	1.8	0.6	158
66	0.50	5	-	10	-	$NaBH_4$	1	514	0.81	1.37	17.02	0.27	-	-	-
67	0.50	5	-	15	-	$NaBH_4$	1	514	0.82	1.36	16.93	0.27	1.6	0.5	163
68	0.50	5	-	-	5	$NaBH_4$	1	515	1.23	1.18	25.82	0.13	4.0	1.0	164
69	0.50	5	-	-	10	$NaBH_4$	1	521	1.34	1.24	9.88	0.27	6.2	2.2	158
70	0.50	5	-	-	15	$NaBH_4$	1	526	1.27	1.25	2.39	0.57	6.7	2.4	156

71	0.50	8	-	-	-	$NaBH_4$	1	515	1.43	1.09	30.87	0.09	6.5	1.3	164
72	0.50	8	5	-	-	$NaBH_4$	1	800	1.17	0.81	0.96	0.96	-	-	-
73	0.50	8	10	-	-	$NaBH_4$	1	748	1.47	0.01	0.93	0.72	-	-	-
74	0.50	8	15	-	-	$NaBH_4$	1	787	1.82	0.00	0.87	0.27	-	-	-
75	0.50	8	-	5	-	$NaBH_4$	1	514	0.89	1.40	17.73	0.25	1.8	0.6	165
76	0.50	8	-	10	-	$NaBH_4$	1	514	0.86	1.39	17.17	0.26	1.9	0.4	161
77	0.50	8	-	15	-	$NaBH_4$	1	515	0.82	1.39	17.57	0.27	1.7	0.5	161
78	0.50	8	-	-	5	$NaBH_4$	1	525	1.32	1.19	2.61	0.52	-	-	-
79	0.50	8	-	-	10	$NaBH_4$	1	514	1.06	1.16	1.28	0.81	-	-	-
80	0.50	8	-	-	15	$NaBH_4$	1	514	1.02	1.14	1.24	0.85	-	-	-
81	0.50	10	-	-	-	$NaBH_4$	1	520	1.61	1.11	28.06	0.08	10.0	3.5	160
82	0.50	10	5	-	-	$NaBH_4$	1	529	1.08	0.05	1.10	0.85	-	-	-
83	0.50	10	10	-	-	$NaBH_4$	1	783	1.70	0.01	0.89	0.44	-	-	-
84	0.50	10	15	-	-	$NaBH_4$	1	784	2.75	0.00	0.41	0.46	-	-	-
85	0.50	10	-	5	-	$NaBH_4$	1	513	0.95	1.40	15.38	0.27	1.8	0.5	165
86	0.50	10	-	10	-	$NaBH_4$	1	518	0.89	1.40	17.62	0.26	1.8	0.6	171
87	0.50	10	-	15	-	$NaBH_4$	1	518	0.90	1.39	16.52	0.27	1.9	0.5	160
88	0.50	10	-	-	5	$NaBH_4$	1	518	1.11	1.16	1.32	0.78	-	-	-
89	0.50	10	-	-	10	$NaBH_4$	1	510	1.02	0.77	1.19	0.88	-	-	-
90	0.50	10	-	-	15	$NaBH_4$	1	514	1.03	0.33	1.17	0.88	-	-	-
91	0.25	5	-	-	-	$NaBH_4$	1	514	1.26	0.57	24.81	0.11	5.5	2.1	153
92	0.25	8	-	-	-	$NaBH_4$	1	510	1.27	0.57	29.92	0.10	4.4	1.2	161
93	0.25	10	-	-	-	$NaBH_4$	1	514	1.29	0.57	30.91	0.10	5.2	1.3	167
94	0.25	4	-	-	-	$NaBH_4$	1	510	1.16	0.56	26.91	0.15	3.8	0.7	207
95	0.5	2	-	-	-	$NaBH_4$	1	535	1.79	0.72	7.16	0.30	50	-	30
96 (1)	0.1	5	-	-	-	$NaBH_4$	1	510	1.24	0.23	26.83	0.11	-	-	-
97 (61)	0.5	5	-	-	-	$NaBH_4$	2	508	1.18	1.11	28.96	0.12	4.0	0.8	195
98	0.5	5	1	-	-	$NaBH_4$	2	505	1.12	1.12	27.89	0.14	3.2	0.8	157
99	0.5	5	2	-	-	$NaBH_4$	2	508	1.16	1.13	27.76	0.13	3.8	1	163
100	0.5	5	3	-	-	$NaBH_4$	2	512	1.24	1.13	33.13	0.11	3.8	1	166
101	0.5	5	4	-	-	$NaBH_4$	2	512	1.32	1.11	31.87	0.10	5.1	1.4	167
102	0.5	5	5	-	-	$NaBH_4$	2	519	1.44	1.12	29.63	0.10	6.2	1.7	177
103	1	5	-	5	-	$NaBH_4$	2	501	0.52	1.33	17.82	0.42	1.9	0.6	169
104	2	5	-	5	-	$NaBH_4$	2	504	0.49	1.32	12.67	0.52	1.7	0.5	178
105	3	5	-	5	-	$NaBH_4$	2	511	0.56	1.27	3.37	0.88	1.6	0.5	155
106	4	5	-	5	-	$NaBH_4$	2	514	0.52	1.13	2.48	1.04	1.9	0.5	159
107	5	5	-	5	-	$NaBH_4$	2	507	0.51	0.57	10.60	0.47	3.0	1.0	121
108	0.5	5	-	-	-	$HAuCl_4$	2	509	1.21	1.10	27.13	0.12	4.1	1.1	192
109	0.5	5	5	-	-	$HAuCl_4$	2	515	1.41	1.33	38.41	0.08	5.8	1.6	151
110	0.5	5	-	5	-	$HAuCl_4$	2	513	0.66	1.16	19.23	0.30	1.7	0.5	154
111	0.5	5	-	-	5	$HAuCl_4$	2	513	1.22	1.04	26.60	0.13	3.8	1.3	163

117	0.5	5	-	0.0	-	$NaBH_4$	3	508	1.17	1.11	30.47	0.13	-	-	-
118	0.5	5	-	0.5	-	$NaBH_4$	3	X	X	1.35	18.84	X	-	-	-
119	0.5	5	-	1.0	-	$NaBH_4$	3	X	X	1.35	18.07	X	1.7	0.6	176
120	0.5	5	-	1.5	-	$NaBH_4$	3	X	X	1.35	17.48	X	-	-	-
121	0.5	5	-	2.0	-	$NaBH_4$	3	X	X	1.35	17.11	X	1.7	0.6	158
122	0.5	5	-	2.5	-	$NaBH_4$	3	X	X	1.34	17.63	X	-	-	-
123	0.5	5	-	3.0	-	$NaBH_4$	3	X	X	1.34	17.54	X	-	-	-
124	0.5	5	-	3.5	-	$NaBH_4$	3	X	X	1.32	17.95	X	-	-	-
125	0.5	5	-	4.0	-	$NaBH_4$	3	X	X	1.34	16.68	X	-	-	-
126	0.5	5	-	4.5	-	$NaBH_4$	3	X	X	1.34	17.46	X	-	-	-
127	0.5	5	-	5.0	-	$NaBH_4$	3	X	X	1.34	17.48	X	2.0	0.4	182
128	0.5	5	-	0.0	-	$NaBH_4$	4	509	1.19	1.10	29.69	0.12	4.1	0.9	173
129	0.5	5	-	0.1	-	$NaBH_4$	4	505	1.11	1.21	26.10	0.15	3.2	0.8	165
130	0.5	5	-	0.2	-	$NaBH_4$	4	501	1.05	1.30	21.41	0.17	2.5	0.6	168
131	0.5	5	-	0.3	-	$NaBH_4$	4	485	1.00	1.34	20.71	0.19	2.5	0.7	162
132	0.5	5	-	0.4	-	$NaBH_4$	4	X	X	1.36	17.25	X	-	-	-
133	0.5	5	-	0.5	-	$NaBH_4$	4	X	X	1.38	19.06	X	2.1	0.7	165
134	0.5	5	-	0.6	-	$NaBH_4$	4	X	X	1.36	18.18	X	-	-	-
135	0.5	5	-	0.7	-	$NaBH_4$	4	X	X	1.38	18.65	X	-	-	-
136	0.5	5	-	0.8	-	$NaBH_4$	4	X	X	1.38	18.49	X	-	-	-
137	0.5	5	-	0.9	-	$NaBH_4$	4	X	X	1.37	17.72	X	-	-	-
138	0.5	5	-	1.0	-	$NaBH_4$	4	X	X	1.38	14.91	X	-	-	-

A ‘X’ indicates that the spr is challenging to identify, typically observed for samples prepared with PVP, as detailed in examples of UV-vis spectra provided below. A ‘-‘ indicates that the corresponding TEM grid was not prepared and therefore the data are not available. The number in parenthesis in the column # correspond to experiments number to be compared to due to identical experimental conditions (equivalent to repeats).

6. UV-vis characterization

Below, the results in **Figure S4** illustrate mainly the effect of using increasing amount of $NaBH_4$/Au molar ratio, leading to UV-vis spectra with higher λ_{spr} values and/of higher A_{spr}/A_{450} values, that correlate to larger NPs.

The results **Figure S5** illustrate mainly the effect of using different Additives (or not any).

The results in **Figure S6** illustrate mainly the effect of using increasing amount of Additive/Au molar ratio, leading to UV-vis spectra with higher λ_{spr} values and/or higher A_{spr}/A_{450} values, that correlate to larger NPs and/or unstable colloidal (characterized by low absorption and no clear spr features).

The difference in the results in **Figure S7** between different batches are attributed to different batches of $NaBH_4$ needed to be prepared fresh. The effect of the inverse addition was compared with at least one experiment using the same batch of $NaBH_4$ used to prepare the Au NPs by the direct method. For the range of chemical concentrations and ratio used here, using the direct or inverse method does not have a strong influence on the results. The cases where the order of addition of the chemicals might have the strongest effect is when PVP or NaCt are used. In the case of PVP using the inverse method tend to lead to slightly larger NPs. For NaCt, the inverse effect is observed, in line with the benefits of the inverse method largely documented for various citrate-mediated syntheses, although not necessarily induced by using $NaBH_4$. While it can be challenging to rational those observations at this stage this is likely due to different $HAuCl_4$-Additive-$NaBH_4$ interactions.

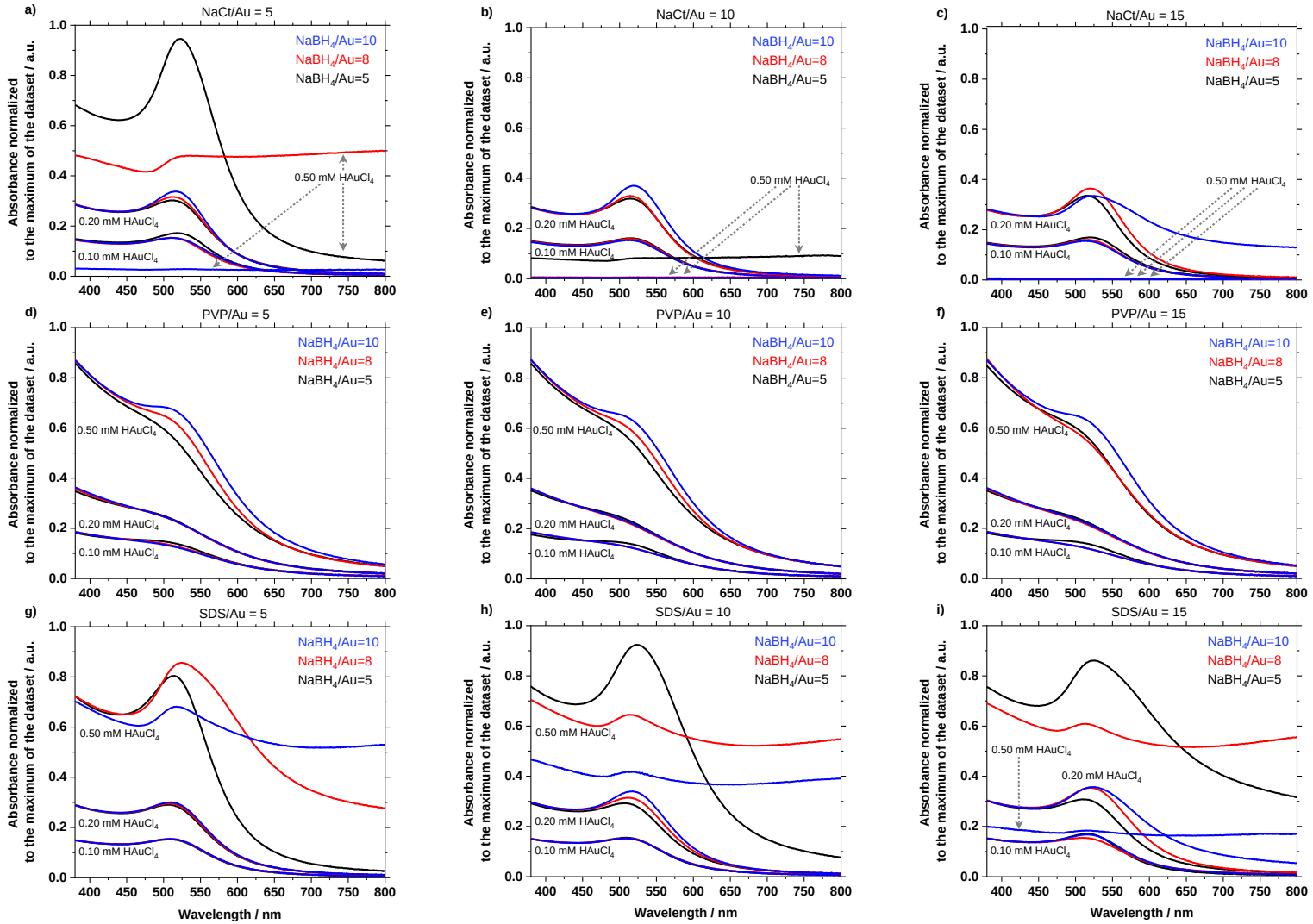

Figure S4. UV-vis spectra for Au NPs obtained using different $HAuCl_4$ concentrations, different $NaBH_4$/Au molar ratio and different additives with different Additive/Au molar ratio, as indicated. (a-c) NaCt, (d-f) PVP, (g-i) SDS, (a, d, g) Additive/Au molar ratio of 5, (b, e, h) Additive/Au molar ratio of 10, (c, f, i) Additive/Au molar ratio of 15. The normalization was performed to the maximum of the overall dataset (including surfactant-free Au NPs not reported here).

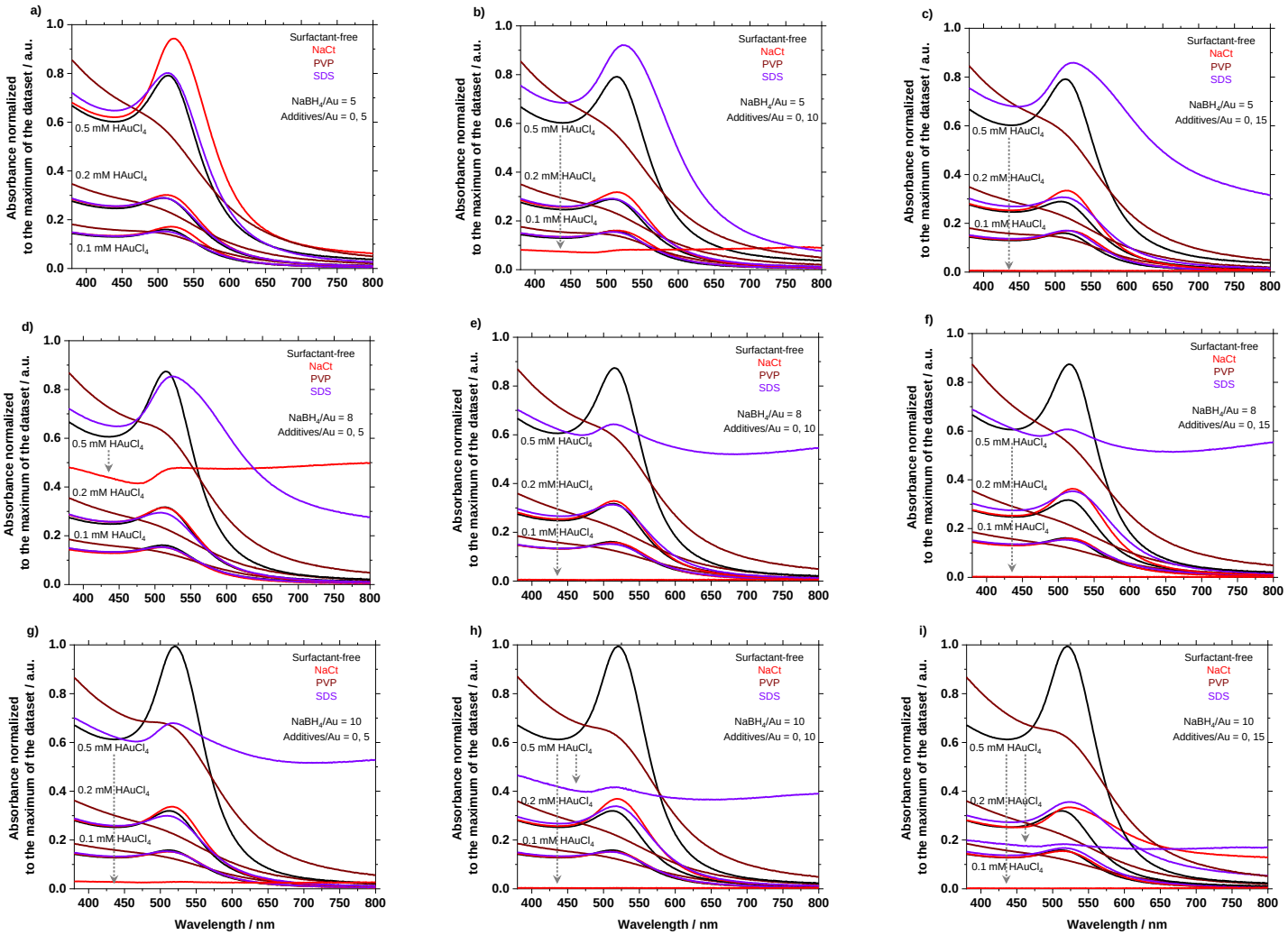

Figure S5. UV-vis spectra for Au NPs obtained using different $HAuCl_4$ concentrations, different $NaBH_4$/Au molar ratio and different additives with different Additive/Au molar ratio, as indicated. (a-c) $NaBH_4$/Au molar ratio of 5, (d-f) $NaBH_4$/Au molar ratio of 8, (g-i) $NaBH_4$/Au molar ratio of 11, (a, d, g) Additive/Au molar ratio of 5, (b, e, h) Additive/Au molar ratio of 10, (c, f,i) Additive/Au molar ratio of 15. The normalization was performed to the maximum of the overall dataset. Panel (a) is the same as **Figure 2b** in the main manuscript, reproduced here to ease the comparison.

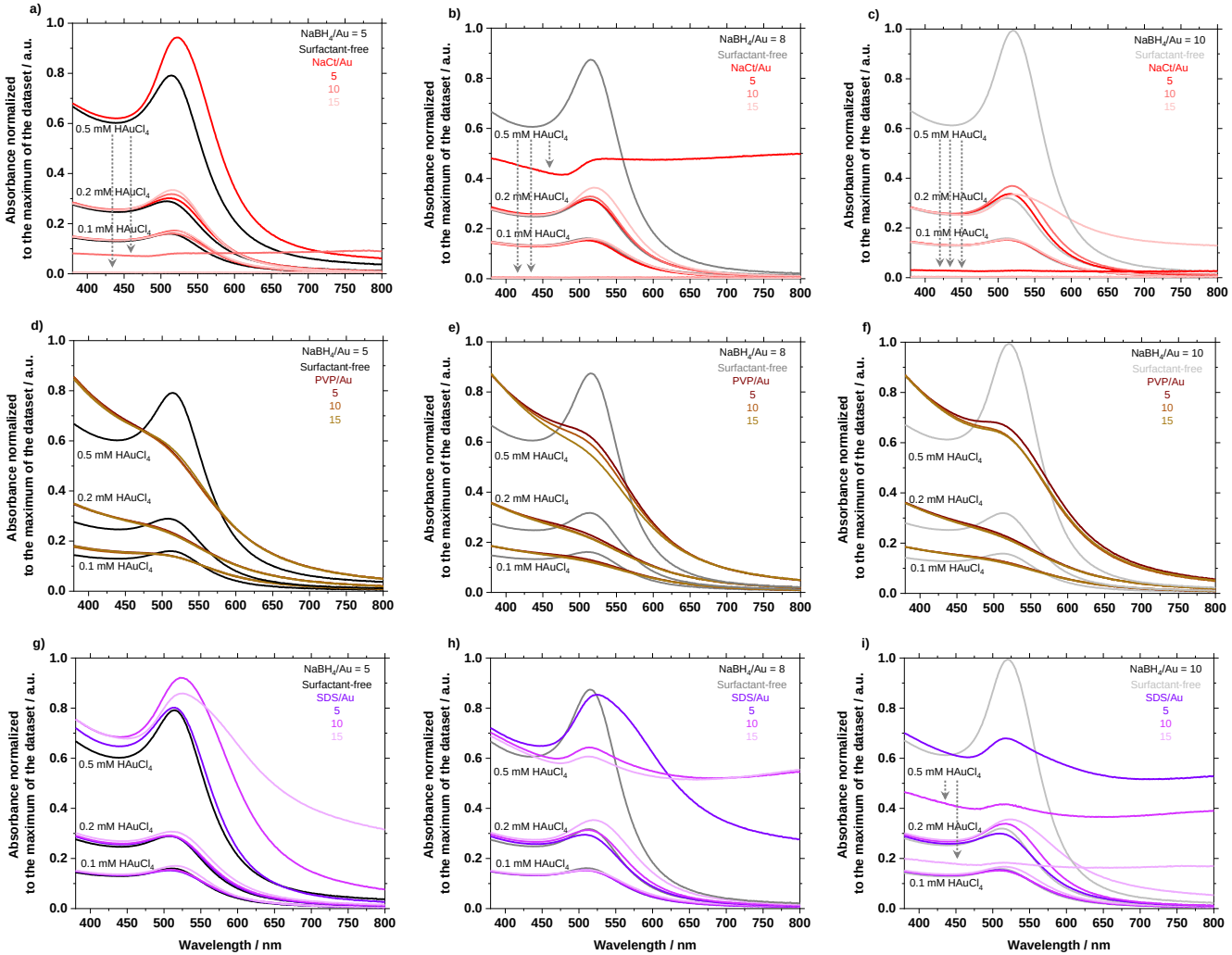

Figure S6. UV-vis spectra for Au NPs obtained using different $HAuCl_4$ concentrations, different $NaBH_4$/Au molar ratio and different additives with different Additive/Au molar ratio, as indicated. (a-c) NaCt, (d-f) PVP, (g-i) SDS, (a, d, g) NaH_4/Au molar ratio of 5, (b, e, h) NaH_4/Au molar ratio of 8, (c, f,i) NaH_4/Au molar ratio of 10. The normalization was performed to the maximum of the overall dataset. Panel (a) is the same as in **Figure 2c** in the main manuscript, reproduced here to ease the comparison.

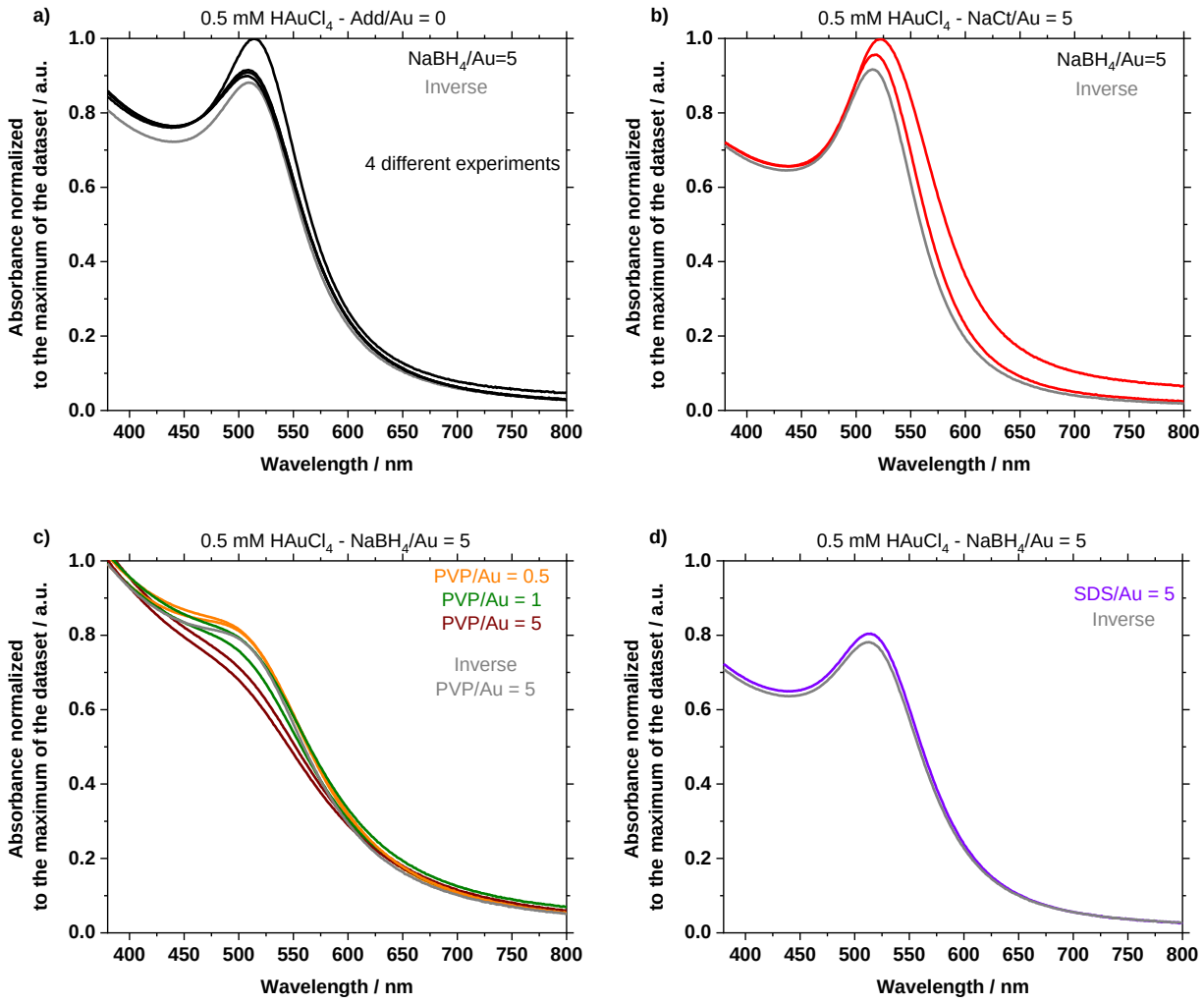

Figure S7. UV-vis spectra for Au NPs obtained using different $HAuCl_4$ concentrations, different $NaBH_4$/Au molar ratio and different additives with different Additive/Au molar ratio, as indicated. A focus is on reproduced results and/or the effect of the order of addition of the chemicals, for (a) surfactant-free synthesis, (b) syntheses using NaCt, (c) syntheses using PVP, and (d) for syntheses using SDS. (a-c) focus on reproducibility and the effect of the order of addition of the chemicals and (d) on the effect of the order of addition of the chemicals only. In (a) 4 different experiments for the *direct* method (adding $NaBH_4$ last) are reported. In grey are the results obtained for the *inverse* method (adding $HAuCl_4$ last).

7. STEM characterization

Note: The numbers used below in **Figure S8**-**S9** correspond to the entry in **Table S3**.

7.1. Direct method

See data on next page.

1) 0.1 mM $HAuCl_4$ – $NaBH_4$/Au = 5 – Additive/Au = 0

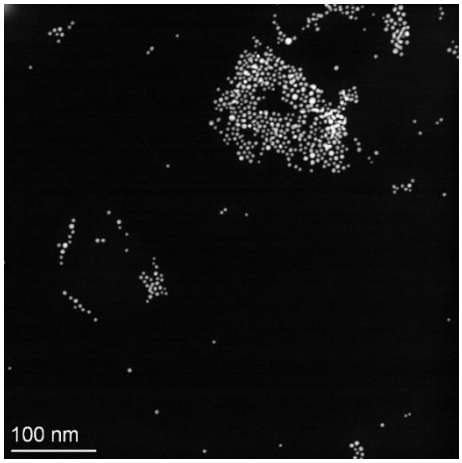

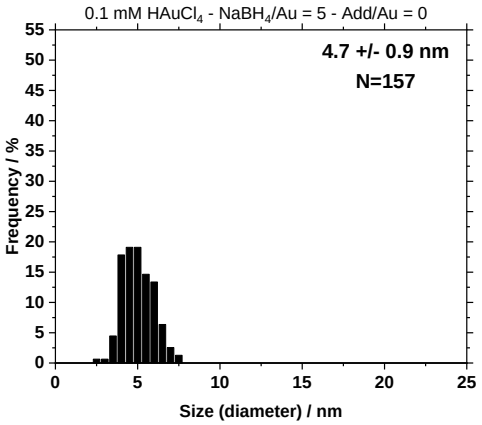

11) 0.1 mM $HAuCl_4$ – $NaBH_4$/Au = 8 – Add/Au = 0

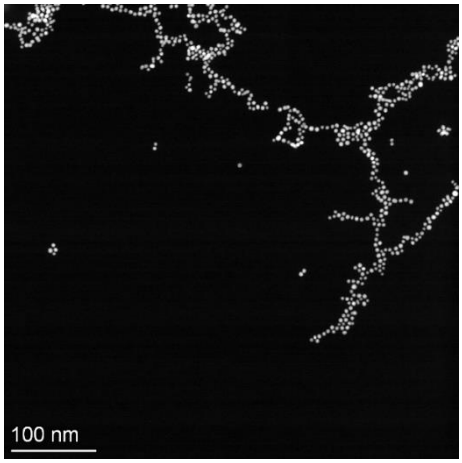

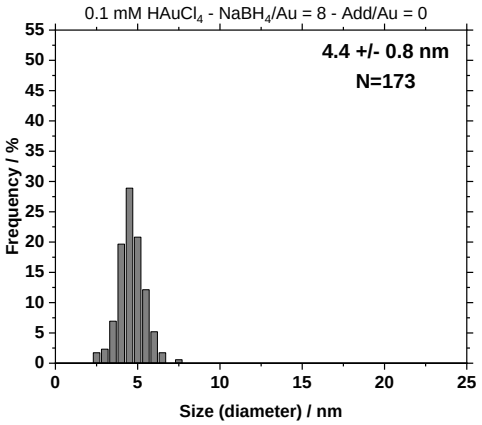

21) 0.1 mM $HAuCl_4$ – $NaBH_4$/Au = 11 – Add/Au = 0

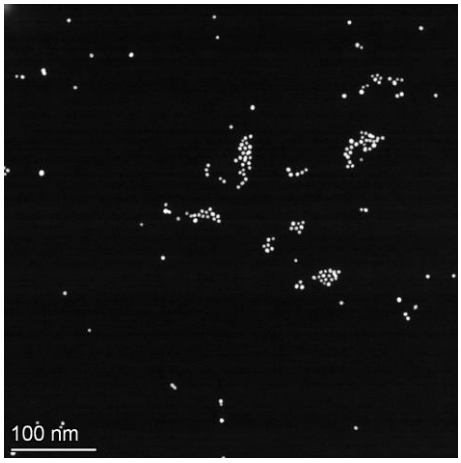

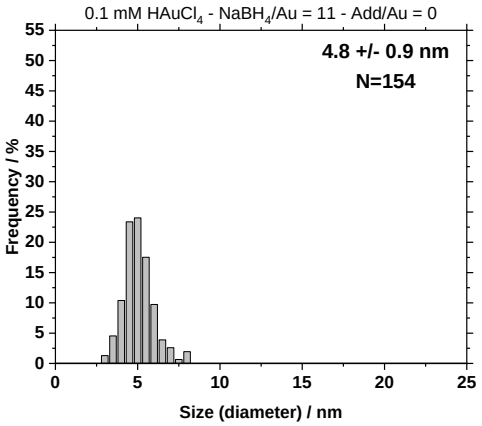

31) 0.2 mM $HAuCl_4$ – $NaBH_4$/Au = 5 – Add/Au = 0

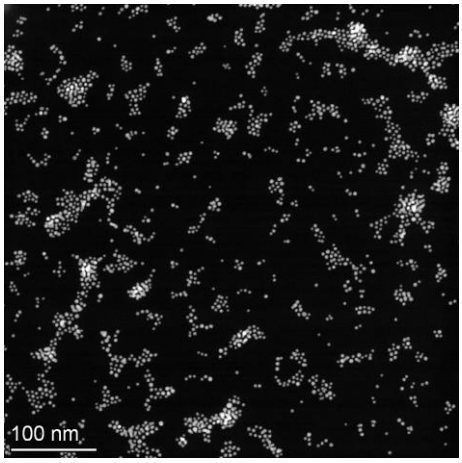

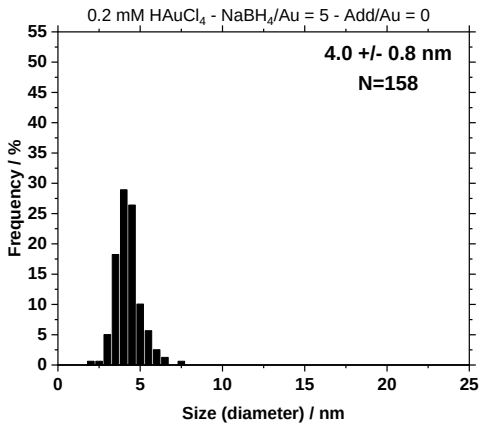

41) 0.2 mM $HAuCl_4$ – $NaBH_4$/Au = 8 – Add/Au = 0

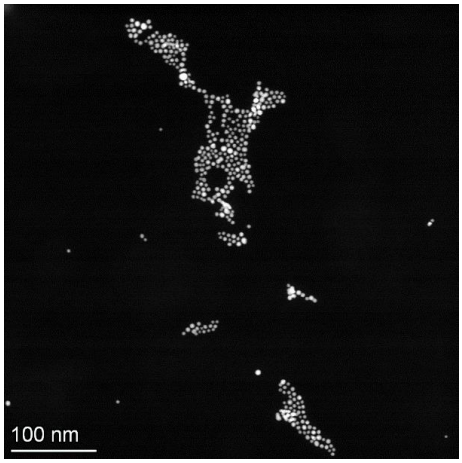

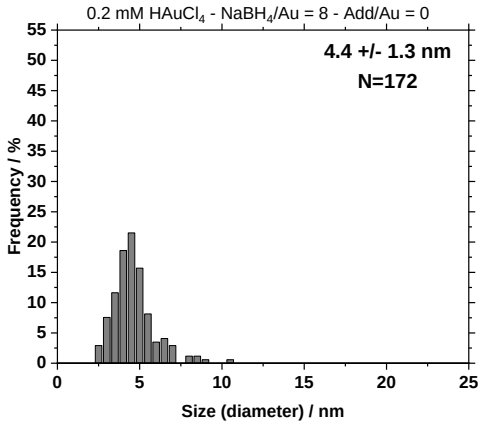

51) 0.2 mM $HAuCl_4$ – $NaBH_4$/Au = 11 – Add/Au = 0

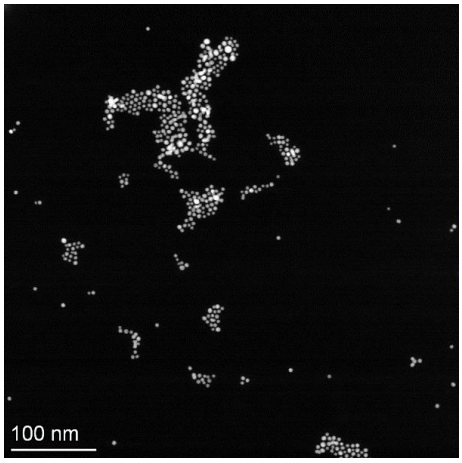

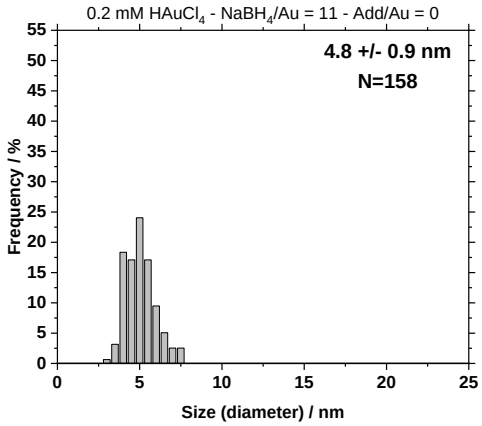

61) 0.5 mM $HAuCl_4$ – $NaBH_4$/Au = 5 – Add/Au = 0

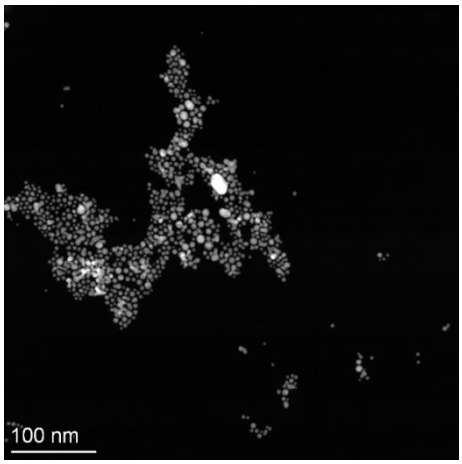

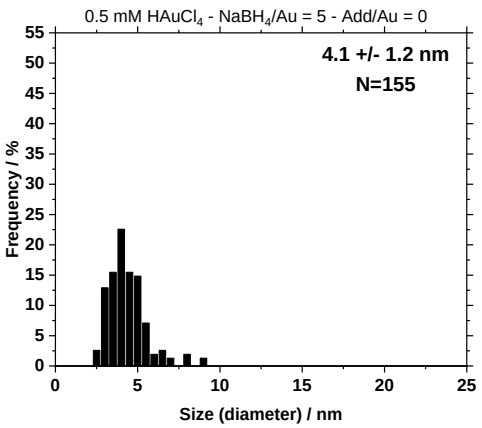

71) 0.5 mM $HAuCl_4$ – $NaBH_4$/Au = 8 – Add/Au = 0

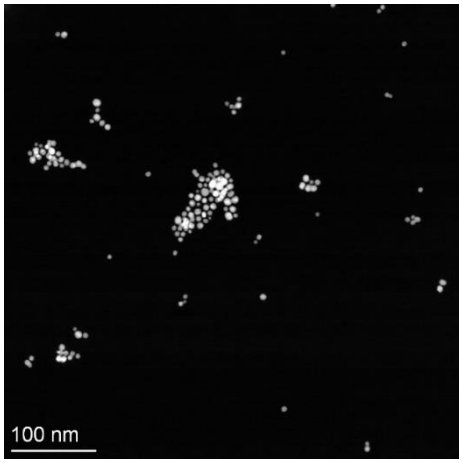

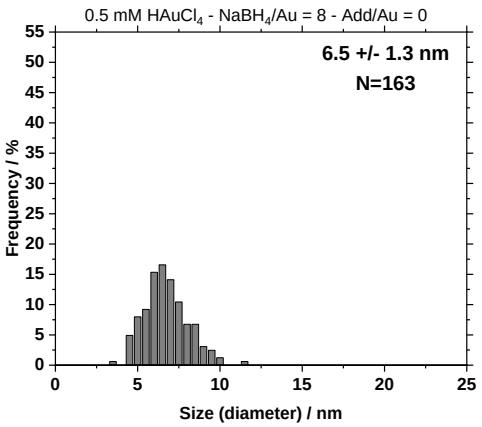

81) 0.5 mM $HAuCl_4$ – $NaBH_4$/Au = 11 – Add/Au = 0

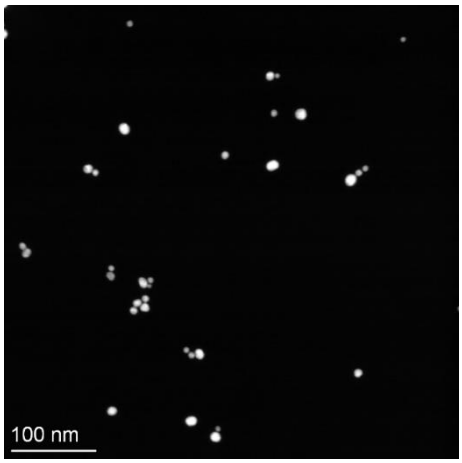

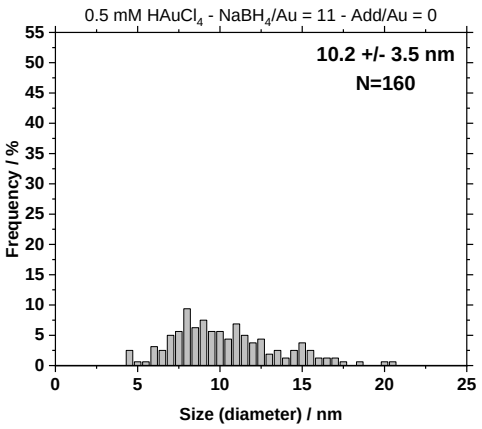

91) 0.25 mM $HAuCl_4$ – $NaBH_4$/Au = 5 – Add/Au = 0

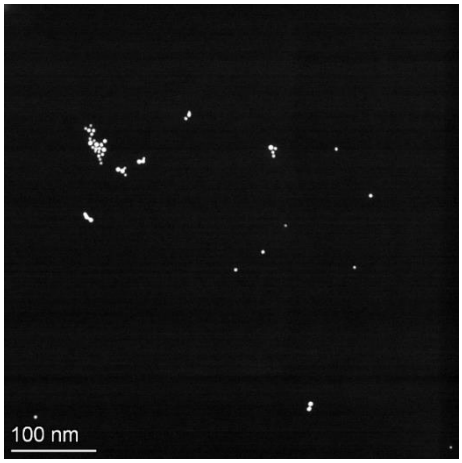

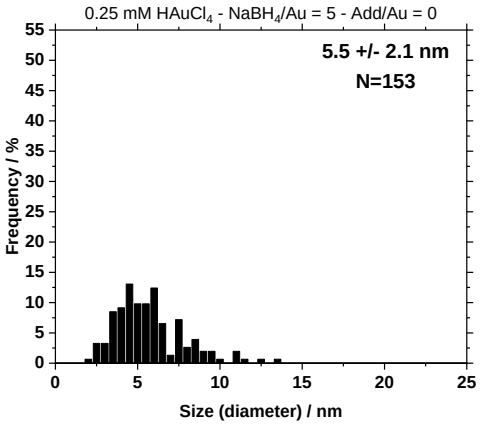

92) 0.25 mM $HAuCl_4$ – $NaBH_4$/Au = 8 – Add/Au = 0

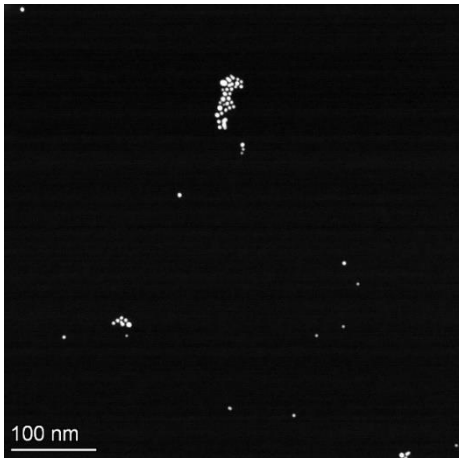

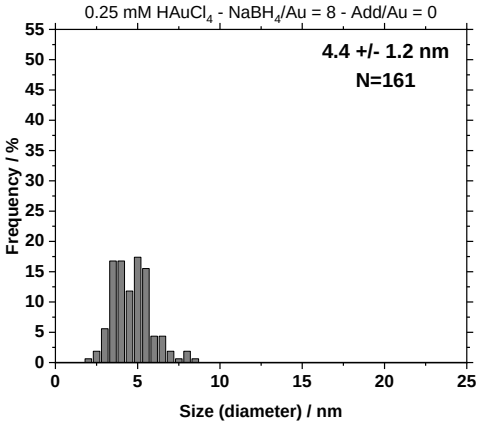

93) 0.25 mM $HAuCl_4$ – $NaBH_4$/Au = 11 – Add/Au = 0

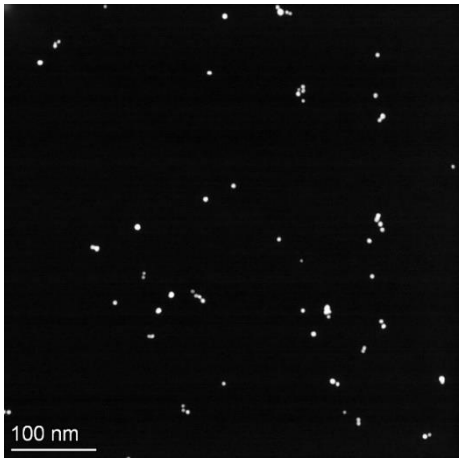

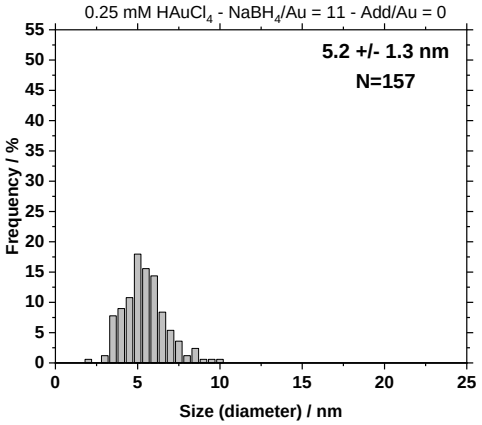

94) 0.25 mM $HAuCl_4$ – $NaBH_4$/Au = 4 – Add/Au = 0

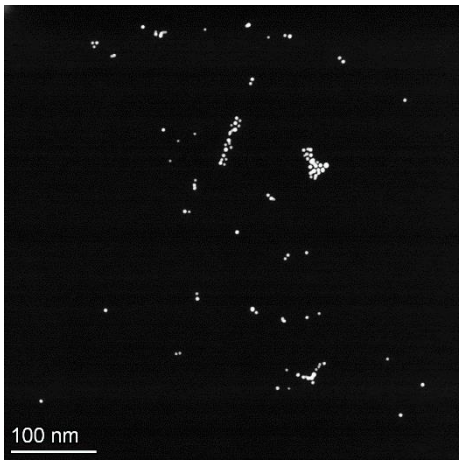

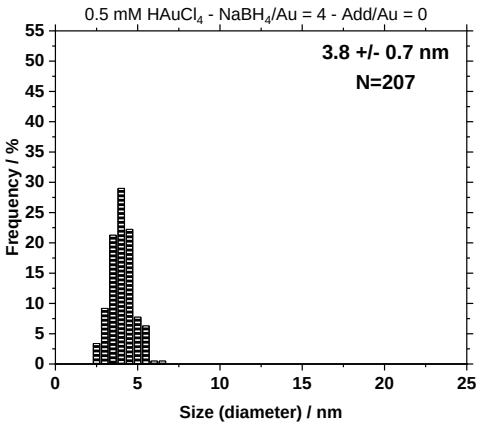

95) 0.25 mM $HAuCl_4$ – $NaBH_4$/Au = 2 – Add/Au = 0

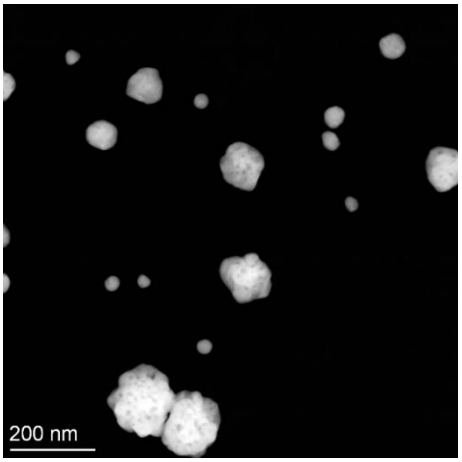

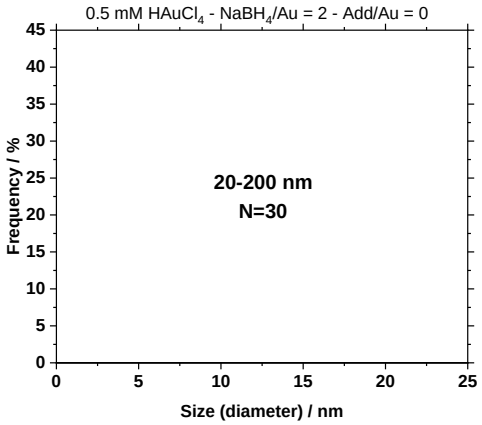

62) 0.5 mM $HAuCl_4$ – $NaBH_4$/Au = 5 – NaCt/Au = 5

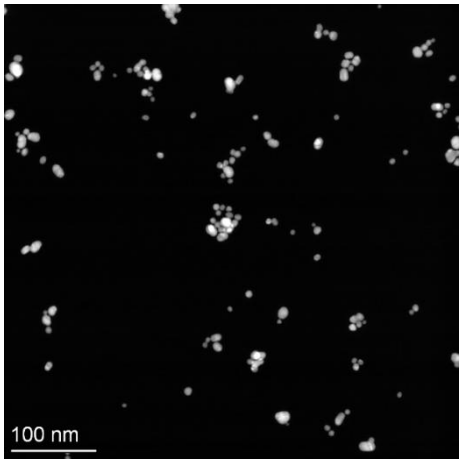

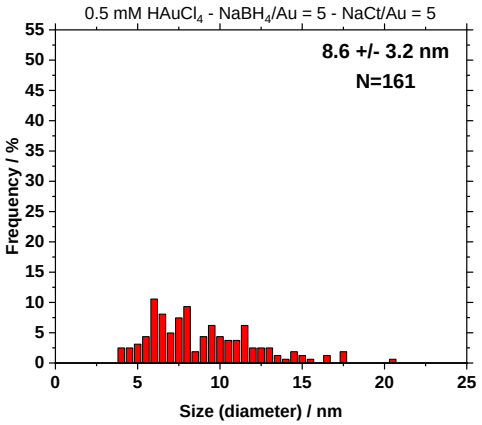

65) 0.5 mM $HAuCl_4$ – $NaBH_4$/Au = 5 – PVP/Au = 5

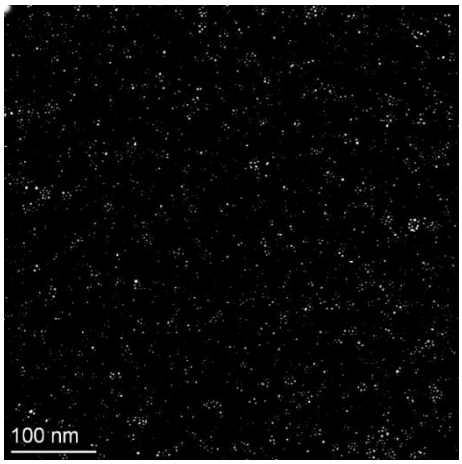

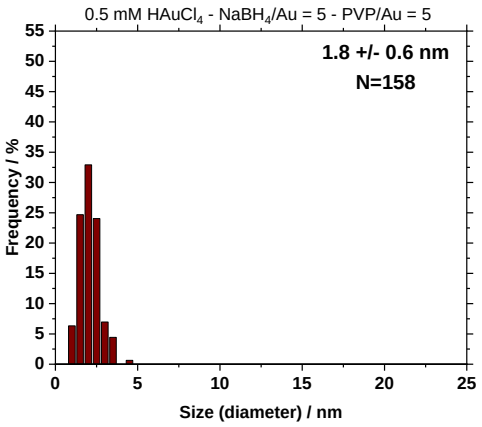

67) 0.5 mM $HAuCl_4$ – $NaBH_4$/Au = 5 – PVP/Au = 15

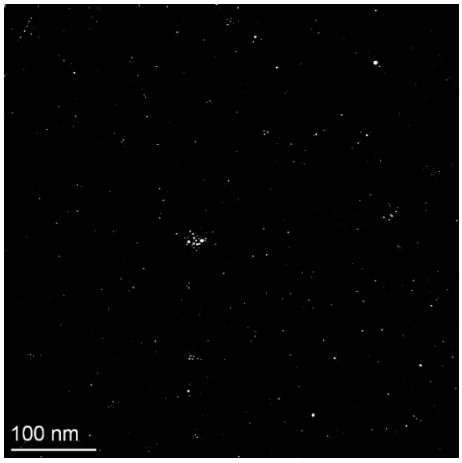

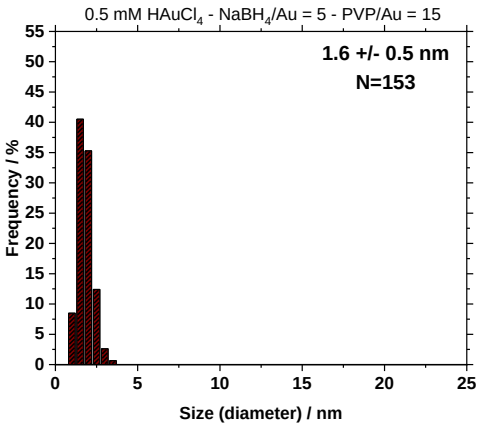

75) 0.5 mM $HAuCl_4$ – $NaBH_4$/Au = 8 – PVP/Au = 5

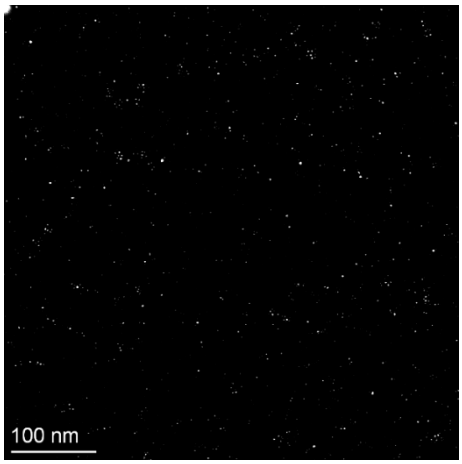

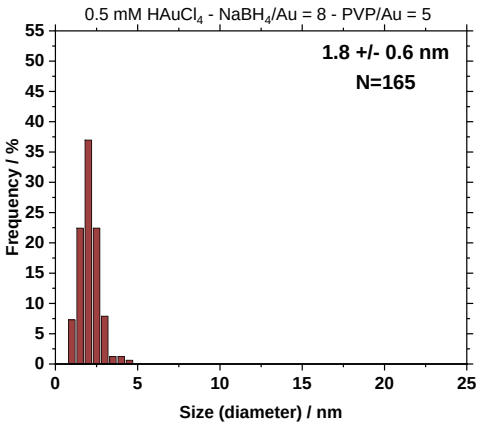

76) 0.5 mM $HAuCl_4$ – $NaBH_4$/Au = 8 – PVP/Au = 10

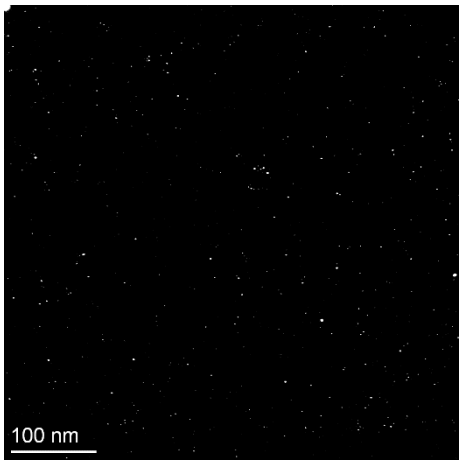

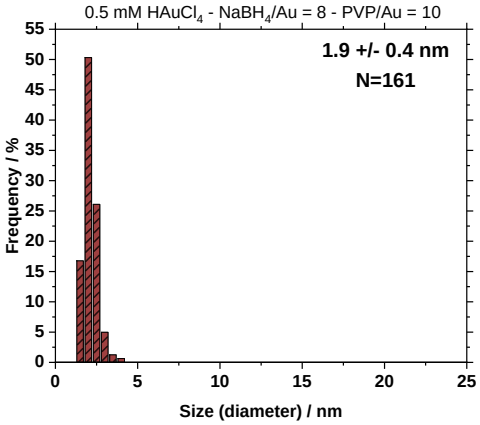

77) 0.5 mM $HAuCl_4$ – $NaBH_4$/Au = 8 – PVP/Au = 15

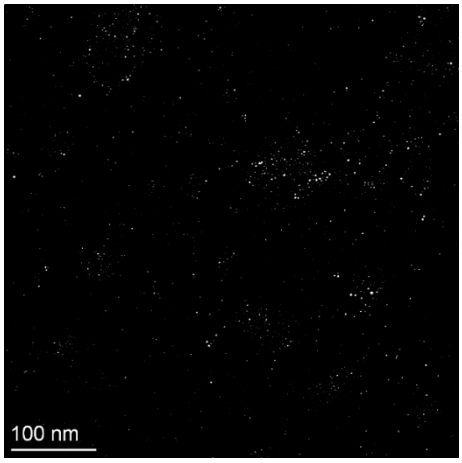

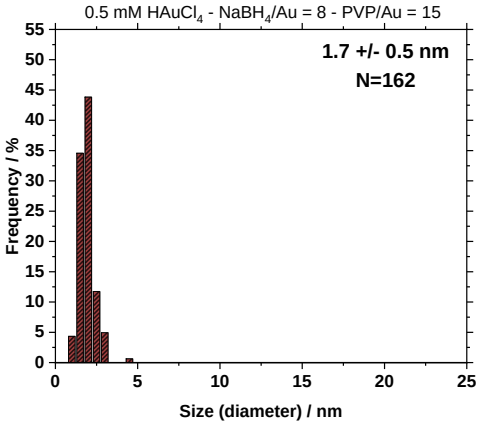

85) 0.5 mM $HAuCl_4$ – $NaBH_4$/Au = 11 – PVP/Au = 5

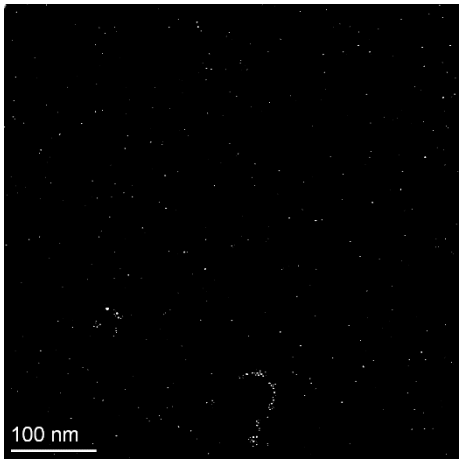

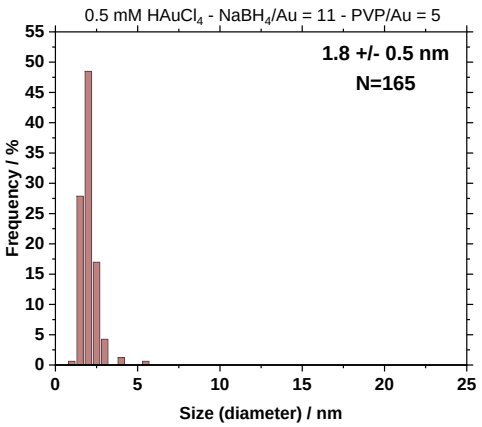

86) 0.5 mM $HAuCl_4$ – $NaBH_4$/Au = 11 – PVP/Au = 10

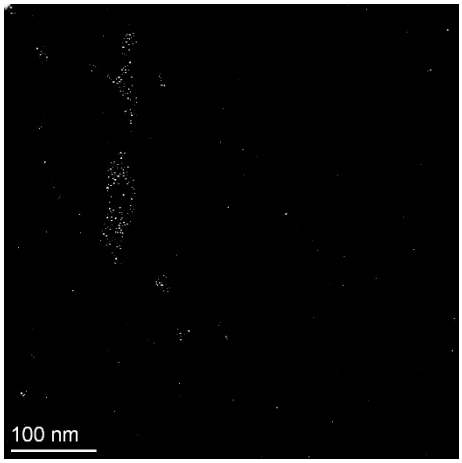

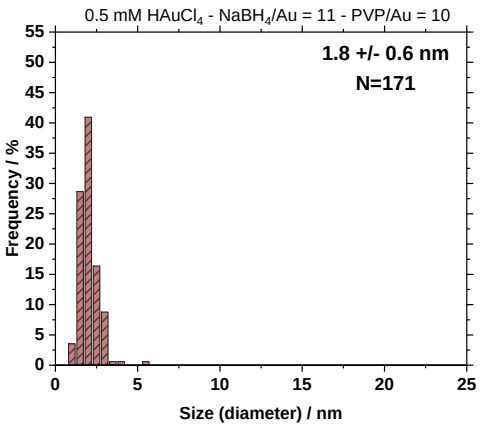

87) 0.5 mM $HAuCl_4$ – $NaBH_4$/Au = 11 – PVP/Au = 15

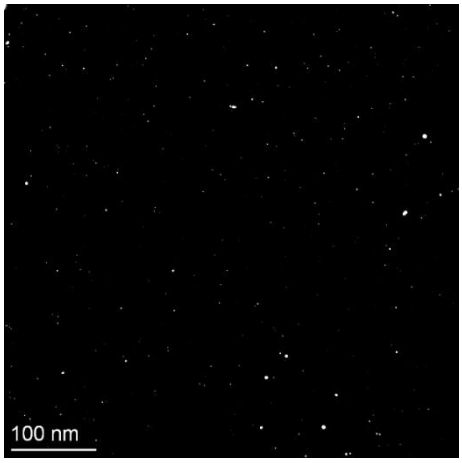

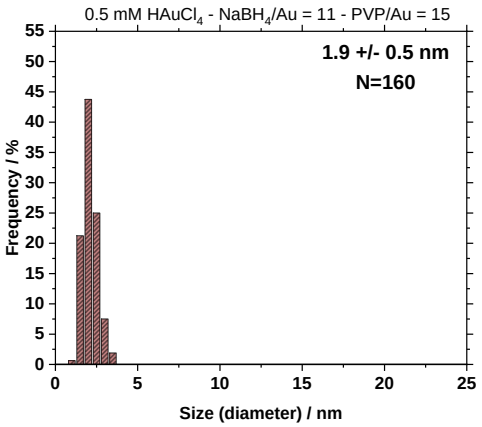

39) 0.2 mM $HAuCl_4$ – $NaBH_4$/Au = 5 – SDS/Au = 10

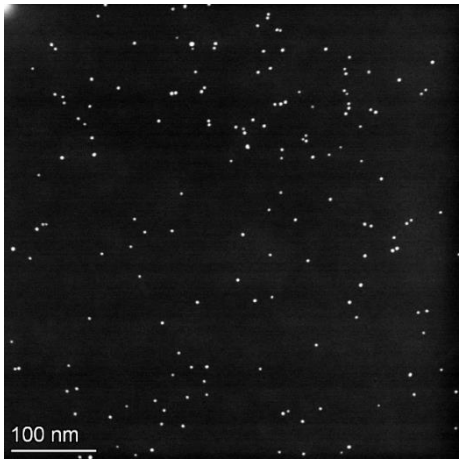

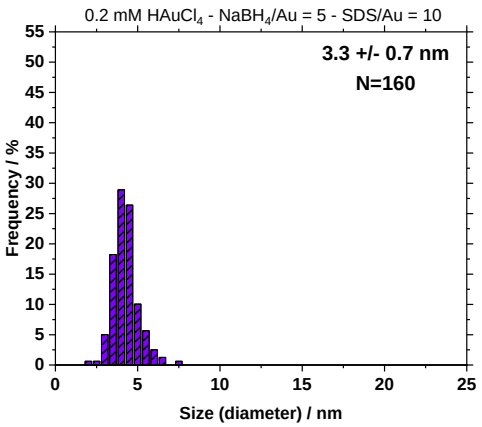

40) 0.2 mM $HAuCl_4$ – $NaBH_4$/Au = 5 – SDS/Au = 15

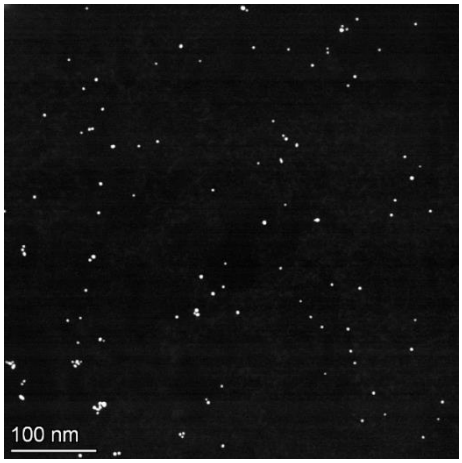

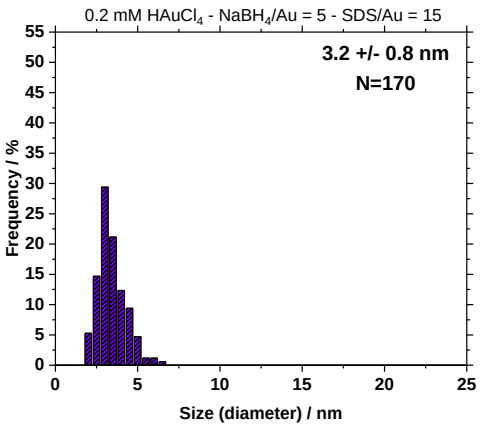

49) 0.2 mM $HAuCl_4$ – $NaBH_4$/Au = 8 – SDS/Au = 10

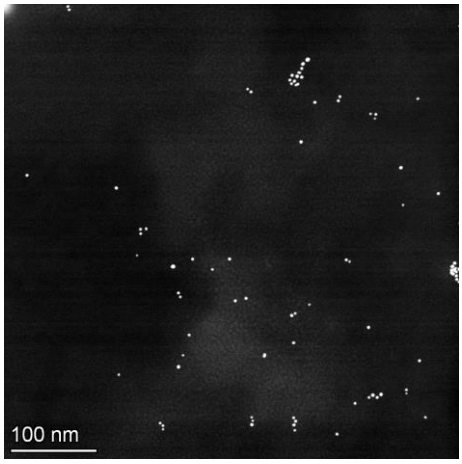

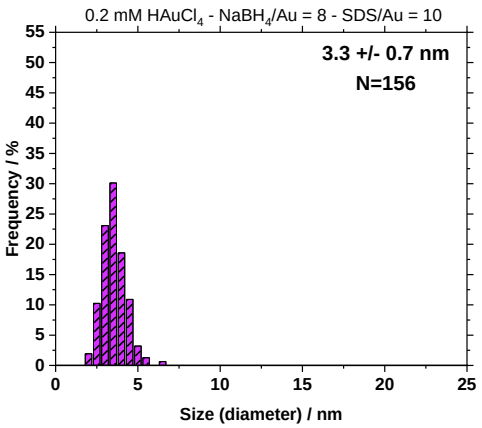

50) 0.2 mM $HAuCl_4$ – $NaBH_4$/Au = 8 – SDS/Au = 15

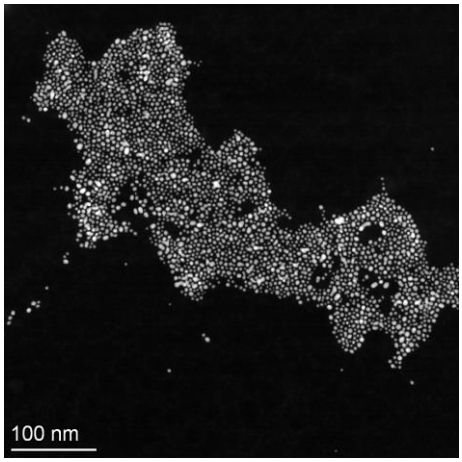

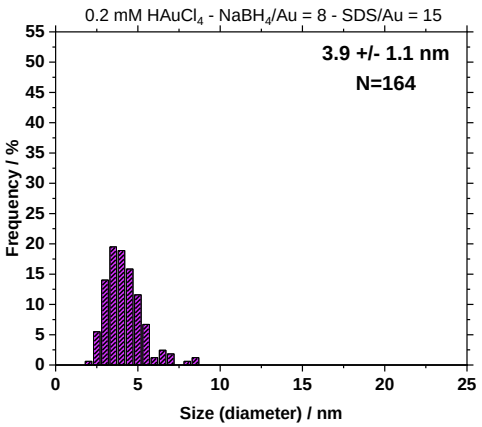

58) 0.2 mM $HAuCl_4$ – $NaBH_4$/Au = 11 – SDS/Au = 5

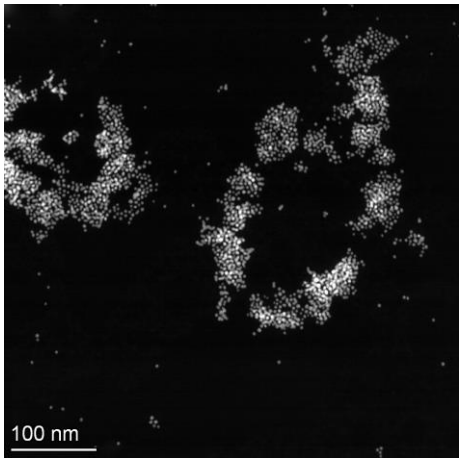

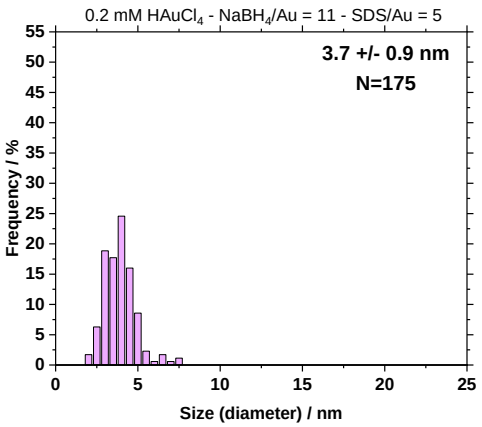

59) 0.2 mM $HAuCl_4$ – $NaBH_4$/Au = 11 – SDS/Au = 10

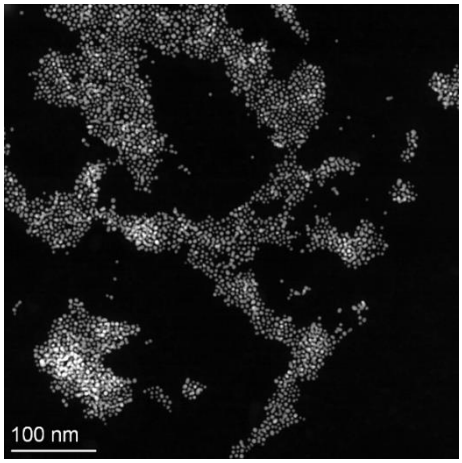

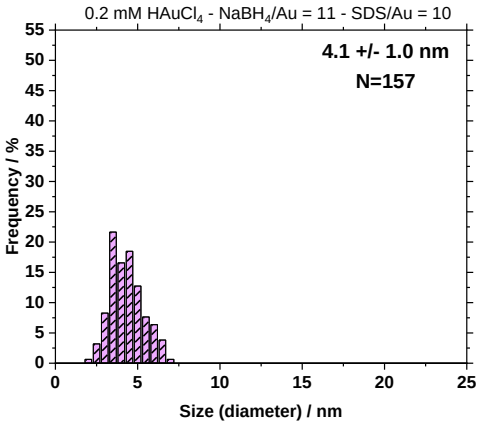

60) 0.2 mM $HAuCl_4$ – $NaBH_4$/Au = 11 – SDS/Au = 15

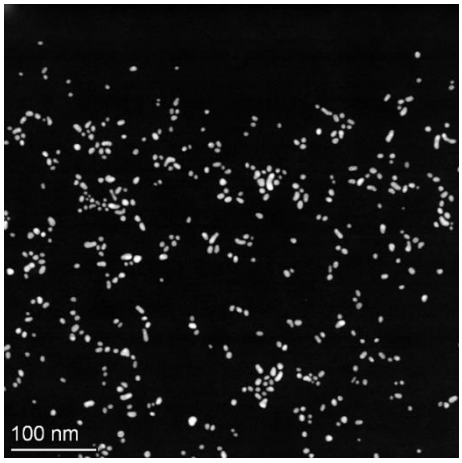

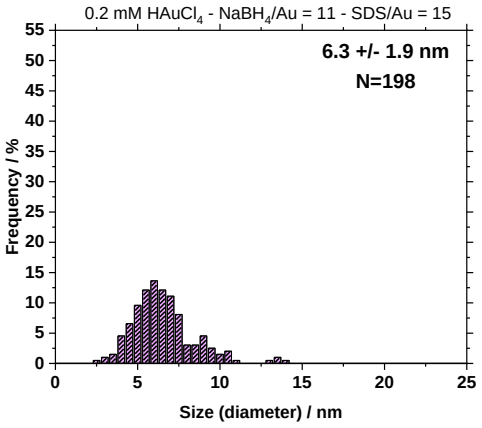

68) 0.5 mM $HAuCl_4$ – $NaBH_4$/Au = 5 – SDS/Au = 5

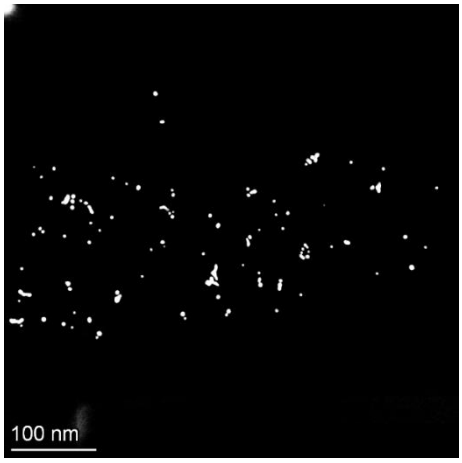

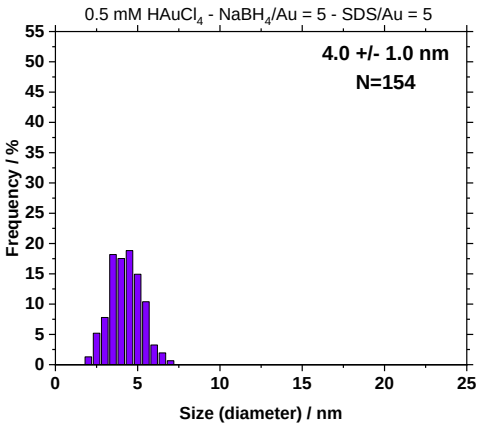

69) 0.5 mM $HAuCl_4$ – $NaBH_4$/Au = 5 – SDS/Au = 10

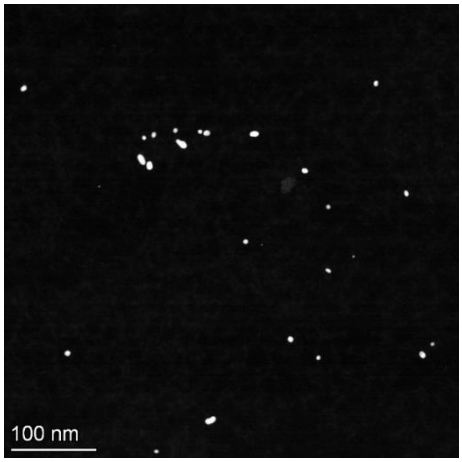

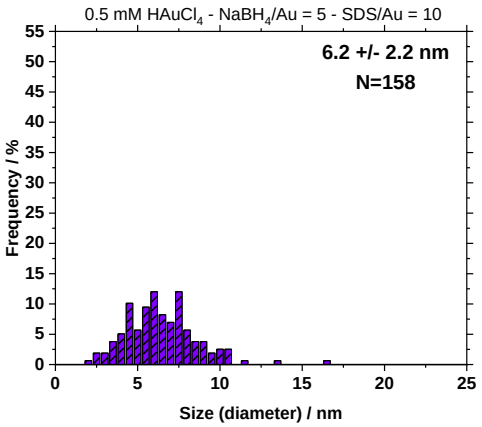

70) 0.5 mM $HAuCl_4$ – $NaBH_4$/Au = 5 – SDS/Au = 15

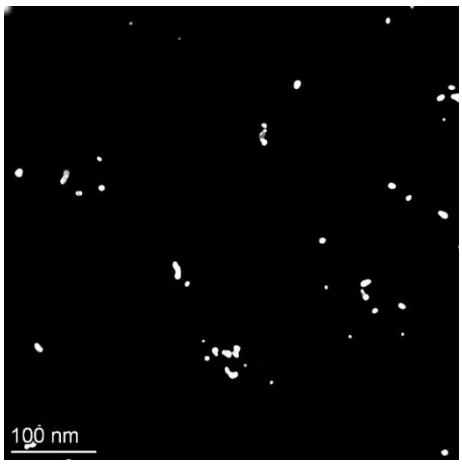

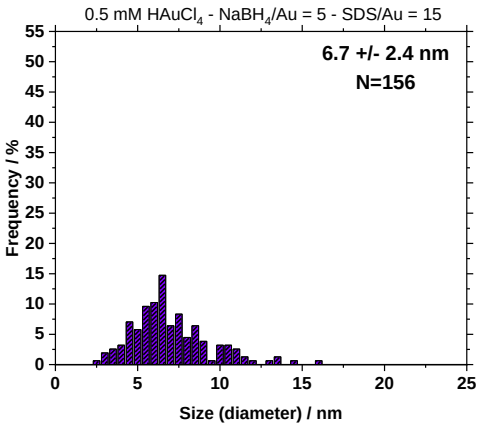

Figure S8. STEM data for the Au NPs prepared according to **Table S3**. The numbers indicate the entry in **Table S3**. STEM micrographs are on the left-hand side column and the retrieved size distributions are on the right-hand side.

7.2. Inverse method

108) 0.5 mM $HAuCl_4$ – $NaBH_4$/Au = 5 – Add/Au = 0 - Inverse

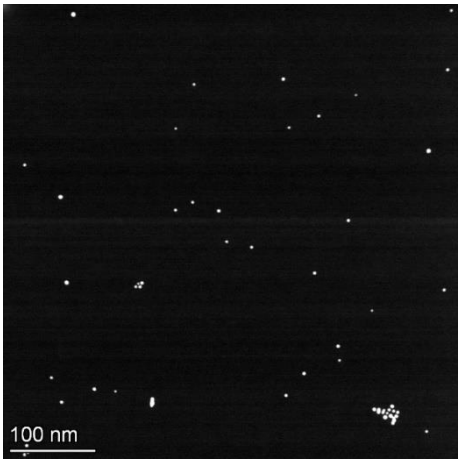

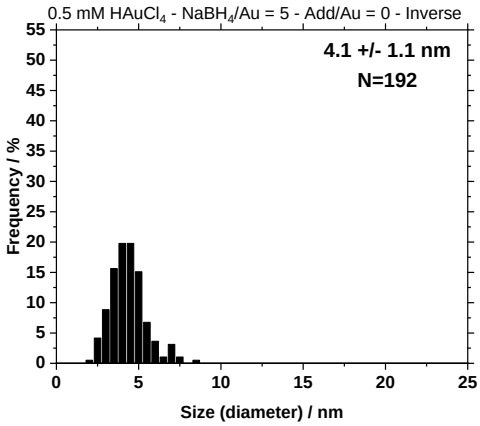

109) 0.5 mM $HAuCl_4$ – $NaBH_4$/Au = 5 – NaCt/Au = 5 – Inverse

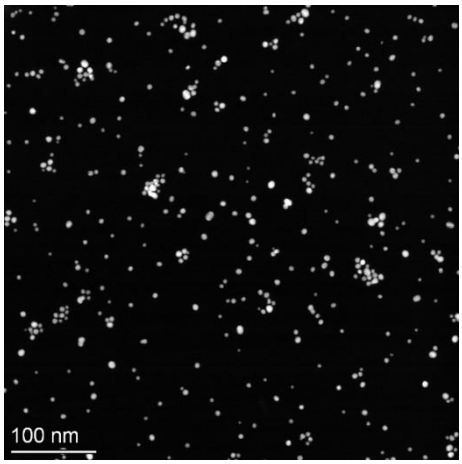

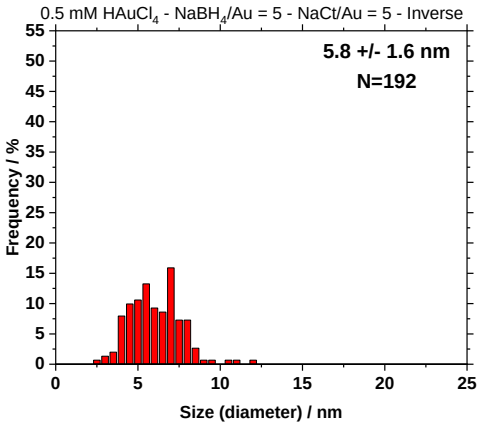

110) 0.5 mM $HAuCl_4$ – $NaBH_4$/Au = 5 – PVP/Au = 5 – Inverse

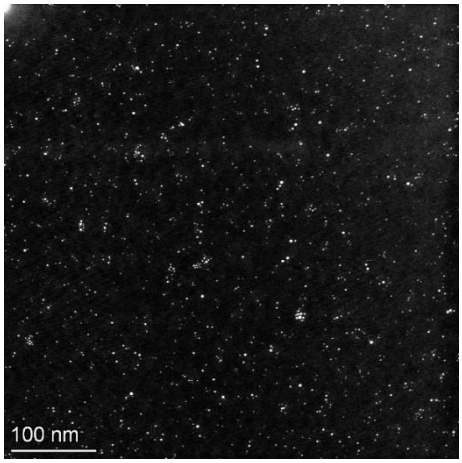

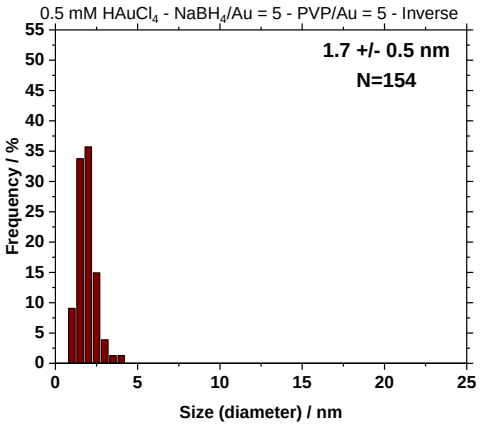

111) 0.5 mM $HAuCl_4$ – $NaBH_4$/Au = 5 – SDS/Au = 5 – Inverse

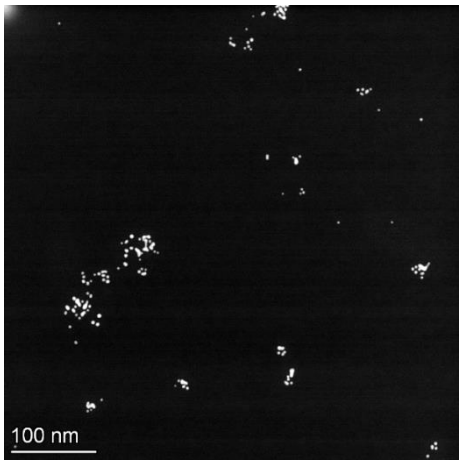

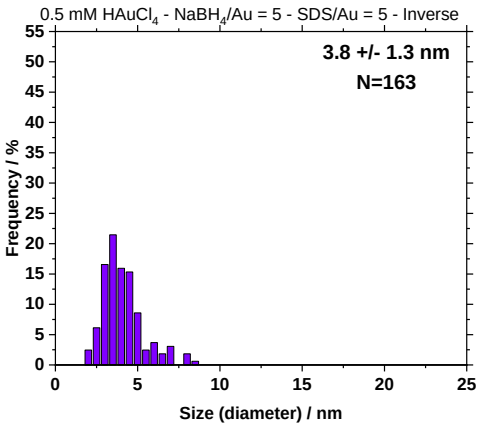

Figure S9. STEM data for the Au NPs prepared using the *inverse* approach. The numbers indicate the entry in **Table S3**. STEM micrographs are on the left-hand side column and the retrieved size distributions are on the right-hand side.

7.3. Optimization for Au NPs prepared in presence of NaCt

A)

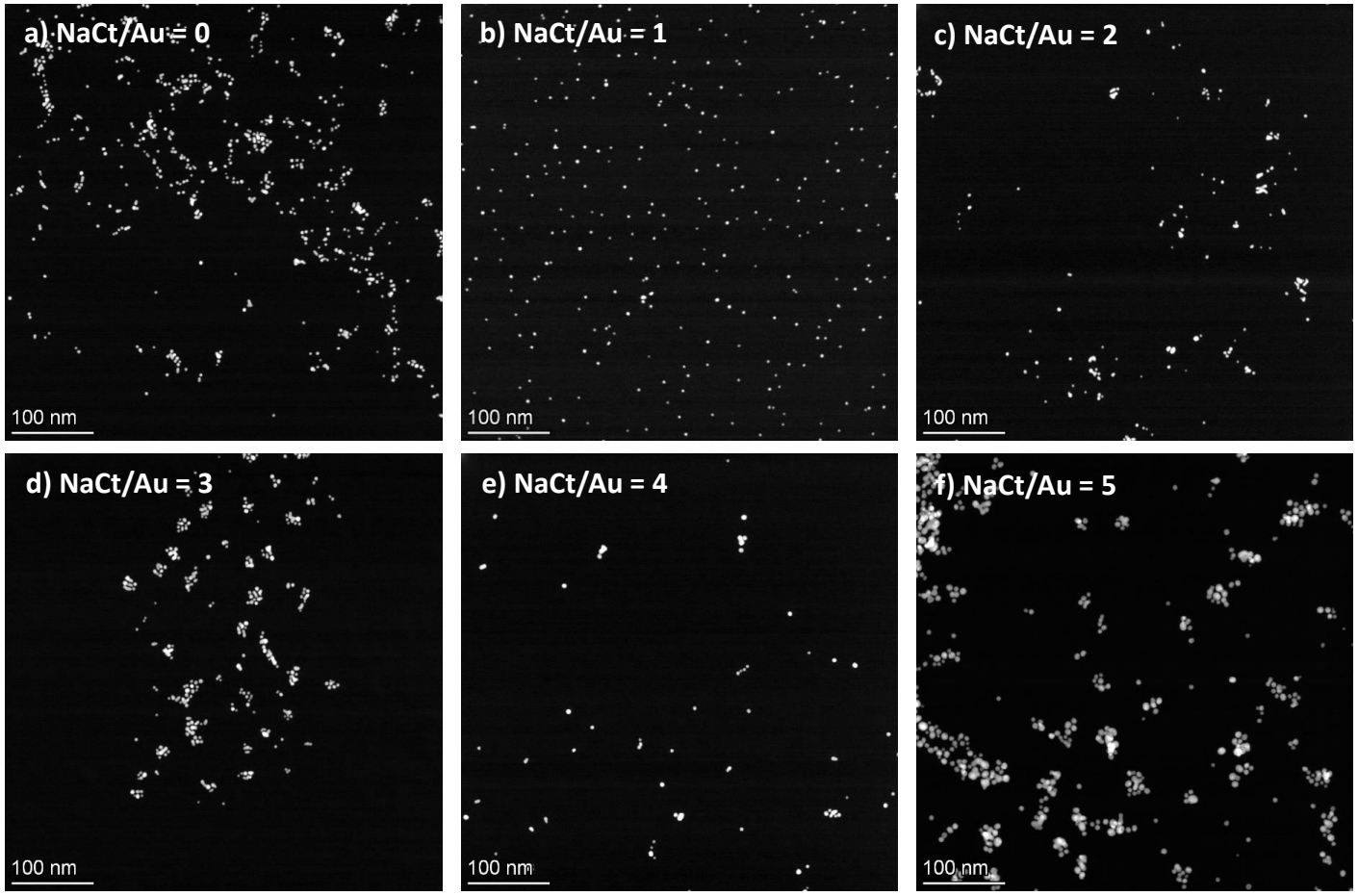

B)

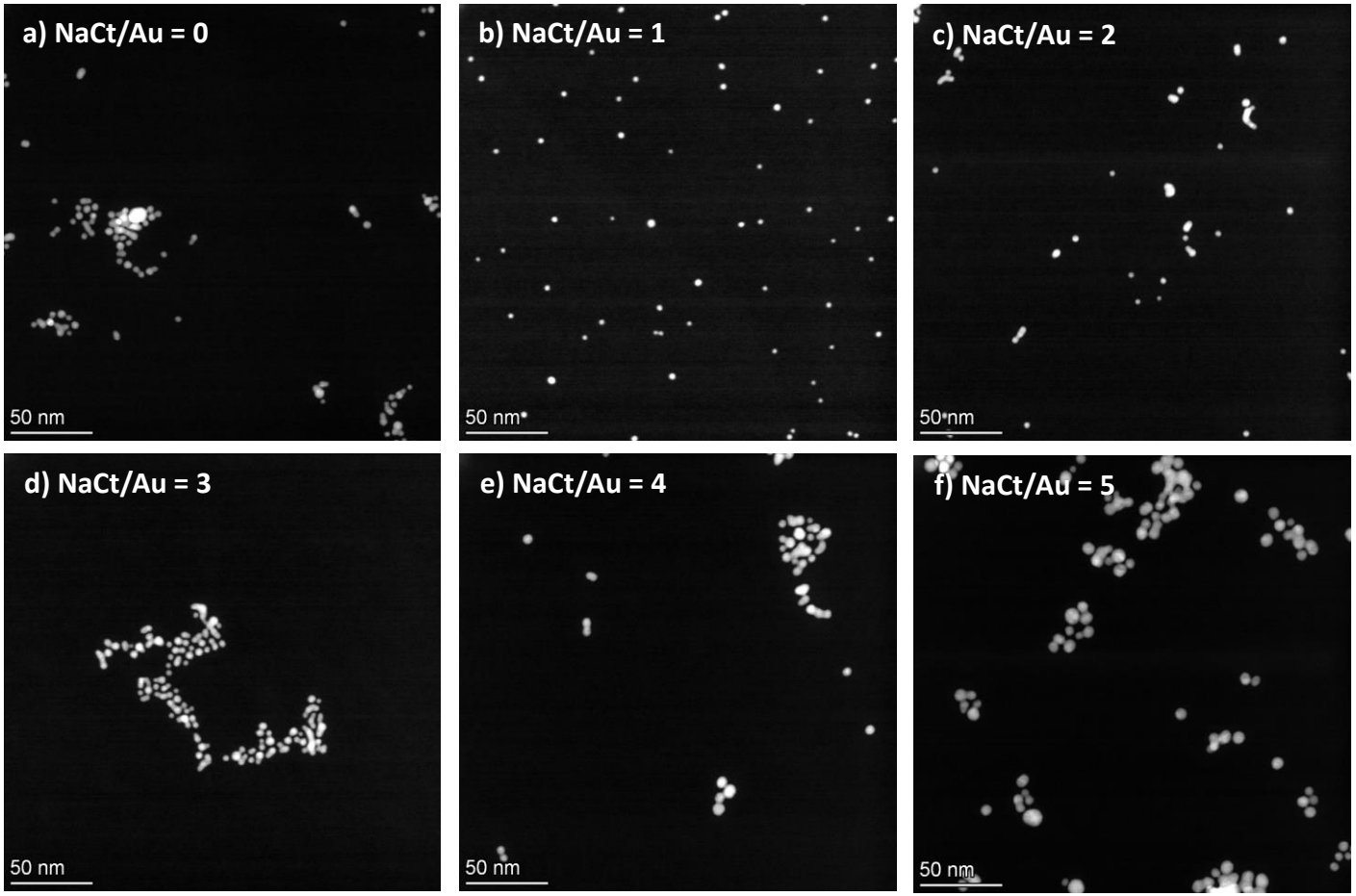
a) NaCt/Au = 0
50 nm
b) NaCt/Au = 1
50 nm
c) NaCt/Au = 2
50 nm
d) NaCt/Au = 3
50 nm
e) NaCt/Au = 4
50 nm
f) NaCt/Au = 5
50 nm

C)

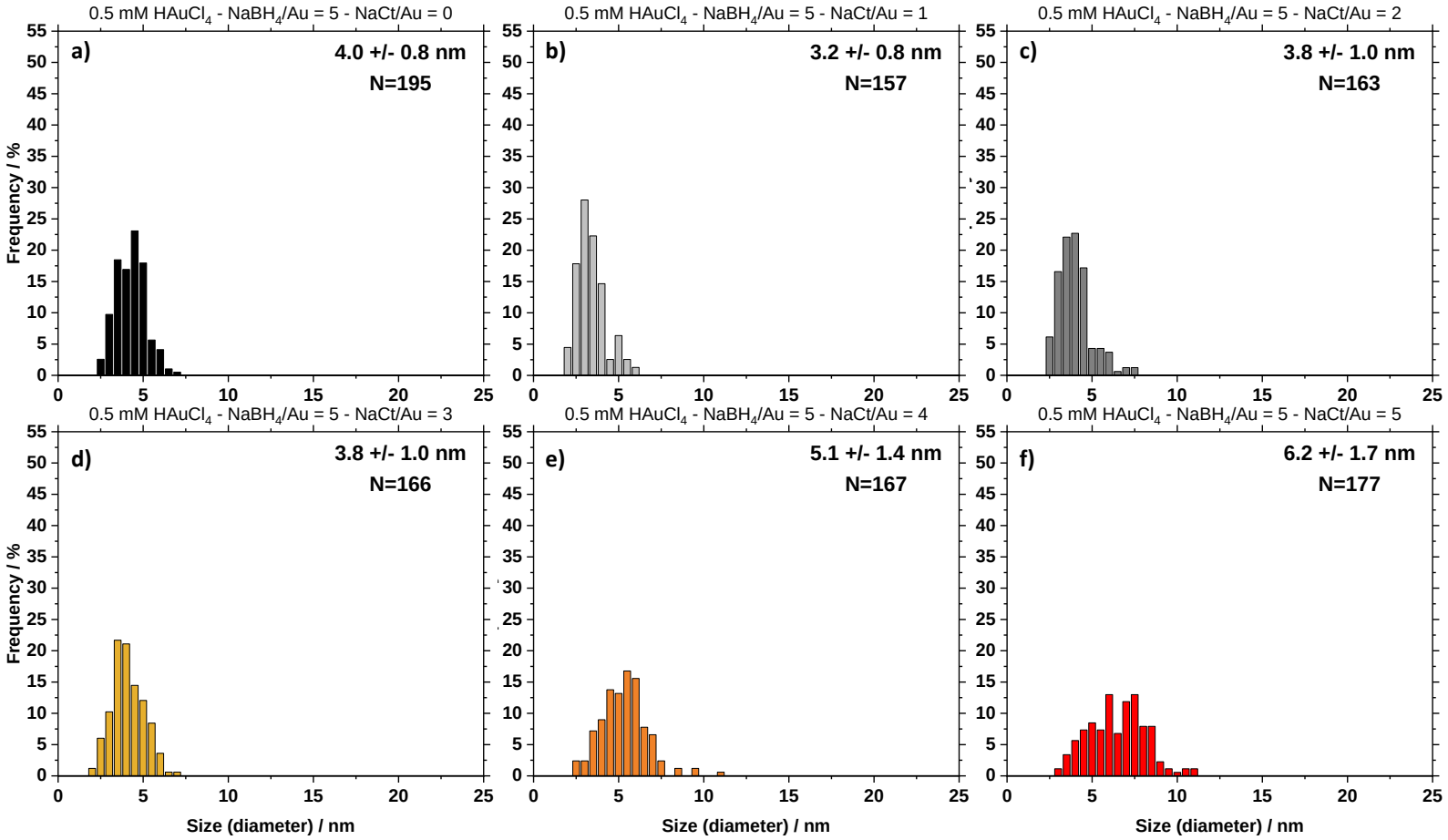

Figure S10. (A, B) STEM micrographs of Au NPs prepared using NaCt at different magnifications for sample prepared using different NaCt/Au molar ratio of (a) 0, (b) 1, (c) 2, (d) 3, (e) 4 and (f) 5. (C) Size distribution retrieved from STEM data analysis for the corresponding samples, as indicated. 0.5 mM $HAuCl_4$ and a $NaBH_4$/Au molar ratio of 5 was used in all cases. The samples correspond to the entry in **Table S3**: (a) 97, (b) 98, (c) 99, (d) 100, (e) 101, (f) 102.

7.4. Optimization for Au NPs prepared in presence of PVP – Effect of $HAuCl_4$ concentration

A)

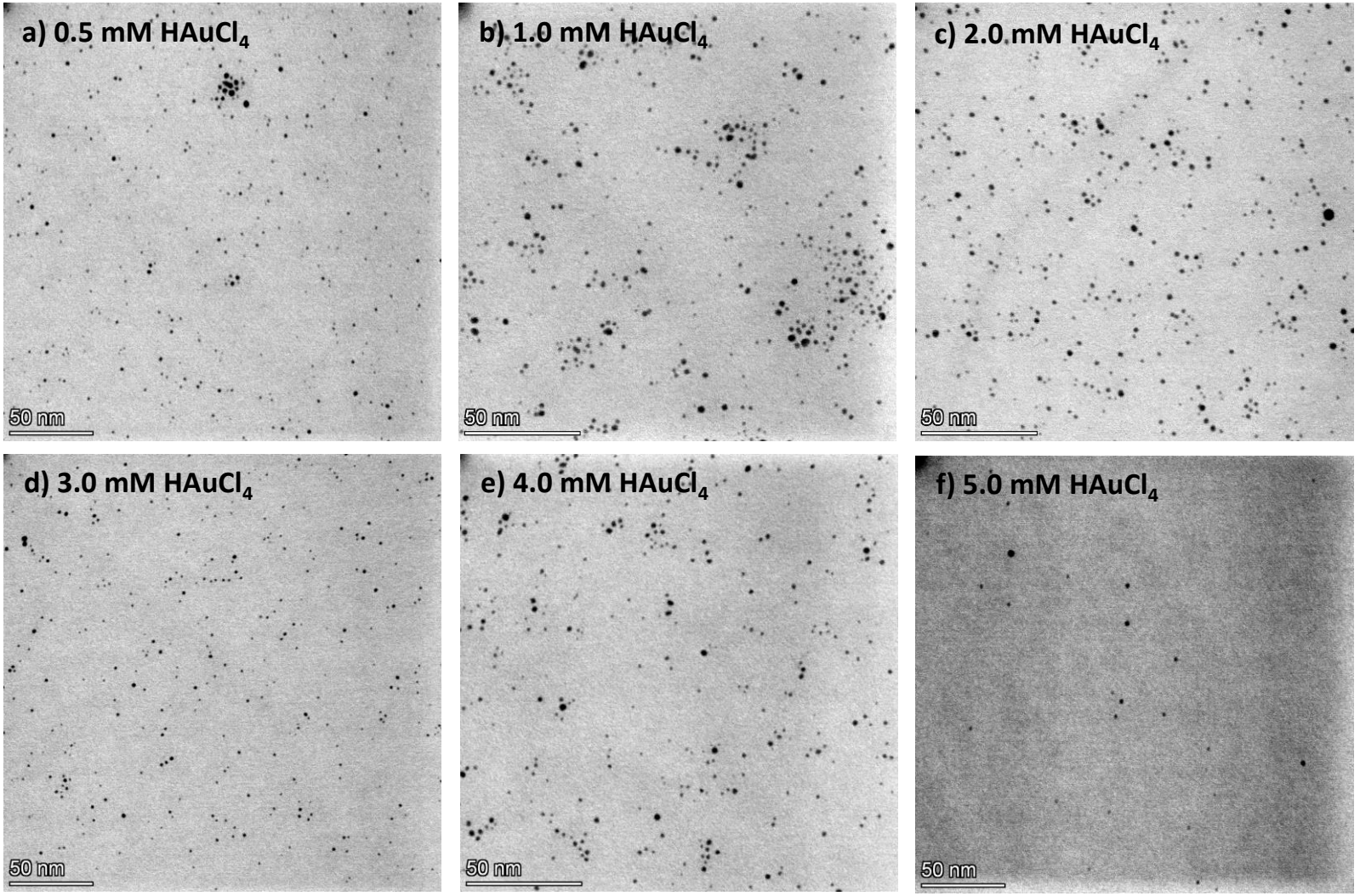

B)

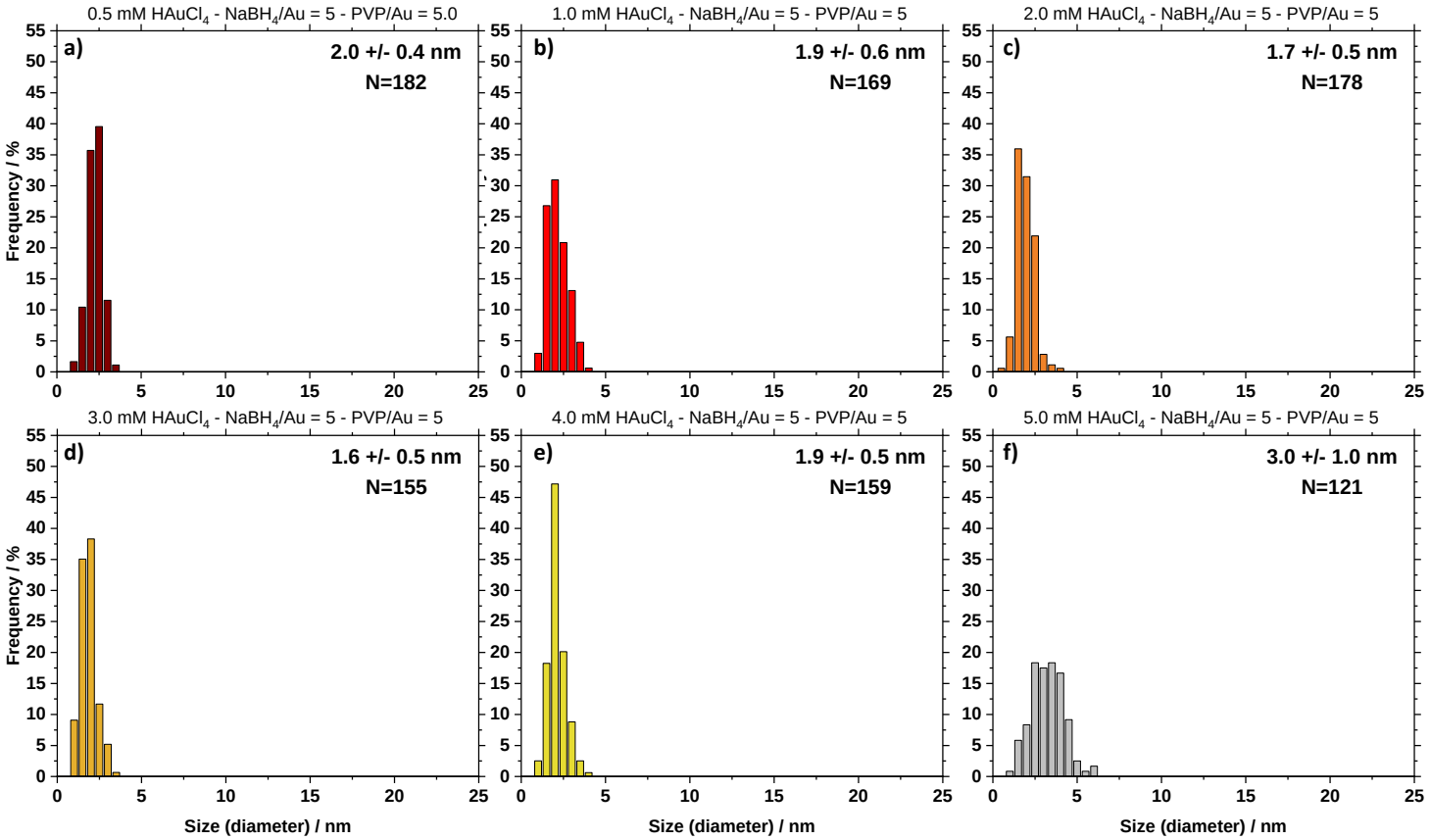

Figure S11. (A) STEM micrographs (bright field detector) of Au NPs prepared using PVP and different concentrations of $HAuCl_4$ of (a) 0.5 mM, (b) 1.0 mM, (c) 2.0 mM, (d) 3.0 mM, (e) 4.0 mM and (f) 5.0 mM. (B) Size distribution retrieved from STEM data analysis for the corresponding samples, as indicated. A $NaBH_4$/Au molar ratio of 5 and a PVP/Au molar ratio of 5 were used in all cases. The samples correspond to the entry in **Table S3**: (a) 127, (b) 103, (c) 104, (d) 105, (e) 106, (f) 107.

7.5. Optimization for Au NPs prepared in presence of PVP – Effect of PVP/Au molar ratio

128) 0.5 mM $HAuCl_4$ – $NaBH_4$/Au = 5 – PVP/Au = 0

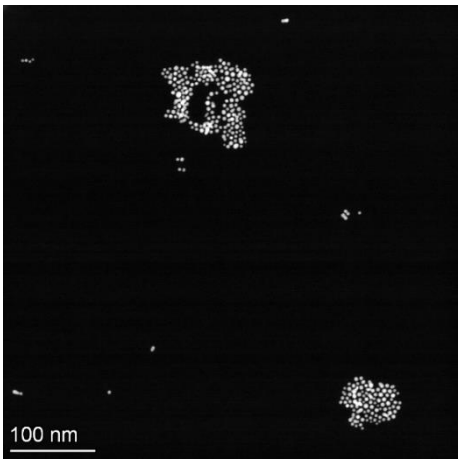

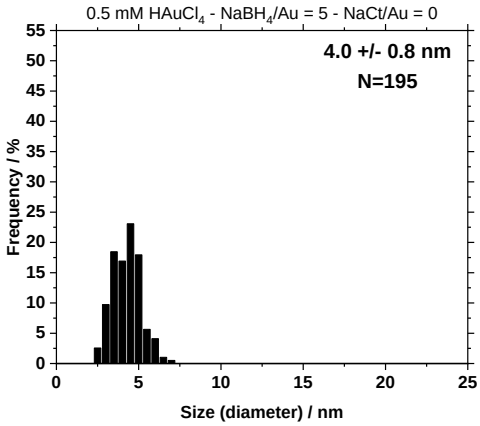

129) 0.5 mM $HAuCl_4$ – $NaBH_4$/Au = 5 – PVP/Au = 0.1

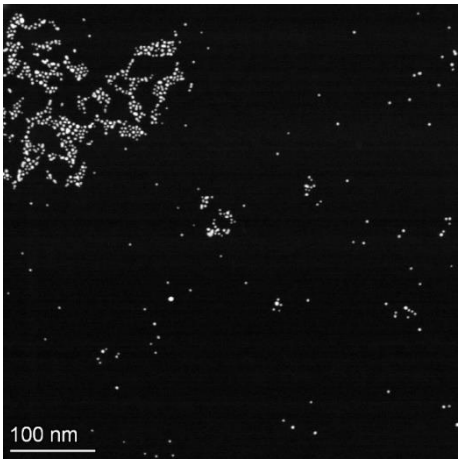

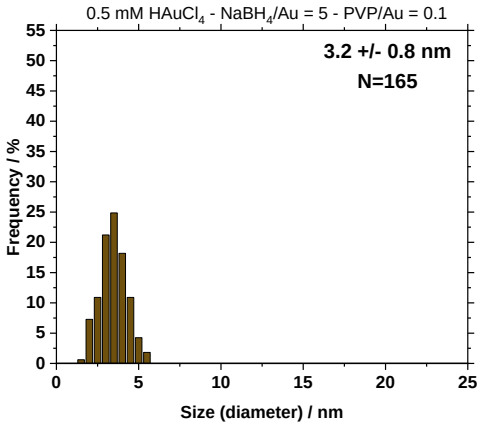

130) 0.5 mM $HAuCl_4$ – $NaBH_4$/Au = 5 – PVP/Au = 0.2

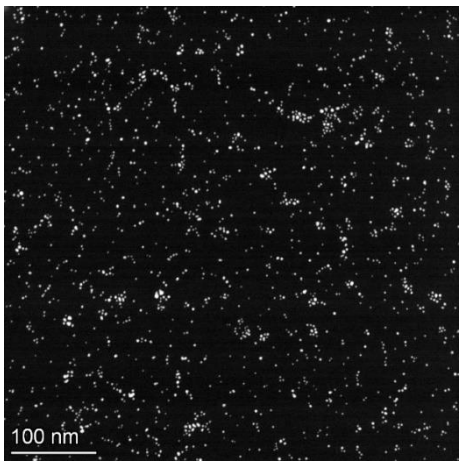

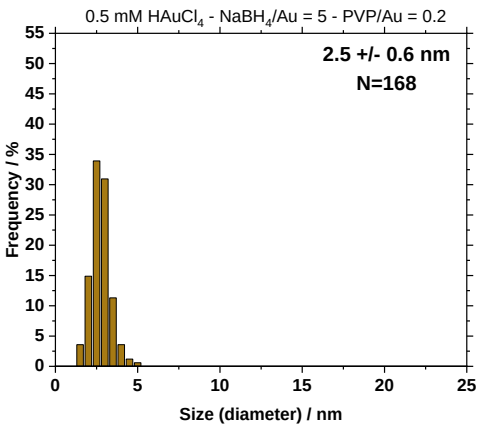

131) 0.5 mM $HAuCl_4$ – $NaBH_4$/Au = 5 – PVP/Au = 0.3

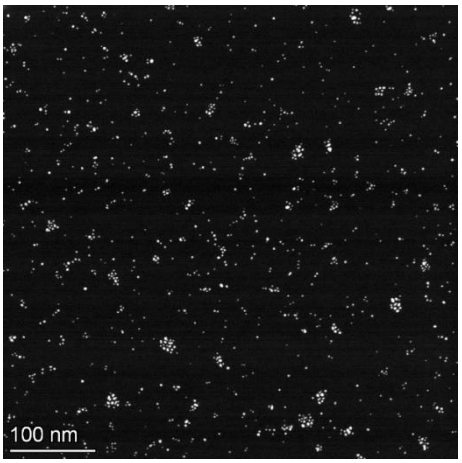

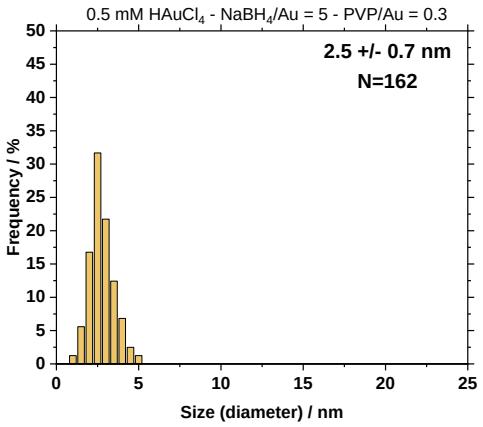

133) 0.5 mM $HAuCl_4$ – $NaBH_4$/Au = 5 – PVP/Au = 0.5

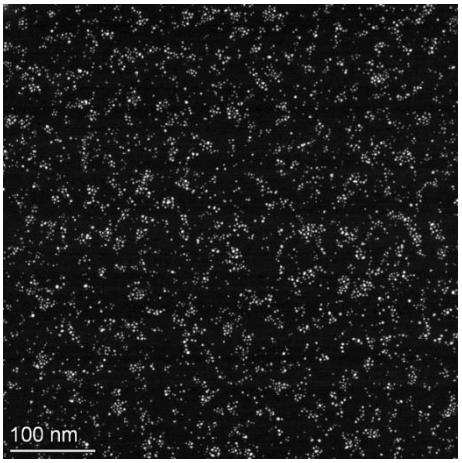

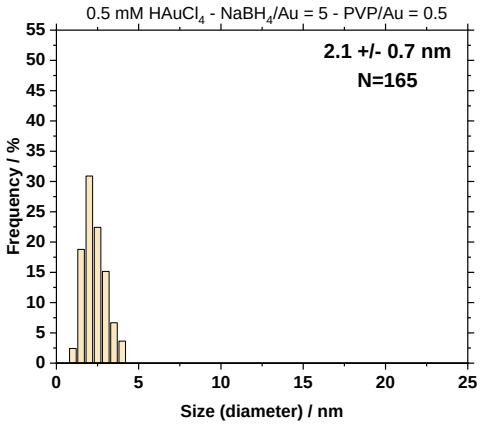

119) 0.5 mM $HAuCl_4$ – $NaBH_4$/Au = 5 – PVP/Au = 1

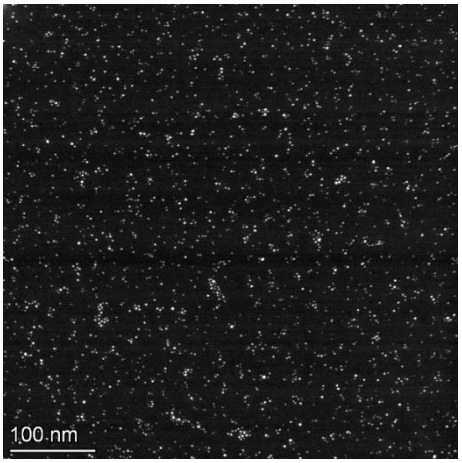

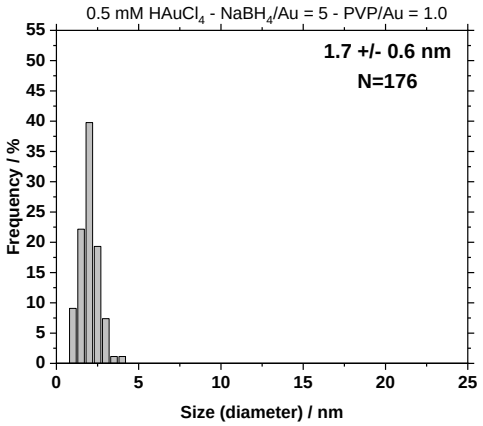

121) 0.5 mM $HAuCl_4$ – $NaBH_4$/Au = 5 – PVP/Au = 2

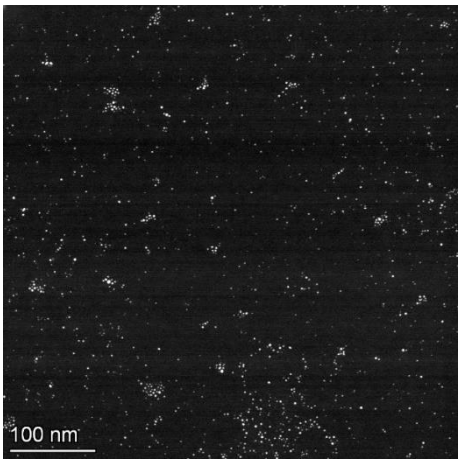

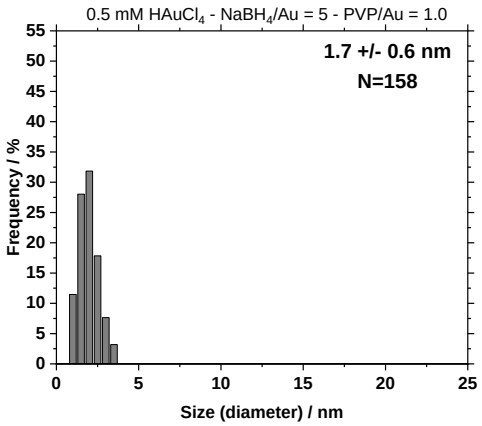

127) 0.5 mM $HAuCl_4$ – $NaBH_4$/Au = 5 – PVP/Au = 5

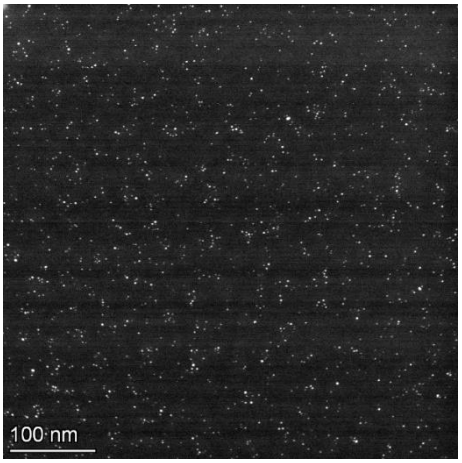

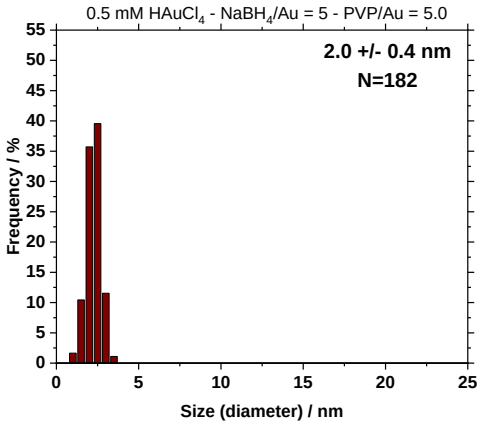

Figure S12. STEM data for the Au NPs prepared according to **Table S3**. The numbers indicate the entry in **Table S3**. STEM micrographs are on the left-hand side column and the retrieved size distributions are on the right-hand side. The focus is on samples with different PVP/Au molar ratio, as indicated.

8. Stability

Most samples did not show any significant changes over time based on colors and UV-vis data. In this section, only the samples that showed significant changes are detailed. The samples with the most pronounced changes were those obtained with higher $NaBH_4$/Au molar values and/or higher $HAuCl_4$ concentrations. In all cases in the graphs below the UV-vis spectra recorded after a day are shown as D1 in thicker lines and the same samples measured after a month are indicated as M1 with a thinner line.

Figure S13 provides and overview of the samples showing the most significant changes. It can be seen that the samples are overall stable over time. The surfactant-free approach leads to stable colloids as illustrated in **Figure S13a**. The use of NaCt tends to lead to more stable NPs, as illustrated in **Figure S13b** when 0.2 mM $HAuCl_4$ is used. The relative stability of the Au NPs obtained using NaCt is also illustrated in **Figure S13c**. When PVP is used, **Figure S13d-f**, the NPs remain relatively stable with a tendency to observe a more pronounced spr over time, in particular when higher $NaBH_4$/Au molar ratios are used. In the cases were SDS was used a systematic increases of the A_{spr} was observed, as illustrated in **Figure S13g-i**. As illustrated in **Figure S13**, that focuses on the samples with the most significant changes, the A_{400} values were very close with a relative decrease typically less than 3%.

Importantly, the changes in size observed are not less pronounced when an additive is used compared to the surfactant-free synthesis, apart when NaCt and PVP are used and a lower $HAuCl_4$ concentration of $HAuCl_4$ is preferred. This shows that as the concentration of $HAuCl_4$ increases, there is no clear benefits of using additives to stabilize the NPs. This is further exemplified in **Figure S14**. **Figure S14a,b** illustrate why a $NaBH_4$/Au molar ratio high enough is needed to obtained stable Au NPs in the surfactant-free approach. With a $NaBH_4$/Au molar ratio of 2 for 0.5 mM $HAuCl_4$, **Figure S14b,** the NPs are not stable as colloids and the overall absorption decreases over time. Whether the reverse or direct methods are used, as illustrated in **Figure S14c** and **Figure S14d**, respectively, all samples show some degree of changes overtime in particular when 0.5 mM $HAuCl_4$ is used. This stresses further that there is no strong difference nor benefits to use the direct or inverse methods and the direct method was preferred as detailed above.

Figure S15 illustrates how the stability over time conferred by using NaCt or PVP increases with the amount of additive used.

Finally, **Figure S16** illustrate that when PVP is used and rather high concentrations of $HAuCl_4$ are used, the colloids remain relatively stable over time with a likely minor growth of the NPs due to the formation of more pronounced spr features. The changes in the features of the spectra are minimal considering the high concentrations of $HAuCl_4$ at which the synthesis is successful (3-4 mM), although it can be seen that dilution of the stock solutions to lower concentration at 0.5 mM $HAuCl_4$ can help to minimize this further growth.

In conclusion, the NPs here obtained under various conditions are relatively stable. And there is overall no major benefits to use the Additives to improve the stability of the NPs. Note that those results need to take into account the fact that in contrast to a current practices, the colloidal NPs here were not stored in a fridge but at room temperature, i.e. the assessment was performed in a 'worst-case-scenario' without incentive to keep the NPs in potentially more optimal condition for storage. This choice was made to stress the benefits of surfactant-free approaches and also to minimize the energy cost and footprint that the use of a fridge would generate, in line with the guidance of more sustainable practices in the laboratory.[15]

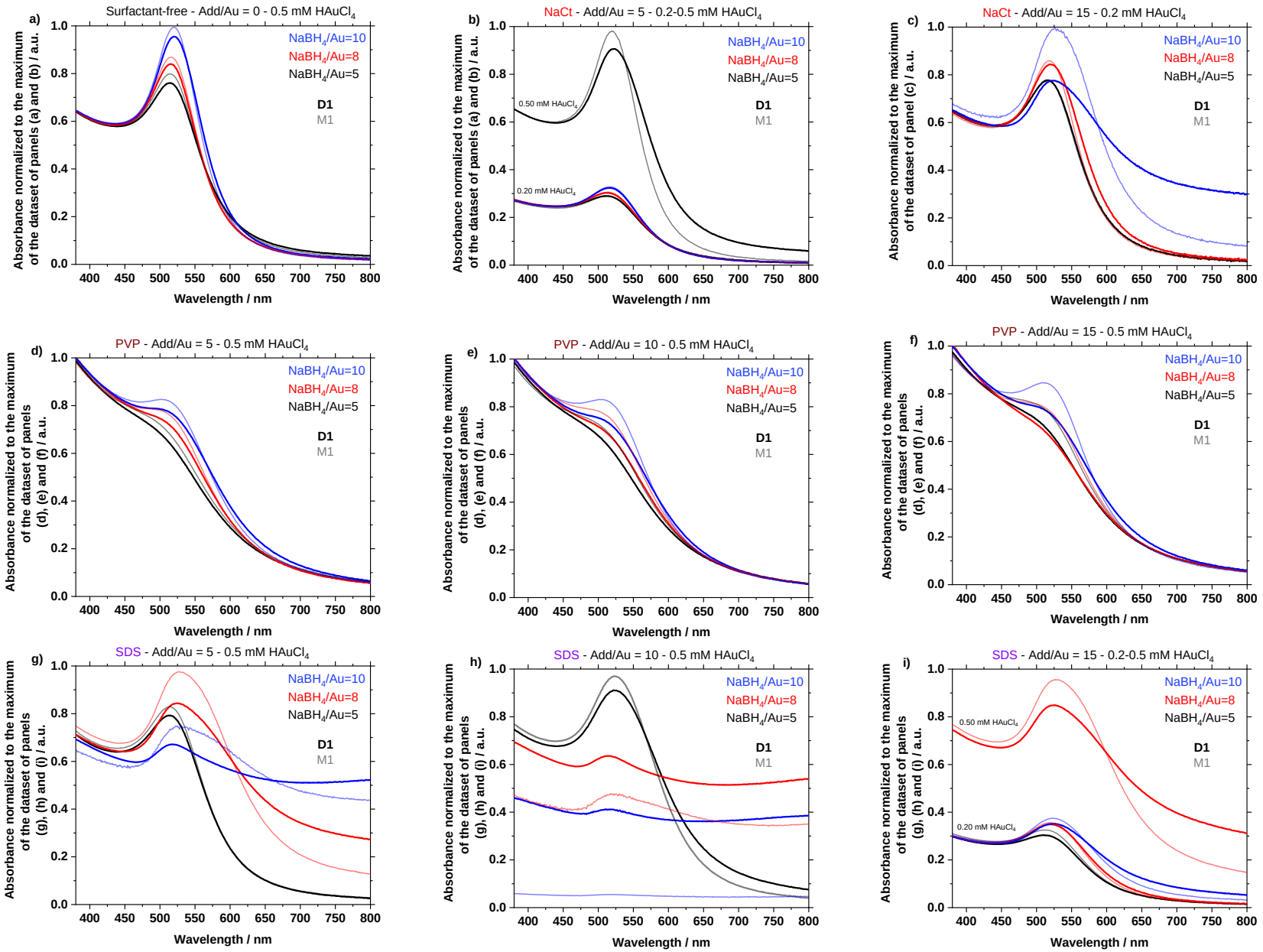
a)
Surfactant-free - Add/Au = 0 - 0.5 mM HAuCl4
b)
NaCt - Add/Au = 5 - 0.2-0.5 mM HAuCl4
0.50 mM HAuCl4
0.20 mM HAuCl4
c)
NaCt - Add/Au = 15 - 0.2 mM HAuCl4
d)
PVP - Add/Au = 5 - 0.5 mM HAuCl4
e)
PVP - Add/Au = 10 - 0.5 mM HAuCl4
f)
PVP - Add/Au = 15 - 0.5 mM HAuCl4
g)
SDS - Add/Au = 5 - 0.5 mM HAuCl4
h)
SDS - Add/Au = 10 - 0.5 mM HAuCl4
i)
SDS - Add/Au = 15 - 0.2-0.5 mM HAuCl4
0.50 mM HAuCl4
0.20 mM HAuCl4
NaBH4/Au=10
NaBH4/Au=8
NaBH4/Au=5
D1
M1
Absorbance normalized to the maximum of the dataset of panels (a) and (b) / a.u.
Absorbance normalized to the maximum of the dataset of panel (c) / a.u.
Absorbance normalized to the maximum of the dataset of panels (d), (e) and (f) / a.u.
Absorbance normalized to the maximum of the dataset of panels (g), (h) and (i) / a.u.
Wavelength / nm

Figure S13. UV-vis spectra for Au NPs obtained using different $HAuCl_4$ concentrations, different $NaBH_4$/Au molar ratio and different additives with different Additive/Au molar ratio, as indicated. In each case the UV-vis spectra recorded 24 hours after the synthesis (D1) and after a month (M1) are reported. (a) Surfactant-free Au NPs obtained with 0.5 mM $HAuCl_4$ and various $NaBH_4$/Au molar ratios, as indicated. (b,c) For Au NPs prepared using NaCt and (b) a NaCt/Au molar ratio of 5, 0.2 or 0.5 mM $HAuCl_4$, and various $NaBH_4$/Au molar ratios, as indicated, and (c) a NaCt/Au molar ratio of 15, 0.2 mM $HAuCl_4$, and various $NaBH_4$/Au molar ratios, as indicated. (d-f) For Au NPs prepared using PVP, 0.5 mM $HAuCl_4$ and (d) a PVP/Au molar ratio of 5, (e) a PVP/Au molar ratio of 10, (f) a PVP/Au molar ratio of 15, and various $NaBH_4$/Au molar ratios, as indicated. (g-i) For Au NPs prepared using SDS, 0.5 mM $HAuCl_4$ and (g) a SDS/Au molar ratio of 5, (h) a SDS/Au molar ratio of 10, (i) a SDS/Au molar ratio of 15, and various $NaBH_4$/Au molar ratios, as indicated.

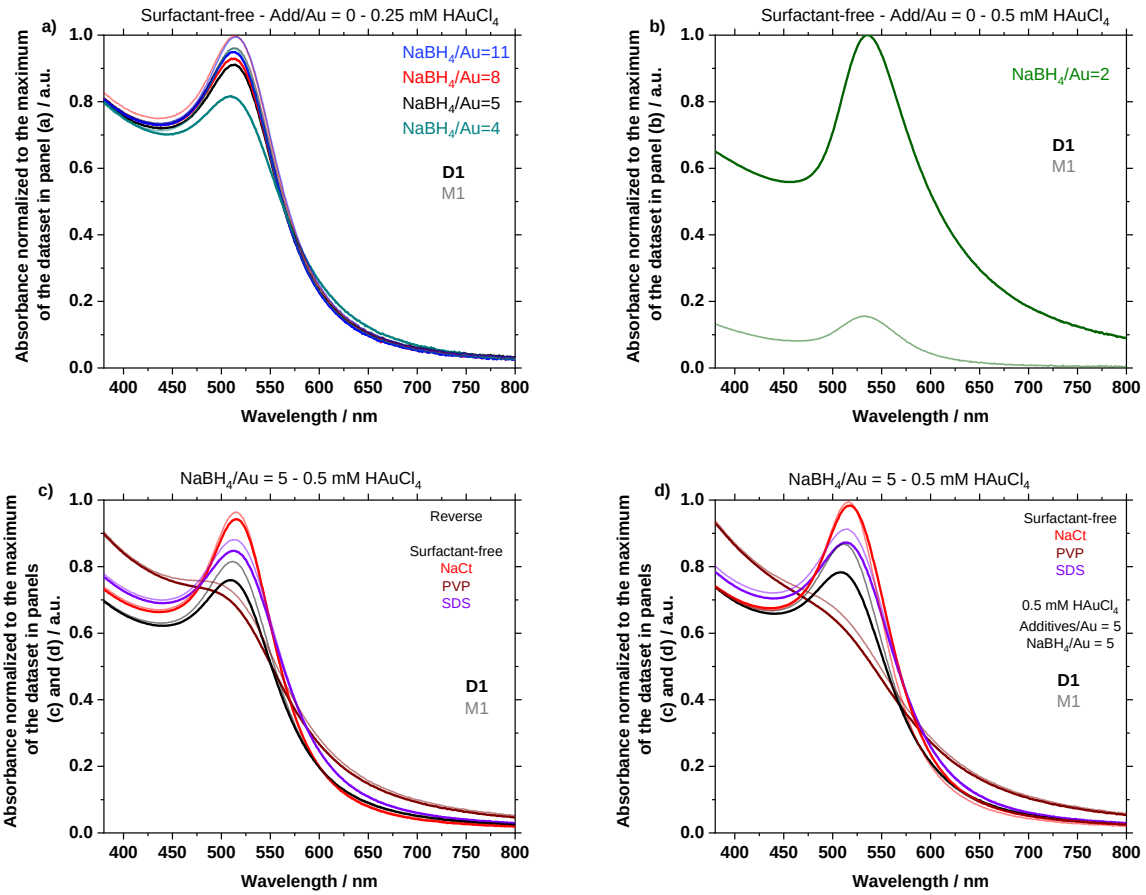

Figure S14. UV-vis spectra for Au NPs obtained using different $HAuCl_4$ concentrations, different $NaBH_4$/Au molar ratio and different additives with different Additive/Au molar ratio, as indicated. In each case the UV-vis spectra recorded 24 hours after the synthesis (D1) and after a month (M1) are reported. (a) Surfactant-free Au NPs obtained with 0.25 mM $HAuCl_4$ and various $NaBH_4$/Au molar ratios, as indicated. (b) Surfactant-free Au NPs obtained with 0.5 mM $HAuCl_4$ and a $NaBH_4$/Au molar ratio of 2. (c,d) Au NPs obtained using 0.5 mM $HAuCl_4$, a $NaBH_4$/Au molar ratio of 5, an Additive/Au molar ratio of 0 or 5 and no additive, NaCt, PVP or SDS, as indicated for (c) the inverse and (d) the direct method.

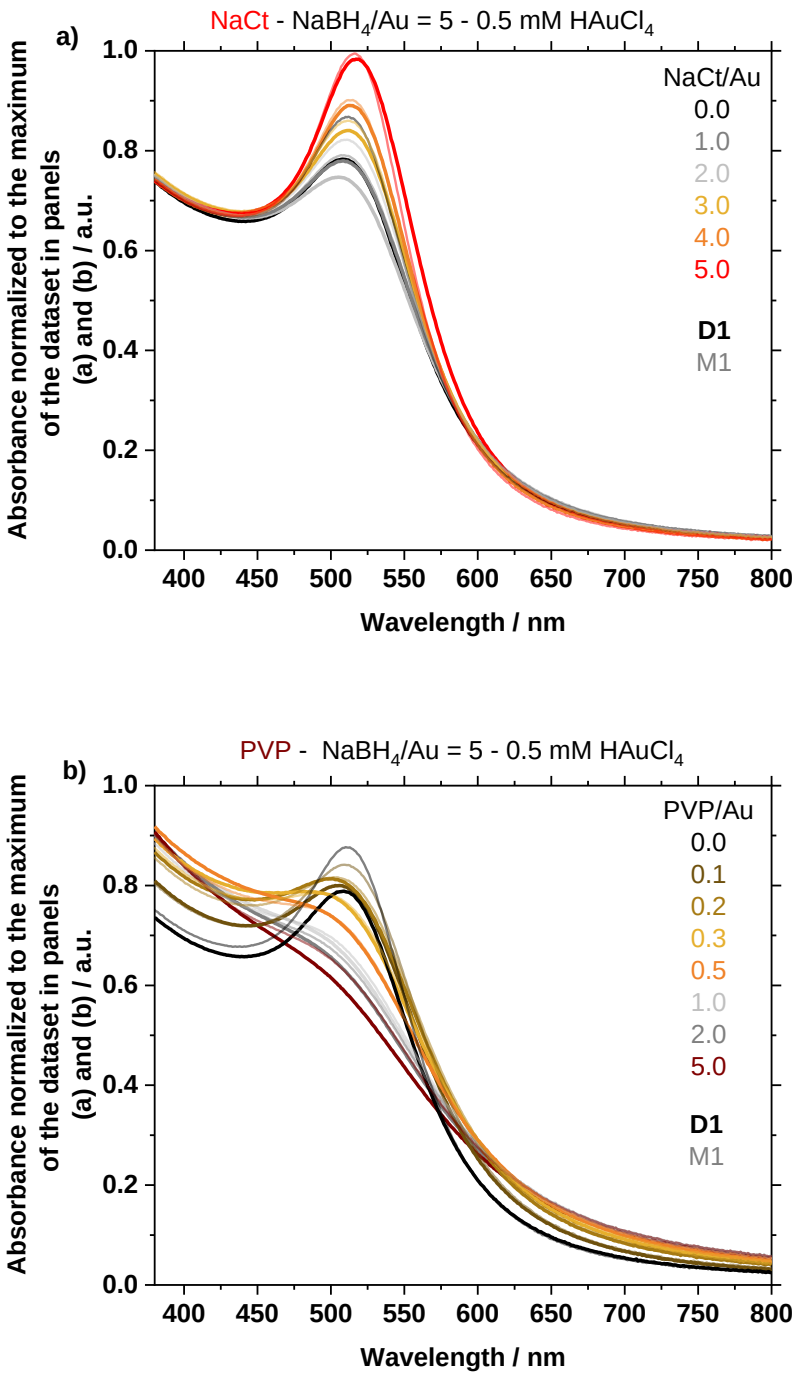

Figure S15. UV-vis spectra for Au NPs obtained using 0.5 mM $HAuCl_4$ concentrations, a $NaBH_4$/Au molar ratio of 5, and (a) NaCt and (b) PVP at different Additive/Au molar ratio, as indicated. In each case the UV-vis spectra recorded 24 hours after the synthesis (D1) and after a month (M1) are reported.

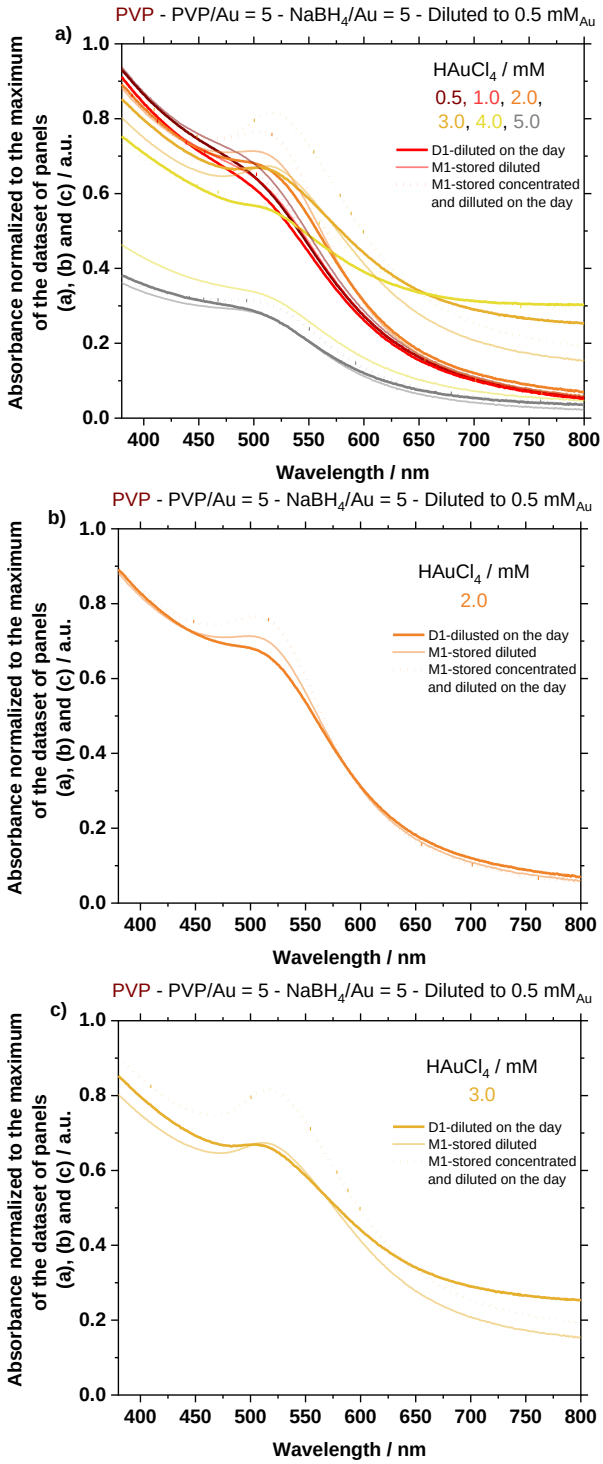

Figure S16. UV-vis spectra for Au NPs obtained using a $NaBH_4$/Au molar ratio of 5, a PVP/Au molar ratio of 5 and (a) various concentrations of $HAuCl_4$. (b) and (c) isolate data relative to the use of 2 mM and 3 mM $HAuCl_4$, respectively. All solutions were diluted to 0.5 mM equivalent of Au for measurement. The data therefore represent the sample diluted and measured after 24 hours (D1, plain thick line), this same samples at 0.5 mM kept at room temperature in a drawer and measured after a month (M1, thinner line), but also samples obtained by dilution of the stock solution at high concentrations kept at room temperature for one month in a drawer, and diluted to 0.5 mM after a month for measurement.

9. Catalysis

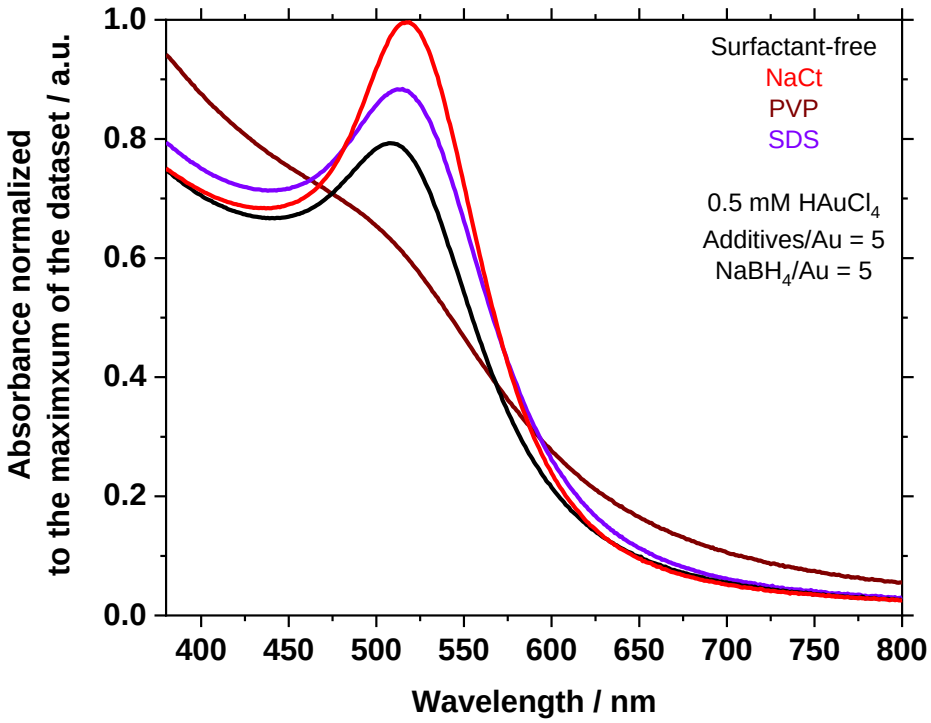

Figure S17. UV-vis data of the samples considered for catalytic experiments. The samples correspond to entries 97, 102, 65, 67 in **Table S3** and so to samples prepared without surfactant, with NaCt, PVP and SDS, respectively, for sizes: 4.0 ± 0.8, 6.2 ±1.7, 1.8 ± 0.6, 4.0 ± 1.0 nm, respectively. In all cases 0.5 mM $HAuCl_4$ was used, a $NaBH_4$/Au molar ratio of 5 and an Additive/Au molar ratio of 5.

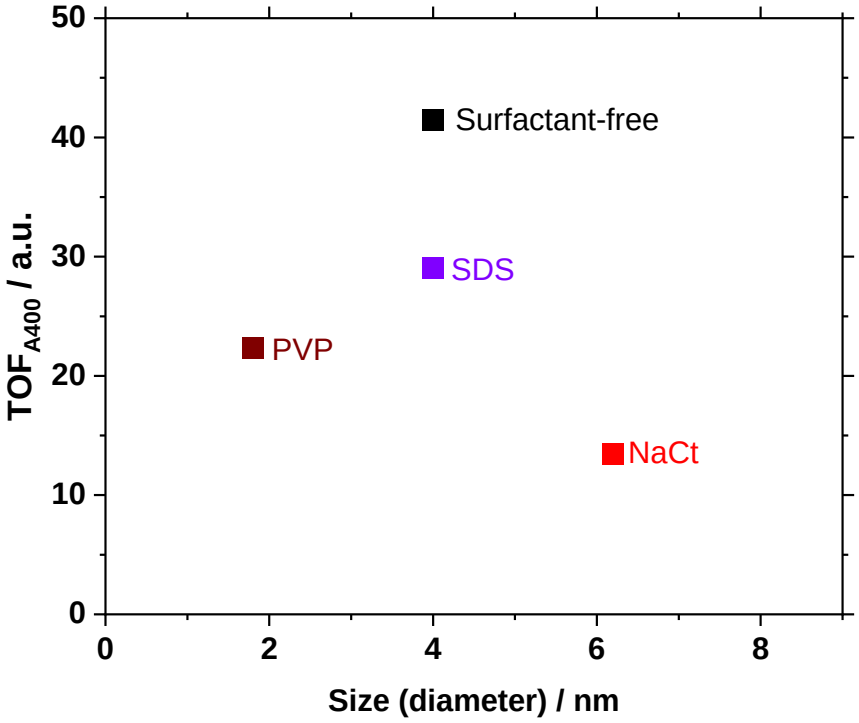

Figure S18. TOF values normalized by the A_{400} values retrieved from UV-vis spectroscopy for samples prepared without additives, with NaCt, with PVP or SDS, as indicated and as detailed in **Figure S17**.

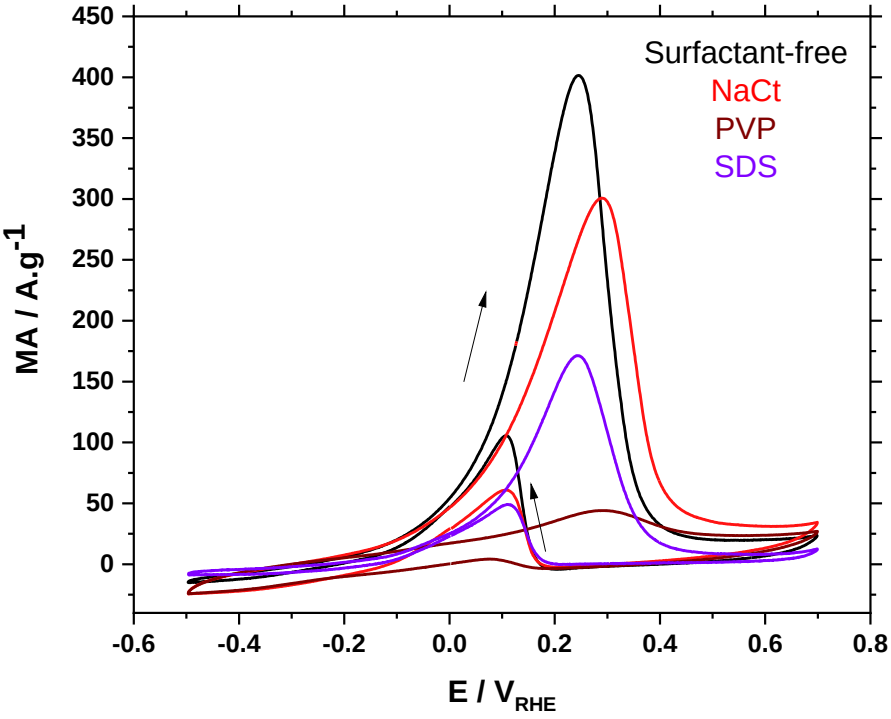

Figure S19. Illustrative cyclic voltammograms for the EOR catalyzed by Au NPs prepared using different additives, as indicated, and prepared using 0.5 mM $HAuCl_4$, a $NaBH_4$/Au molar ratio of 5 and an Additive/Au molar ratio of 5. 20 µL of a solution at 0.5 mM Au, a scan rate of 50 mV s^{-1} and 1 M KOH with 1 M ethanol were used. The forward and backward scans are indicated.

The highest MA in the forward scan, around 0.2-0.3 V_{RHE} correspond to the EOR. The highest MA on the backward scan around 0.1 V_{RHE} correspond to the cleaning of the NP surface.[38]

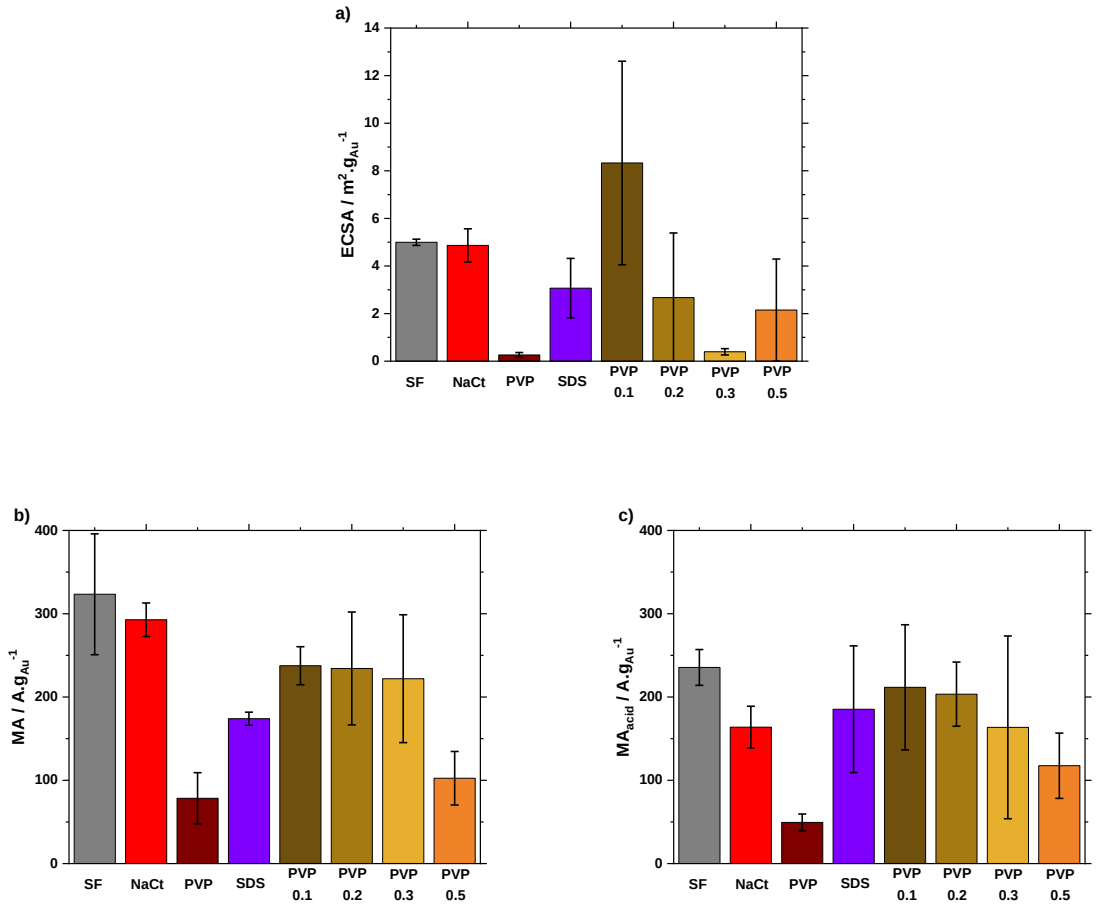

Figure S20. (a) ECSA values (b) MA values and (c) MA values obtained after an acid treatment, for samples prepared without additives, with NaCt, with PVP (with various PVP/Au molar ratio of 0.1, 0.2, 0.3 or 0.5) or SDS, as indicated. Unless otherwise specified the Au NPs were prepared using 0.5 mM $HAuCl_4$, $NaBH_4$/Au molar ratio of 5 and an Additive/Au molar ratio of 5.

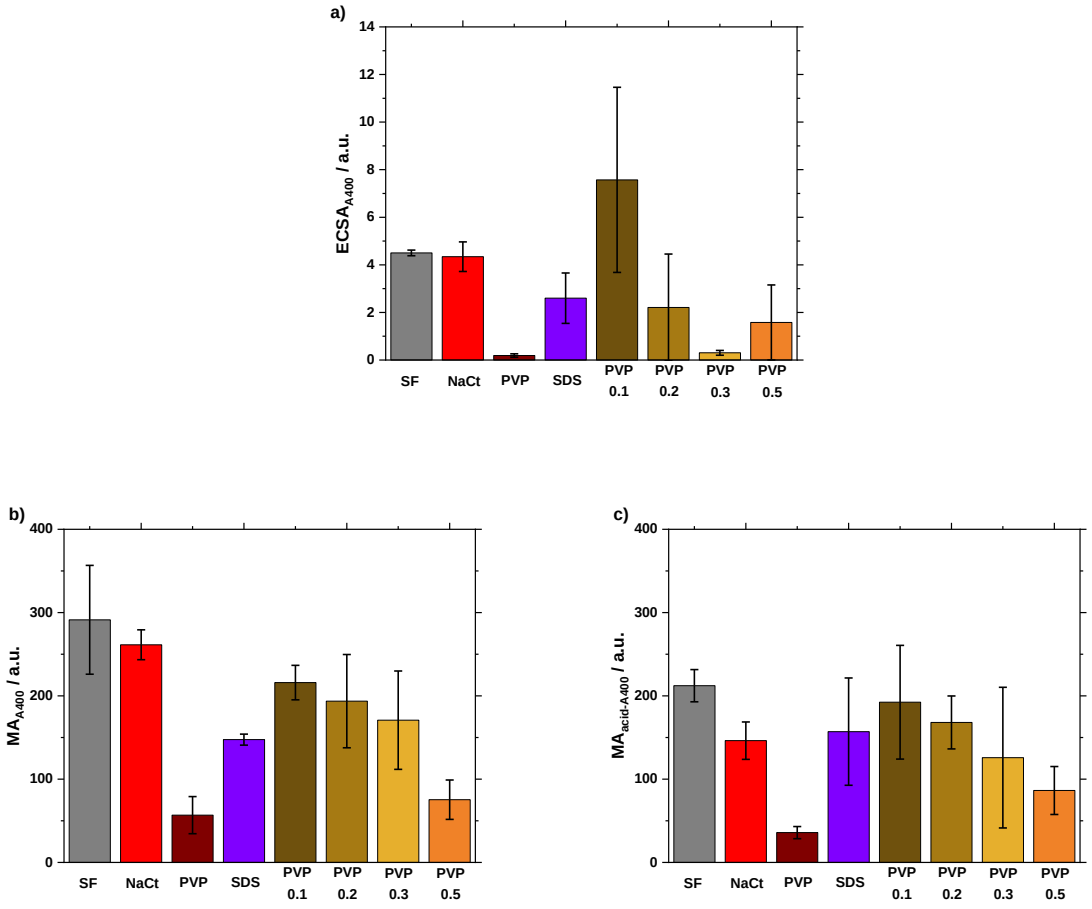

Figure S21. (a) ECSA values (b) MA values and (c) MA values obtained after an acid treatment, all normalized by the A_{400} values retrieved from UV-vis spectroscopy, for samples prepared without additives, with NaCt, with PVP (with various PVP/Au molar ratio of 0.1, 0.2, 0.3 or 0.5) or SDS, as indicated. Unless otherwise specified the Au NPs were prepared using 0.5 mM $HAuCl_4$, $NaBH_4$/Au molar ratio of 5 and an Additive/Au molar ratio of 5.

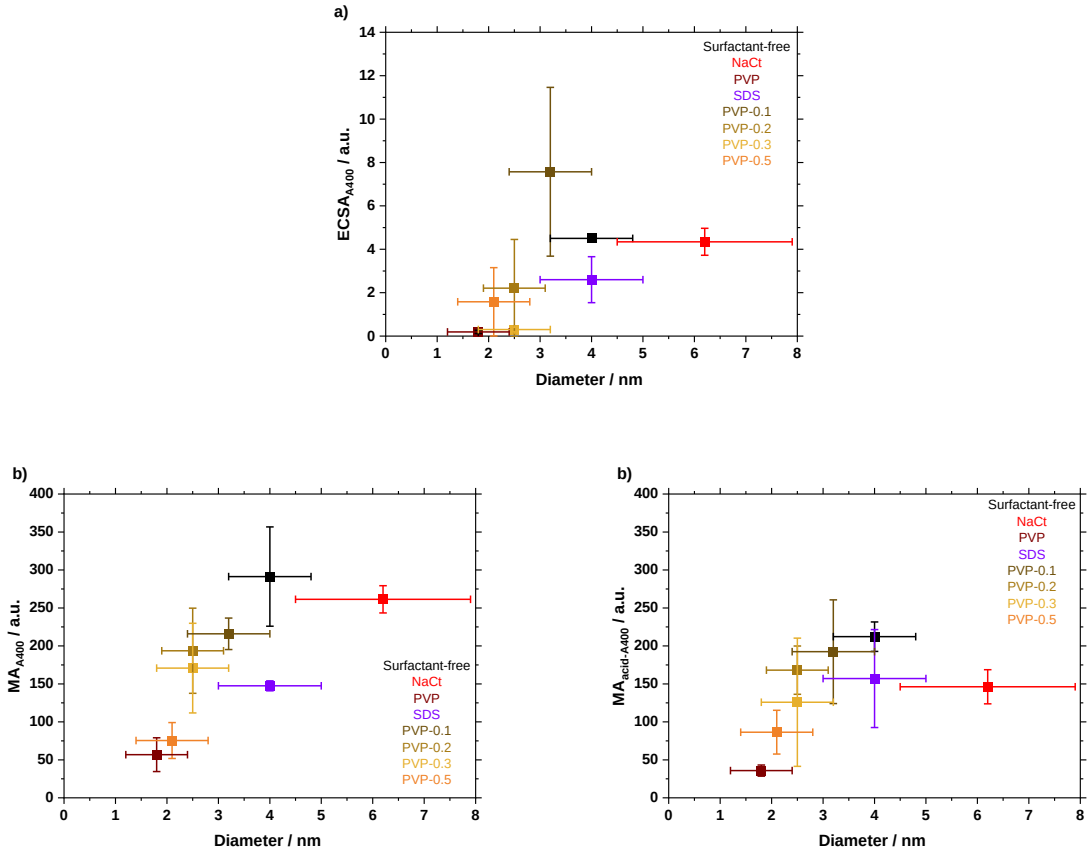

Figure S22. (a) ECSA values (b) MA values and (c) MA values obtained after an acid treatment, all normalized by the A_{400} values retrieved from UV-vis spectroscopy, as a function of the NP diameter for samples prepared without additives, with NaCt, with PVP (with various PVP/Au molar ratio of 0.1, 0.2, 0.3 or 0.5) or SDS, as indicated. Unless otherwise specified the Au NPs were prepared using 0.5 mM $HAuCl_4$, $NaBH_4$/Au molar ratio of 5 and an Additive/Au molar ratio of 5. The data point that might appear without deviation actually have a very small deviation.

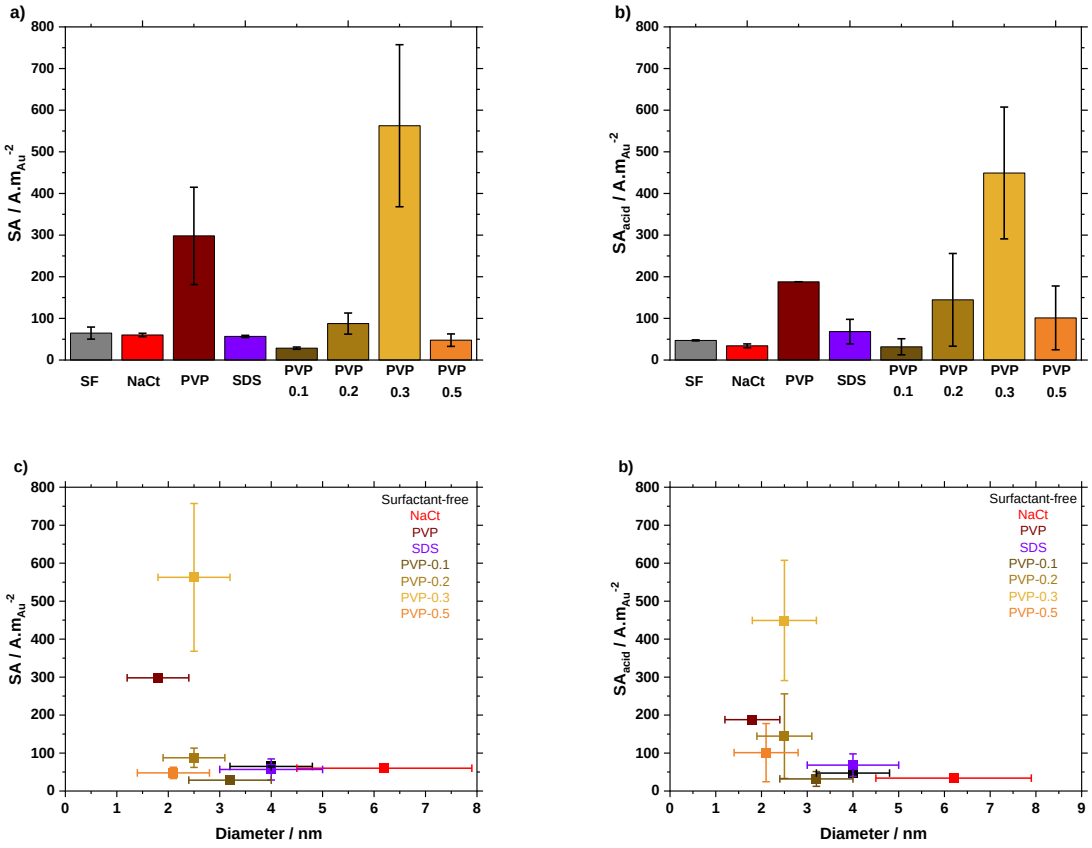

Figure S23. (a) SA values (b) SA values after acidic treatment, (c) (a) SA values a function of diameter and (d) SA values a function of diameter after acidic treatment, for samples prepared without additives, with NaCt, with PVP (with various PVP/Au molar ratio of 0.1, 0.2, 0.3 or 0.5) or SDS, as indicated. Unless otherwise specified the Au NPs were prepared using 0.5 mM $HAuCl_4$, $NaBH_4$/Au molar ratio of 5 and an Additive/Au molar ratio of 5. The data point that might appear without deviation actually have a very small deviation.

The SA values reported in **Figure S23** are reported for the convenience of the reader. Since the SA is obtained by multiplication of the MA divided by the ECSA, the very low ECSA retrieved for some experimental measurement accounts for the relatively high values obtained for PVP-based syntheses, especially for samples prepared with a PVP/Au molar ratio of 0.3 (PVP-0.3) and 5 (PVP).

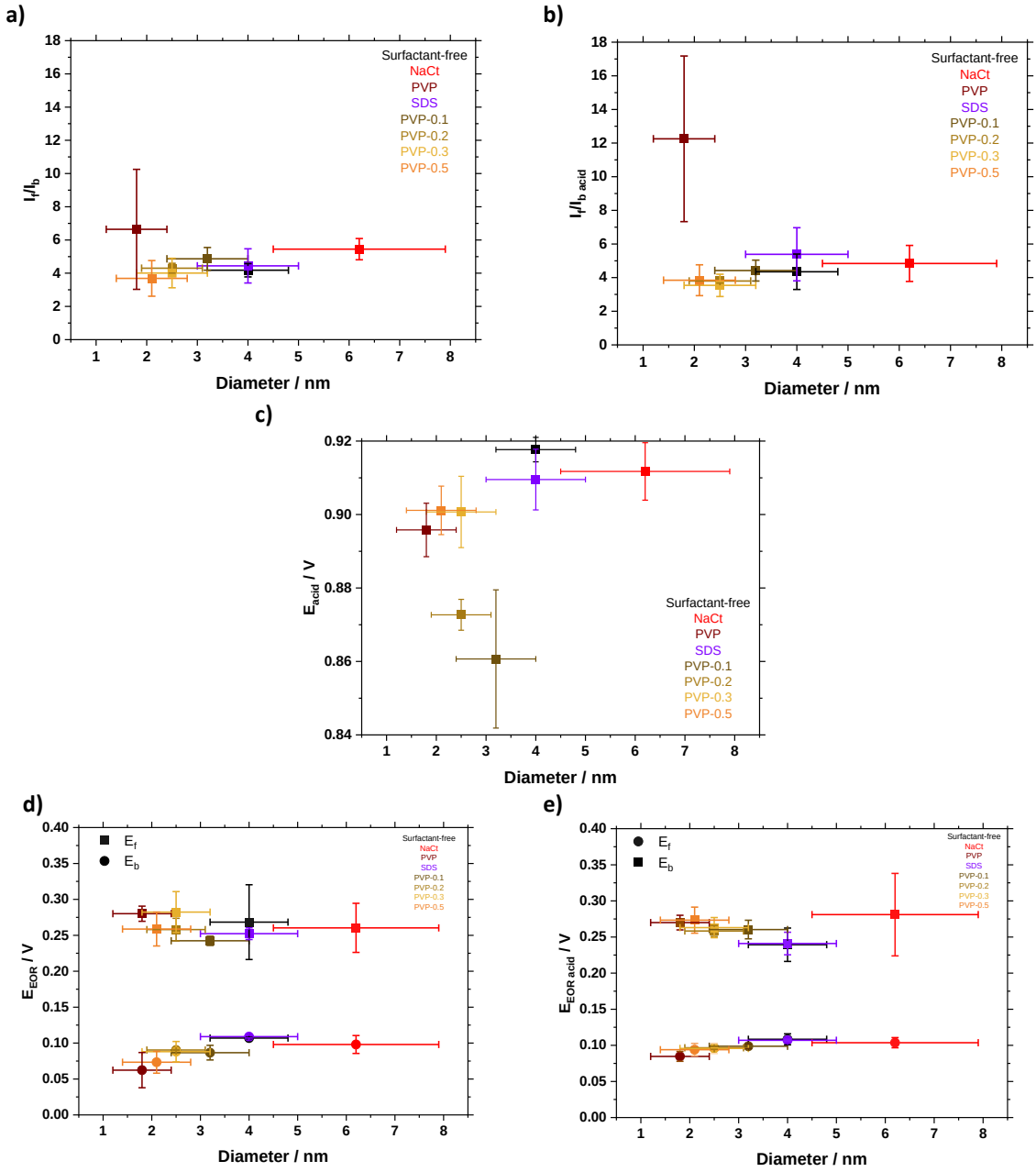

Figure S24. (a) I_f/I_b, (b) $I_f/I_{b\ acid}$, (c) E_{acid}, (d) E_{OR} and (e) $E_{EOR\ acid}$ as a function of NP diameter for samples prepared without additives, with NaCt, with PVP (with various PVP/Au molar ratio of 0.1, 0.2, 0.3 or 0.5) or SDS, as indicated. Unless otherwise specified the Au NPs were prepared using 0.5 mM $HAuCl_4$, $NaBH_4$/Au molar ratio of 5 and an Additive/Au molar ratio of 5. The value under scripted with 'acid' correspond to values retrieved from the Protocol B detailed in the Materials and methods section. Without under script 'acid' the data correspond to the Protocol A detailed in the Materials and Methods section. I_f/I_b is the ratio of the maximum activity retrieved from the forward and backwards scans from the 10th CV. The forward scan shows a maximum at a value E_f and the backward scan at a value E_b. The value E_{acid} corresponds to the position of the reduction peak evaluated in acid following Protocol A detailed in the Materials and methods section. E_{EOR} corresponds to the voltage where a maximum is observed, in the forward (E_f) or backward (E_b) scans, as indicated.

The I_f/I_b and $I_f/I_{b\ acid}$ values in **Figure S24a,b** are in the typical range for Au NPs for the EOR, see **Table S4**. An outstanding value is obtained with Au NPs prepared with a PVP/Au molar ratio of 5 and is attributed to the fact that for those Au NPs the activity is overall very low and therefore the measurements more challenging in general. The potential E_{acid} of the reduction peak observed in acidic electrolyte is consistent around 0.91 V_{RHE}, **Figure S24c**. This values decreases as the amount of PVP increases, indicating a more challenging reduction when PVP is use, in line with the passivating effect of PVP. The position of the oxidation peak in the forward scan, E_f, **Figure S24d-e** tends to be around 0.25-0.30 V_{RHE}, and tends to increase as the amount of PVP increases. The position of the oxidation peak in the backward scan, E_b, **Figure S24d-e** tends to be around 0.05-0.10 V_{RHE}, and tends to decrease as the amount of PVP increases. In all cases those trends suggest the passivating role of PVP rather than a size effect.

Table S4. Comparison of the properties of different Au NPs for the EOR. Parts in grey are made with strong assumptions because the information is not directly available (e.g. conversion of the potentials expressed versus one type of reference electrode to another). Typically no errors (standard deviations) are reported. This is a completed table from [38,39]. It is a general challenge to compare results from the literature due to different protocols being used and/or not reported in detail.

Ref.	Catalyst	Reaction	Size nm	Method	Electrolytes	Scan rate $mV\ s^{-1}$	Scan range	# Scans	Counter	ECSA $m^2\ g^{-1}$	Mass Activity* $A\ g^{-1}$	Specific activity $A\ m^{-2}$	I_f/I_b	Sequence of electrochemical steps
[45]	Au	EOR	-	Solid phase	1 M Ethanol 1 M KOH	50	0.8 to 1.7 V_{SCE}	?	Pt	-	22	-	-	NO
[46]	Au	EOR	1900	Reduction with H_2O_2	1 M Ethanol 1 M KOH	20	-0.6 to 0.6 V_{SCE} 0.47 to 1.67 V_{RHE}	?	?	-	23	-	3-4	NO
[47]	Au	EOR	6-50	Aerogels	0.5 M Ethanol 1 M KOH	50	-0.4 to 0.6 $V_{Ag/AgCl}$ 0.6 to 1.6 V_{RHE}	1000	Pt	1.2	30-36	25-30	4	NO
[48]	Au/C	EOR	22	Reduction with $NaBH_4$	1 M Ethanol 0.5 M KOH	50	-1.0 to 0.8 $V_{Ag/AgCl}$ 0.0 to 1.8 V_{RHE}	?	Pt	-	54	-	2-3	NO
[49]	Au/C	EOR	6	Reduction with $NaBH_4$ in presence of support	1 M Ethanol 0.5 M KOH	50	-0.4 to 0.6 V_{SCE} 0.67 to 1.67 V_{RHE}	?	Pt	6.1	82	13.4	3	NO
[50]	Au/C	EOR	< 10	Reduction with $NaBH_4$ in presence of support	1 M Ethanol 1 M KOH	50	-0.4 to 0.6 V_{SCE} 0.67 to 1.67 V_{RHE}	?	Graphite	2	128	-	4	NO
[51]	Au/C	EOR	4-5	Laser	1 M Ethanol 1 M KOH	50	-0.9 to 0.8 $V_{Hg/HgO}$ 0.02 to 1.72 V_{RHE}	?	Pt	9.4	146	10.3	4-5	NO
[52]	Au	EOR	5-6	Aerogel Citrate Aerogel No surfactant	1 M Ethanol 1 M NaOH	50	-0.8 to 0.5 $V_{Ag/AgCl}$ 0.2 to 1.5 V_{RHE}	?	Pt	11 16	45 145	4.5 11	10 4	NO
[53]	Au/C	EOR	20	Reduction with glycerol	1 M Ethanol 0.5 M NaOH	50	–0.6 to 0.6 $V_{Ag/AgCl}$ 0.4 to 1.6 V_{RHE}	?	Pt	3	94-150	30	2	NO
[54]	Au/NC	EOR	5	Reduction with $NaBH_4$ in presence of support	0.02-0.6 M Ethanol 1 M NaOH	10-100	-0.8 to 0.5 V_{SCE} 0.27 to 1.57 V_{RHE}	?	Pt	11	200	17.5	4	NO
[55]	Au/C	EOR	5	Reduction with KBH_4 in presence of support	1 M Ethanol 0.1 M KOH	20	-0.4 to 0.6 $V_{Hg/HgO}$ 0.52 to 1.52 V_{RHE}	?	C	-	300	-	3-4	NO
[39]	Au	EOR	10	Surfactant-free colloids (alcohol-mediated)	1 M Ethanol 1 M KOH	50	0.57-1.57 V_{RHE}	25	C	5-6	150	25	3-4	YES
[38]	Au	EOR	5, 10, 13, 15, 22	Surfactant-free colloids (ethanol-mediated)	1 M Ethanol 1 M KOH	50	0.37-1.57 V_{RHE}	10	C	4-7	167-295	~ 50	3-5	YES
Our previous work [11]	Au	EOR	5-20	Surfactant-free colloids ($NaBH_4$-mediated)	1 M Ethanol 1 M KOH	50	0.37-1.57 V_{RHE}	10	C	5-9	300-587	~ 50-100	5-7	YES
This work	Au	EOR	2-6	PVP, NaCt, SDS Surfactant-free colloids ($NaBH_4$-mediated)	1 M Ethanol 1 M KOH	50	0.37-1.57 V_{RHE}	10	C	0-8	75-325	~ 50-100	5-6	YES

* typically quoted as the maximum current per mass observed on the forward *oxidative* scan while cycling from low to high voltages.

10. References

1 Lin, C., Tao, K., Hua, D., Ma, Z. & Zhou, S. Size Effect of Gold Nanoparticles in Catalytic Reduction of p-Nitrophenol with $NaBH_4$. *Molecules* **18**, 12609-12620 (2013). https://doi.org/10.3390/molecules181012609

2 De Souza, C. D., Nogueira, B. R. & Rostelato, M. Review of the methodologies used in the synthesis gold nanoparticles by chemical reduction. *Journal of Alloys and Compounds* **798**, 714-740 (2019). https://doi.org/10.1016/j.jallcom.2019.05.153

3 Xia, N. & Wu, Z. K. Controlling ultrasmall gold nanoparticles with atomic precision. *Chemical Science* **12**, 2368-2380 (2021). https://doi.org/10.1039/d0sc05363e

4 Deraedt, C. *et al.* Sodium borohydride stabilizes very active gold nanoparticle catalysts. *Chemical Communications* **50**, 14194-14196 (2014). https://doi.org/10.1039/c4cc05946h

5 Elnagar, M. *et al.* Water-soluble ionic carbon nitride as unconventional stabilizer for highly catalytically active ultrafine gold nanoparticles. *Nanoscale* **15**, 19268-19281 (2023). https://doi.org/10.1039/d3nr03375a

6 Iqbal, M. *et al.* Preparation of gold nanoparticles and determination of their particles size via different methods. *Materials Research Bulletin* **79**, 97-104 (2016). https://doi.org/10.1016/j.materresbull.2015.12.026

7 Larm, N. E., Thon, J. A., Vazmitsel, Y., Atwood, J. L. & Baker, G. A. Borohydride stabilized gold-silver bimetallic nanocatalysts for highly efficient 4-nitrophenol reduction. *Nanoscale Advances* **1**, 4665-4668 (2019). https://doi.org/10.1039/c9na00645a

8 Larm, N. *et al.* Role of Heavy Water in the Synthesis and Nanocatalytic Activity of Gold Nanoparticles. *ACS Nanoscience Au* **5**, 52-59 (2025). https://doi.org/10.1021/acsnanoscienceau.4c00069

9 Andersen, K. J. *et al.* Positive Thinking: Countercation Effects in Colloidal Syntheses of Gold Nanoparticles. N*ano Letters* **25**, 15436–15442 (2025). https://doi.org/10.1021/acs.nanolett.5c04815

10 Sørensen, M. P. *et al.* Room temperature surfactant-free syntheses of colloidal gold nanoparticles: comparison of the precursors $HAuCl_4$ and $HAuBr_4$. *ChemRxiv* **Preprint** (2025). https://doi.org/10.26434/chemrxiv-2025-l8w54

11 Fokam, H. K., Smolska, A. & Quinson, J. Surfactant-free $NaBH_4$-mediated synthesis of gold nanoparticles in water at room temperature: fine size control for active nanocatalysts. *ChemRxiv* **Preprint** (2025). https://doi.org/10.26434/chemrxiv-2025-rwh33

12 Wuithschick, M. *et al.* Turkevich in New Robes: Key Questions Answered for the Most Common Gold Nanoparticle Synthesis. *ACS Nano* **9**, 7052-7071 (2015). https://doi.org/10.1021/acsnano.5b01579

13 Quinson, J. *et al.* Surfactant-free colloidal syntheses of gold-based nanomaterials in alkaline water and mono-alcohol mixtures. *Chemistry of Materials* **35**, 2173–2190 (2023). https://doi.org/10.1021/acs.chemmater.3c00090

14 Quinson, J. Influence of the alcohol and water grades on surfactant-free colloidal syntheses of gold nanoparticles in alkaline water-alcohol mixtures. *Gold Bulletin* **57**, 27-31 (2024). https://doi.org/10.1007/s13404-024-00345-7

15 Freese, T., Elzinga, N., Heinemann, M., Lerch, M. M. & Feringa, B. L. The relevance of sustainable laboratory practices. *RSC Sustainability* **2**, 1300-1336 (2024). https://doi.org/10.1039/D4SU00056K

16 Hutchison, J. E. The Road to Sustainable Nanotechnology: Challenges, Progress and Opportunities. *ACS Sustainable Chemistry & Engineering* **4**, 5907-5914 (2016). https://doi.org/10.1021/acssuschemeng.6b02121
17 Gilbertson, L. M., Zimmerman, J. B., Plata, D. L., Hutchison, J. E. & Anastas, P. T. Designing nanomaterials to maximize performance and minimize undesirable implications guided by the Principles of Green Chemistry. *Chemical Society Reviews* **44**, 5758-5777 (2015). https://doi.org/10.1039/c4cs00445k
18 Duan, H. H., Wang, D. S. & Li, Y. D. Green chemistry for nanoparticle synthesis. *Chemical Society Reviews* **44**, 5778-5792 (2015). https://doi.org/10.1039/c4cs00363b
19 Yuan, H. F. *et al.* Reshaping anisotropic gold nanoparticles through oxidative etching: the role of the surfactant and nanoparticle surface curvature. *RSC Advances* **5**, 6829-6833 (2015). https://doi.org/10.1039/c4ra14237c
20 Wall, M. A. *et al.* Surfactant-Free Shape Control of Gold Nanoparticles Enabled by Unified Theoretical Framework of Nanocrystal Synthesis. *Advanced Materials* **29**, 1605622 (2017). https://doi.org/10.1002/adma.201605622
21 Yuan, X. *et al.* Balancing the Rate of Cluster Growth and Etching for Gram- Scale Synthesis of Thiolate- Protected Au25 Nanoclusters with Atomic Precision. *Angewandte Chemie-International Edition* **53**, 4623-4627 (2014). https://doi.org/10.1002/anie.201311177
22 Rasmussen , D. R., Lock , N. & Quinson , J. Lights on the synthesis of surfactant-free colloidal gold nanoparticles in alkaline mixtures of alcohols and water. *ChemSusChem* **18**, e202400763 (2025). https://doi.org/10.1002/cssc.202400763
23 Oestreicher, V., Garcia, C. S., Soler-Illia, G. & Angelome, P. C. Gold Recycling at Laboratory Scale: From Nanowaste to Nanospheres. *ChemSusChem* **12**, 4882-4888 (2019). https://doi.org/10.1002/cssc.201901488
24 Rodrigues, T. S. *et al.* Synthesis of Colloidal Metal Nanocrystals: A Comprehensive Review on the Reductants. *Chemistry-a European Journal* **24**, 16944-16963 (2018). https://doi.org/10.1002/chem.201802194
25 Mourdikoudis, S., Pallares, R. M. & Thanh, N. T. K. Characterization techniques for nanoparticles: comparison and complementarity upon studying nanoparticle properties. *Nanoscale* **10**, 12871-12934 (2018). https://doi.org/10.1039/c8nr02278j
26 Villa, A. *et al.* Characterisation of gold catalysts. *Chemical Society Reviews* **45**, 4953-4994 (2016). https://doi.org/10.1039/c5cs00350d
27 Pal, A., Shah, S. & Devi, S. Preparation of silver-gold alloy nanoparticles at higher concentration using sodium dodecyl sulfate. *Australian Journal of Chemistry* **61**, 66-71 (2008). https://doi.org/10.1071/CH07165
28 Silva, L. *et al.* Gold nanoparticles produced using $NaBH_4$ in absence and in the presence of one-tail or two-tail cationic surfactants: Characteristics and optical responses induced by aminoglycosides. *Colloids and Surfaces A-Physicochemical and Engineering Aspects* **614**, 126174 (2021). https://doi.org/10.1016/j.colsurfa.2021.126174
29 Varga, M. & Quinson, J. Fewer, but better: on the benefits for surfactant-free colloidal syntheses of nanomaterials. *ChemistrySelect* **10**, e202404819 (2025). https://doi.org/10.1002/slct.202404819
30 Panariello, L., Radhakrishnan, A. N. P., Papakonstantinou, I., Parkin, I. P. & Gavriilidis, A. Particle Size Evolution during the Synthesis of Gold Nanoparticles Using In Situ Time-Resolved UV-Vis Spectroscopy: An Experimental and Theoretical Study Unravelling the Effect of Adsorbed Gold Precursor Species. *Journal of Physical Chemistry C* **124**, 27662-27672 (2020). https://doi.org/10.1021/acs.jpcc.0c07405

31 Jæger, F., Pedersen, A. A., Wacherhausen, P. S., Smolska, A. & Quinson, J. Surfactant-free gold nanoparticles synthesized in alkaline water-ethanol mixtures: leveraging lower grade chemicals for size control of active nanocatalysts. *RSC Sustainability* **3**, 2870-2875 (2025). https://doi.org/10.1039/D5SU00213C

32 Neal, R., Inoue, Y., Hughes, R. & Neretina, S. Catalytic Reduction of 4-Nitrophenol by Gold Catalysts: The Influence of Borohydride Concentration on the Induction Time. *Journal of Physical Chemistry C* **123**, 12894-12901 (2019). https://doi.org/10.1021/acs.jpcc.9b02396

33 Pradhan, N., Pal, A. & Pal, T. Catalytic reduction of aromatic nitro compounds by coinage metal nanoparticles. *Langmuir* **17**, 1800-1802 (2001). https://doi.org/10.1021/la000862d

34 Larm, N. E., Bhawawet, N., Thon, J. A. & Baker, G. A. Best practices for reporting nanocatalytic performance: lessons learned from nitroarene reduction as a model reaction. *New Journal of Chemistry* **43**, 17932-17936 (2019). https://doi.org/10.1039/c9nj01745c

35 Hendel, T. *et al.* In Situ Determination of Colloidal Gold Concentrations with UV-Vis Spectroscopy: Limitations and Perspectives. *Analytical Chemistry* **86**, 11115-11124 (2014). https://doi.org/10.1021/ac502053s

36 Wu, D. S. *et al.* Platinum-Group-Metal High-Entropy-Alloy Nanoparticles. *Journal of the American Chemical Society* **142**, 13833-13838 (2020). https://doi.org/10.1021/jacs.0c04807

37 Bai, J., Liu, D. Y., Yang, J. & Chen, Y. Nanocatalysts for Electrocatalytic Oxidation of Ethanol. *ChemSusChem* **12**, 2117-2132 (2019). https://doi.org/10.1002/cssc.201803063

38 Panagopoulos, D., Asghari Alamdari, A. & Quinson, J. Surfactant-free colloidal gold nanoparticles: room temperature synthesis, size control and opportunities for catalysis. *Materials Today Nano* **29**, 100600 (2025). https://doi.org/10.1016/j.mtnano.2025.100600

39 Quinson, J., Nielsen, T. M., Escudero-Escribano, M. & Jensen, K. M. Ø. Room temperature syntheses of surfactant-free colloidal gold nanoparticles: the benefits of mono-alcohols over polyols as reducing agents for electrocatalysis. *Colloids and Surfaces A: Physicochemical and Engineering Aspects*, **675**, 131853 (2023). https://doi.org/10.1016/j.colsurfa.2023.131853

40 Padayachee, D., Golovko, V., Ingham, B. & Marshall, A. T. Influence of particle size on the electrocatalytic oxidation of glycerol over carbon-supported gold nanoparticles. *Electrochimica Acta* **120**, 398-407 (2014). https://doi.org/10.1016/j.electacta.2013.12.100

41 Haiss, W., Thanh, N. T. K., Aveyard, J. & Fernig, D. G. Determination of size and concentration of gold nanoparticles from UV-Vis spectra. *Analytical Chemistry* **79**, 4215-4221 (2007). https://doi.org/10.1021/ac0702084

42 Merk, V. *et al.* In Situ Non-DLVO Stabilization of Surfactant-Free, Plasmonic Gold Nanoparticles: Effect of Hofmeister's Anions. *Langmuir* **30**, 4213-4222 (2014). https://doi.org/10.1021/la404556a

43 Ye, Y. J., Lv, M. X., Zhang, X. Y. & Zhang, Y. X. Colorimetric determination of copper(II) ions using gold nanoparticles as a probe. *RSC Advances* **5**, 102311-102317 (2015). https://doi.org/10.1039/c5ra20381c

44 Agarwal, S. *et al.* Citrate-capped gold nanoparticles for the label-free detection of ubiquitin C-terminal hydrolase-1. *Analyst* **140**, 1166-1173 (2015). https://doi.org/10.1039/c4an01935k

45 Zhang, A. *et al.* Enhanced Electrocatalytic Activities toward the Ethanol Oxidation of Nanoporous Gold Prepared via Solid-Phase Reaction. *ACS Applied Energy Materials* **3**, 336-343 (2020). https://doi.org/10.1021/acsaem.9b01588

46 Zhao, X. D. *et al.* Sulfhydryl-functionalized carbon dots modified ball cactus-like Au composites facilitating the electrocatalytic ethanol oxidation through adsorption effect. *Journal of Applied Electrochemistry* **50**, 925-933 (2020). https://doi.org/10.1007/s10800-020-01445-w

47 Wang, C. *et al.* Facet-Dependent Long-Term Stability of Gold Aerogels toward Ethylene Glycol Oxidation Reaction. *ACS Applied Materials & Interfaces* **12**, 39033-39042 (2020). https://doi.org/10.1021/acsami.0c08914

48 Maumau, T. R., Modibedi, R. M. & Mathe, M. K. Electro-oxidation of alcohols using carbon supported gold, palladium catalysts in alkaline media. *Materials Today-Proceedings* **5**, 10542-10550 (2018). https://doi.org/10.1016/j.matpr.2017.12.386

49 Li, T. F. *et al.* Carbon supported ultrafine gold phosphorus nanoparticles as highly efficient electrocatalyst for alkaline ethanol oxidation reaction. *Electrochimica Acta* **231**, 13-19 (2017). https://doi.org/10.1016/j.electacta.2017.02.044

50 Zhang, G. G. *et al.* Facile synthesis of branched Au nanocrystals with sub-10-nm arms and their applications for ethanol oxidation reaction. *Journal of Nanoparticle Research* **23**, 22 (2021). https://doi.org/10.1007/s11051-020-05126-9

51 Zhu, J. Y. *et al.* Laser-assisted synthesis of Au aerogel with high-index facets for ethanol oxidation. *Nanotechnology* **33**, 225404 (2022). https://doi.org/10.1088/1361-6528/ac56bc

52 Wen, D. *et al.* Gold Aerogels: Three-Dimensional Assembly of Nanoparticles and Their Use as Electrocatalytic Interfaces. *ACS Nano* **10**, 2559-2567 (2016). https://doi.org/10.1021/acsnano.5b07505

53 Kepeniene, V., Stagniunaite, R., Balciunaite, A., Tamasauskaite-Tamasiunaite, L. & Norkus, E. Microwave-assisted synthesis of a $AuCeO_2$/C catalyst and its application for the oxidation of alcohols in an alkaline medium. *New Journal of Chemistry* **44**, 18308-18318 (2020). https://doi.org/10.1039/d0nj03219k

54 Yang, Y., Jin, L., Liu, B., Kerns, P. & He, J. Direct growth of ultrasmall bimetallic AuPd nanoparticles supported on nitrided carbon towards ethanol electrooxidation. *Electrochimica Acta* **269**, 441-451 (2018). https://doi.org/10.1016/j.electacta.2018.03.017

55 Yan, S. H. *et al.* Synthesis of Au/C catalyst with high electrooxidation activity. *Electrochimica Acta* **94**, 159-164 (2013). https://doi.org/10.1016/j.electacta.2013.01.087